**Distribution Agreement**

In presenting this thesis or dissertation as a partial fulfillment of the requirements for an advanced degree from Emory University, I hereby grant to Emory University and its agents the non-exclusive license to archive, make accessible, and display my thesis or dissertation in whole or in part in all forms of media, now or hereafter known, including display on the world wide web. I understand that I may select some access restrictions as part of the online submission of this thesis or dissertation. I retain all ownership rights to the copyright of the thesis or dissertation. I also retain the right to use in future works (such as articles or books) all or part of this thesis or dissertation.

Signature:

_____ _____

James Bogenpohl Date

Metabotropic glutamate and adenosine receptors in the monkey striatopallidal complex and their involvement in Parkinsonism: Anatomy, physiology, and behavior.

By

James W. Bogenpohl II
Doctor of Philosophy
Graduate Division of Biological and Biomedical Science
Neuroscience

_____
Yoland Smith, Ph.D.
Advisor

_____
Thomas Wichmann, M.D.
Committee Member

_____
E. Christopher Muly, M.D./Ph.D.
Committee Member

_____
Randy Hall, Ph.D.
Committee Member

_____
Stewart Factor, D.O.
Committee Member

Accepted:

_____
Lisa A. Tedesco, Ph.D.
Dean of the James T. Laney School of Graduate Studies

_____ Date

Metabotropic glutamate and adenosine receptors in the monkey striatopallidal complex and their involvement in Parkinsonism: Anatomy, physiology, and behavior.

By

James W. Bogenpohl II
B.A., Washington University in St. Louis, 2004

Advisor: Yoland Smith, Ph.D.

An abstract of a dissertation submitted to the Faculty of the James T. Laney School of Graduate Studies of Emory University, in partial fulfillment of the requirements for the degree of Doctor of Philosophy in Graduate Division of Biological and Biomedical Science, Neuroscience
2013

## Abstract

**Metabotropic glutamate and adenosine receptors in the monkey striatopallidal complex and their involvement in Parkinsonism: Anatomy, physiology, and behavior.**

**By James W. Bogenpohl II**

Long term dopamine replacement therapies for Parkinson's disease (PD) induce debilitating side effects. The discovery of non-dopaminergic pharmacotherapeutics for PD which could replace or potentiate dopaminergic drugs represents a strategy whereby side effects could be reduced. In this thesis, anatomical, electrophysiological, and behavioral properties of three potential non-dopaminergic drug targets in the striatopallidal complex were examined.

First, we demonstrated that the metabotropic glutamate receptor 5 (mGluR5) antagonist 3-((2-Methyl-4-thiazolyl)ethynyl)pyridine (MTEP) potentiates the antiparkinsonian effect of low doses of the D2-like dopamine receptor (D2LR) agonist pramipexole in 1-methyl-4-phenyl-1,2,3,6-tetrahydropyridine (MPTP)-treated monkeys. This combination treatment strategy may be able to reduce the development of side effects commonly associated with high doses of D2LR agonists in PD.

The adenosine $A_{2A}$ receptor ($A_{2A}R$) is another attractive non-dopaminergic target for PD pharmacotherapy. In rodents, synergistic antiparkinsonian effects of $A_{2A}R$ and mGluR5 antagonists have been shown. A more detailed localization of these two receptors in the basal ganglia is needed before such therapy can be tested in primates. Using electron microscopy immunohistochemistry, we found that $A_{2A}R$ is located mainly in striatopallidal GABAergic axon terminals in the external globus pallidus and in both

pre- and postsynaptic structures in the striatum. We also found that $A_{2A}R$ was colocalized with mGluR5 in postsynaptic structures in the striatum. These data highlight numerous target sites whereby the combined use of $A_{2A}R$ and mGluR5 antagonists could mediate synergistic antiparkinsonian effects in primates.

Finally, we studied the localization and electrophysiological effects of mGluR4, another non-dopaminergic target with good antiparkinsonian potential, in the monkey striatopallidal complex. We found that mGluR4 is located in both putative glutamatergic and GABAergic terminals and that activation of mGluR4 has multifarious effects on striatal and pallidal neurons, which showed increases and decreases in firing rates, as well as changes in firing patterns, in the striatopallidal complex of normal and MPTP-treated monkeys.

Together, these studies help to lay the foundation for the development of new non-dopaminergic antiparkinsonian treatment strategies in PD.

# Metabotropic glutamate and adenosine receptors in the monkey striatopallidal complex and their involvement in Parkinsonism: Anatomy, physiology, and behavior.

By

James W. Bogenpohl II
B.A., Washington University in St. Louis, 2004

Advisor: Yoland Smith Ph.D.

A dissertation submitted to the Faculty of the
James T. Laney School of Graduate Studies of Emory University
in partial fulfillment of the requirements for the degree of Doctor of Philosophy in
Graduate Division of Biological and Biomedical Science
Neuroscience
2013

**Acknowledgements**

First and foremost, I would like to thank my advisor, Dr. Yoland Smith, for invaluable advice and direction throughout my graduate school career. No matter how busy, he was always there with help and encouragement. Second, I thank Dr. Thomas Wichmann, who was like a second advisor to me. Always helpful and knowledgeable, Thomas always had the right answer. Third, I must thank Dr. Adriana Galvan, whose help and advice were indispensable. She always made herself available, even with matters that weren't her responsibility, and she taught me everything I know about electrophysiology. I would also like to thank my committee: Dr. Randy Hall, Dr. Stewart Factor, Dr. Chris Muly, and Dr. Claudia Testa. Their guidance was a boon, and they always made meetings a nurturing experience. Jean-Francois Pare, Susan Jenkins, and Cindy Hu also deserve thanks for their friendship and technical assistance.

Finally, I would like to thank my friends and family for their undying support and encouragement. My parents, Jim and Mary Bogenpohl, gave me everything I needed to excel, and were always there when I needed them. Dr. Darlene Mitrano has been my rock. Whenever times turned to despair, she was there to help me see the brighter side of life. I am also grateful for all the rest of my friends who helped me through the last eight and a half years. Eric, Jacob, Mike, Meag, Kalynda, Rosa, Anthony, and Sunday, thank you all for being such good friends.

**List of figures**

**List of tables**

# Chapter 1

## *Introduction*

Contains excerpts from:

Bogenpohl JW and Smith Y. Direct Pathway. In: Kompoliti K, and Verhagen Metman L (eds.) Encyclopedia of Movement Disorders, vol. 1, (2010) pp. 310-313 Oxford: Academic Press.

Bogenpohl JW and Smith Y. Indirect Pathway. In: Kompoliti K, and Verhagen Metman L (eds.) Encyclopedia of Movement Disorders, vol. 2, (2010) pp. 68-71 Oxford: Academic Press.

## 1.1 Preface

This dissertation "Metabotropic glutamate and adenosine receptors in the monkey striatopallidal complex and their involvement in Parkinsonism: Anatomy, physiology, and behavior" is presented in five chapters. The first chapter, "Introduction," gives a detailed description of background information deemed necessary to understand the circuitry and neurotransmitter receptors involved in the research described in chapters 2 through 4. The fifth and final chapter, "Discussion," summarizes the findings of this dissertation, examines the limitations of this work, and discusses future directions.

This dissertation explores the anatomical localization, electrophysiological properties, and behavioral effects of three potential non-dopaminergic antiparkinsonian drug targets, the metabotropic glutamate receptors 4 and 5 (mGluR4 and mGluR5), and the adenosine $A_{2A}$ receptor ($A_{2A}R$), in the gold-standard animal model of Parkinson's disease (PD), the 1-methyl-4-phenyl-1,2,3,6-tetrahydropyridine (MPTP)-treated monkey. Drugs acting at all three of these neurotransmitter receptors have been shown to induce antiparkinsonian effects in rodent models of PD, at least in part, through modulation of neurotransmission in the striatopallidal complex. Thus, in order to set the stage for future assessments of the potential therapeutic benefits of targeting these receptors in primates, this dissertation aims at filling gaps of knowledge about their localization, function, and behavioral properties in the monkey basal ganglia.

## 1.2 Rationale

Half a century after the discovery that levodopa can alleviate parkinsonism, dopamine replacement therapy remains the standard treatment for PD, despite the fact

that this treatment strategy often induces the progressive development of debilitating motor and non-motor side effects. Dopamine receptor agonists are often used as a frontline therapy to treat early PD, as this class of drugs has low dyskinetic potential. However, after chronic use, their efficacy decreases, requiring dose escalation, which may induce side effects. Eventually, many patients must be switched to levodopa treatment, which has an even worse side effect profile. An adjunct treatment that could potentiate the effect of dopamine receptor agonists would allow for a reduction in the required agonist dosage, extend their period of usefulness, and reduce or delay the development of side effects. Several non-dopaminergic neurotransmitter receptors in the basal ganglia have generated significant interest as potential targets for PD therapies. Three of the most attractive among these receptors are studied in this dissertation.

The metabotropic glutamate receptor 5 is expressed at high levels in the basal ganglia (Shigemoto et al., 1993; Testa et al., 1994), and antagonists at these receptors may be able to down-regulate glutamatergic transmission at corticostriatal and subthalamofugal synapses, which are overactive in the parkinsonian condition. Furthermore, through an interaction with the $D_2$ dopamine receptor in the striatum, mGluR5 is positioned to alleviate parkinsonism by modulating the binding characteristics of the $D_2$R (Ferre et al., 1999; Popoli et al., 2001). Antagonists of mGluR5 have shown good antiparkinsonian potential in rodent models of PD (Spooren et al., 2000; Breysse et al., 2002; Ossowska et al., 2002; Breysse et al., 2003; Ossowska et al., 2005; Dekundy et al., 2006), but studies examining the anti-dyskinetic effects of these drugs suggested that they have no significant antiparkinsonian effects in primates (Johnston et al., 2010; Morin et al., 2010; Rylander et al., 2010; Berg et al., 2011; Gregoire et al., 2011). However,

these studies administered the antagonist with levodopa in severely parkinsonian subjects with dyskinesia. In this thesis, we conducted behavioral experiments to examine the ability of mGluR5 antagonist to potentiate the effect of low doses of D2LR agonist in moderately parkinsonian, non-dyskinetic monkeys. These experiments are described in Chapter 2 of this dissertation.

Another non-dopaminergic receptor with antiparkinsonian potential, the adenosine $A_{2A}$ receptor, takes part in the interaction between mGluR5 and $D_2$ receptors that was exploited in the behavioral experiments described above. The $A_{2A}R$ is selectively expressed in indirect pathway striatal neurons and physically and functionally interacts with mGluR5 and $D_2R$ (Ferre et al., 1999; Popoli et al., 2001). Combined administration of mGluR5 and $A_{2A}R$ antagonists results in synergistic enhancement of their effects on the binding properties of $D_2R$, as well as on the reversal of parkinsonian signs in rodents (Coccurello et al., 2004; Kachroo et al., 2005). As such, mGluR5 antagonist/$A_{2A}R$ antagonist/D2LR agonist triple combination represents an attractive potential pharmacotherapy for PD. However, before assessing the efficacy of such a therapeutic approach in primates, we need to better characterize the ultrastructural localization of $A_{2A}R$, and elucidate anatomical sites for potential $A_{2A}R$/mGluR5 interactions in the primate basal ganglia. In order to address this issue, we used electron microscopy immunohistochemistry to examine the subcellular localization of $A_{2A}R$, and its colocalization with mGluR5 in the monkey basal ganglia. These experiments are described in Chapter 3 of this dissertation.

Another metabotropic receptor that has recently garnered much attention as a non-dopaminergic antiparkinsonian target is the mGluR4. This receptor is expressed at high

levels in the striatum and pallidum, and previous studies have shown that injection of agonists of mGluR4 into the striatopallidal complex alleviates parkinsonian motor signs in rodent models of PD (Marino et al., 2003; Valenti et al., 2003; Niswender et al., 2008), possibly through modulation of neurotransmission at corticostriatal or striatopallidal synapses (Matsui and Kita, 2003; Valenti et al., 2003; Beurrier et al., 2009; Cuomo et al., 2009). In order to examine the anatomical substrates and physiological effects of mGluR4 activation upon striatal and pallidal neurons in primates, we performed electron microscopy immunohistochemistry to localize mGluR4, as well as local administration of mGluR4 agonist with simultaneous extracellular recording, to assess the effects of mGluR4 activation on the firing rates and patterns of striatal and pallidal neurons in parkinsonian monkeys. These experiments are detailed in Chapter 4 of this dissertation.

Together, these experiments enhance our knowledge of the anatomical localization, electrophysiological effects, and antiparkinsonian potential of three attractive non-dopaminergic drug targets currently under study for the treatment of PD.

## 1.3 The striatum: Main entry to the basal ganglia circuitry

The basal ganglia are a collection of interconnected subcortical nuclei that regulate voluntary movement. Among these nuclei are the striatum, the internal and external globus pallidus, the subthalamic nucleus, and the substantia nigra. The striatum is known as the main input nucleus of the basal ganglia circuit, as it receives a massive glutamatergic projection from the cortex, a glutamatergic input from the thalamus, as well as a significant dopaminergic projection from the substantia nigra pars compacta. Proper striatal function is integral for normal activity throughout the basal ganglia. For example, most of the pathophysiological changes that occur throughout the basal ganglia

circuitry in Parkinson's disease are caused, in part, by the depletion of striatal dopamine and the dysregulated striatal output activity. Additionally, many potential non-dopaminergic PD treatments are thought to regulate striatal activity, and for that reason, the striatum is the most studied structure in this dissertation.

### 1.3.1 Striatal medium spiny neurons

The striatum contains one main type of projection neuron which comprises approximately 70-90% of the total striatal neuronal population: the GABAergic medium spiny neurons (MSN). The dendrites of these neurons are covered with spines targeted by glutamatergic afferents from the cerebral cortex and thalamus. Dopaminergic inputs from the substantia nigra pars compacta (SNc), serotonin afferents from the dorsal raphe, as well as GABAergic and cholinergic inputs from interneurons and MSN axon collaterals represent the bulk of other inputs that impinge upon striatal MSNs. The corticostriatal projection is by far the main source of information to striatal MSNs.

Regardless of their location within the striatum, MSNs can be divided equally into two groups based on their distinct chemical phenotypes and projection targets. Direct pathway (GPi/SNr-projecting) MSNs preferentially express D1 dopamine receptors and the neuropeptides substance P and dynorphin, whereas indirect pathway (GPe-projecting) MSNs preferentially express D2 dopamine receptors, adenosine $A_{2A}$ receptors, and the neuropeptide enkephalin. The direct and indirect striatal output pathways are described in further detail below.

## 1.4 General basal ganglia circuitry

Glutamatergic projections from the cortex and thalamus enter the striatum and contact medium spiny projection neurons. Projections from sensorimotor cortical areas terminate in the posterior putamen, associative cortical inputs terminate in the anterior putamen and caudate nucleus, and limbic inputs terminate in the ventral striatum. From the striatum, segregated functional information is funneled to the basal ganglia output nuclei (the internal globus pallidus and the substantia nigra pars reticulata), which then forward basal ganglia outflow to the thalamus and brainstem. Thalamic output projections are then sent to the cerebral cortex or back to the striatum, through a series of functionally segregated basal ganglia-thalamocortical and basal ganglia-thalamostriatal circuits. (Figure 1.1; Wichmann and DeLong, 2003; Smith et al., 2004).

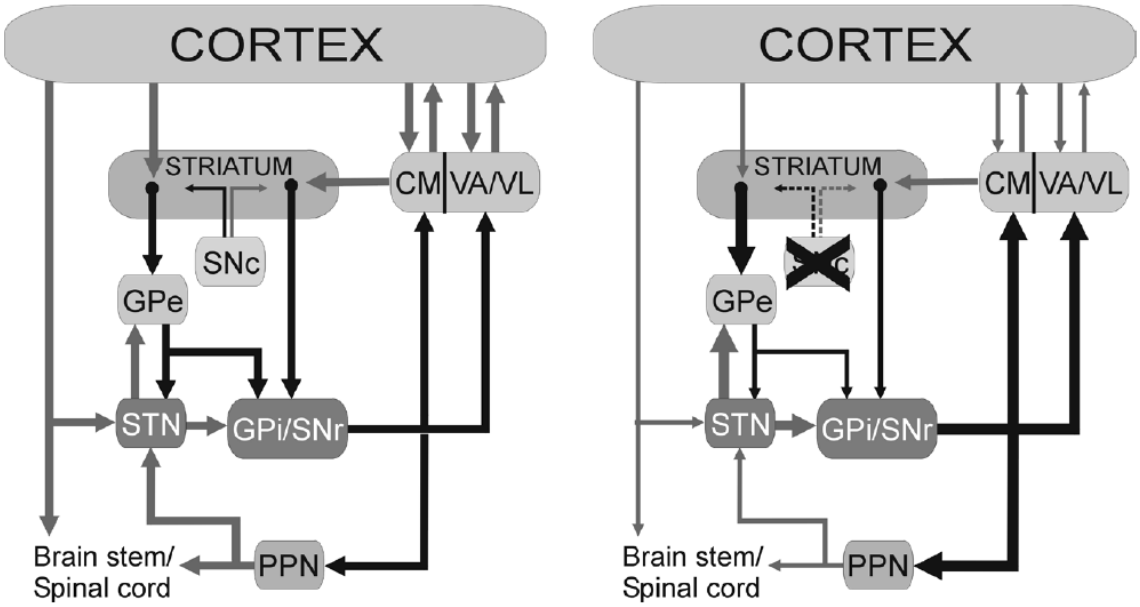


**Figure 1.1** – Simplified schematic diagram of the basal ganglia-thalamocortical circuitry under normal conditions (left) and rate changes in parkinsonism (right). Inhibitory connections are black, and excitatory connections are gray. Weight of arrows correlates to amount of neuronal activity. Figure from (Wichmann and DeLong, 2003).

## 1.5 Direct and indirect pathways

The direct and indirect pathways are the two major tracts through which information flows in the basal ganglia circuitry. The direct pathway received its name by virtue of the fact that it consists of a single projection from the striatum, known as the main basal ganglia input nucleus, directly to the internal globus pallidus and substantia nigra pars reticulata, the two basal ganglia output structures. This GABAergic projection gives rise to the majority of synaptic inputs on the dendrites of neurons in the output nuclei (Shink and Smith, 1995). This system runs in parallel with the "indirect pathway," which conveys information from the striatum to the output nuclei via relays in the external globus pallidus and the subthalamic nucleus.

In addition to their differential expression of neuropeptides and neurotransmitter receptors (see section 1.3.1), other subtle, though functionally important, differences exist in the physiology and morphology of direct and indirect pathway MSNs. D1-containing MSNs are less excitable than D2-containing MSNs, which is likely due to the larger dendritic area of D1-containing MSNs (Gertler et al., 2008). Additionally, indirect pathway MSNs seem to be more responsive to cortical inputs than direct pathway MSNs, as shown by their immediate-early gene expression following microstimulation or pharmacological disinhibition of the motor cortex (Berretta et al., 1997). Both direct and indirect pathway neurons provide significant GABAergic inputs to striatal cholinergic interneurons in primates (Gonzales et al., 2011)

Despite clear phenotypic and hodologic differences, the degree of segregation between the two groups of striatal MSNs may not be as clear-cut as originally thought. For example, the axonal projections of many direct pathway MSNs that arborize

extensively in the GPi and SNr also send axon collaterals to the GPe (Wu et al., 2000). Similarly, some indirect pathway MSNs that project preferentially to the GPe send axon collaterals to the GPi and SNr (Parent et al., 1995; Parent et al., 2000). Additionally, the complete segregation of D1 and D2 dopamine receptors between direct and indirect pathway MSNs has been a subject of debate due to the reported discovery of a certain percentage of striatal projection neurons expressing both receptor subtypes (Lester et al., 1993; Aizman et al., 2000). It is also important to note that direct and indirect pathway MSNs communicate with each other via local axon collaterals in the striatum; connections from D2- to D1-containing MSNs being more common than connections from D1- to D2-positive neurons (Taverna et al., 2008).

The classical view of the indirect pathway relies on the following connectivity network. Extrinsic information from the cerebral cortex and thalamus enters the basal ganglia circuits via the striatum, reaching D2 dopamine receptor-containing, GABAergic MSNs which send projections to the GPe. In turn, the GPe extends a massive GABAergic projection to the subthalamic nucleus, which then provides glutamatergic innervation of the basal ganglia output nuclei. Collateral projections of pallidosubthalamic axons that end in the GPi and SNr, without a relay in the STN, are also part of this system. The following discussion will pertain to the primate indirect pathway; subtle differences exist in rodents.

In nonhuman primates, four major types of GPe projection neurons have been characterized based on their projection targets. About half of all GPe neurons project to the STN and SNr, while the remaining half is split about evenly between neurons projecting to the STN & GPi; the STN, GPi, & SNr; or to the striatum (Sato et al.,

2000a). Several groups have shown that the GPe projections to the striatum originate from different neurons than those giving rise to projections to the STN, GPi or SNr (Bevan et al., 1998; Kita and Kitai, 1994). In rats, these pallidostriatal neurons display pre-pro-enkephalin mRNA (Hoover and Marshall, 1999) and fire with a different phase relationship to the STN (Mallet et al., 2012). Most GPe projection neurons also give rise to local axon collaterals that terminate on the cell bodies of other GPe neurons.

GPe projection neurons of the most prevalent type send axons that form a highly focused, dense field of terminals that innervate the whole extent of the somatodendritic domain of individual STN neurons. Axon collaterals from this projection descend into the SNr, where they form dense pericellular baskets around the somata of SNr output neurons. The next two types of GPe projection neuron follow a similar path, creating highly focused pericellular projections to GPi output neurons. These GPe projections are distributed in a highly specific and topographic fashion with respect to functional regions in the target structures. Axons from the subset of GPe neurons that send reciprocal connections to the striatum terminate in a widespread fashion throughout the structure, where they give rise to GABAergic terminals that preferentially target interneurons, at least in rodents (Bevan et al., 1998).

The final step in the indirect pathway is the glutamatergic projection from the STN to the output nuclei. These excitatory inputs from the indirect pathway converge with inhibitory terminals from the direct pathway at projection neurons of the output nuclei. Balanced activity between these opposing inputs modulates the basal ganglia outflow to thalamocortical neurons. Like other projections in the indirect pathway, STN projection neurons have axons that collateralize and terminate in multiple structures. In

addition to GPi and SNr, STN efferents contact the striatum, the substantia nigra pars compacta, the pedunculopontine nucleus, the spinal cord, and send reciprocal projections to the GPe. In nonhuman primates, the most common types of STN projection neurons are those collateralizing to both GPi and GPe (comprising about half), followed by neurons contacting GPe, GPi, and SNr (comprising about 20%), striatum only (~17%), and GPe only (~10%) (Sato et al., 2000b). The STN terminals have a similar morphology in all target nuclei and form asymmetric synapses with dendrites and perikarya. The STN projections to the output nuclei and GPe are highly topographic and functionally organized such that neurons related to the same functional modality remain connected through segregated loops. In addition to the striatum, the STN is another site of entry of extrinsic information into the basal ganglia circuitry, receiving direct inputs from the cerebral cortex (so-called the "hyperdirect pathway"), thalamus, and brainstem (Carpenter et al., 1981).

## 1.6 Basal ganglia disorders

Basal ganglia dysfunction is known to be associated with several disorders. Not surprisingly, most of these disorders have a prominent motor component. In this thesis, we will focus our discussion on PD, but many other neurodegenerative and neurochemical disorders of the basal ganglia have been recognized, including Huntington's disease, hemiballismus, dystonia, attention deficit hyperactivity disorder, Tourette's syndrome, and more. Many of these conditions are quite disabling, but none is as prevalent as PD.

PD is the second most common neurodegenerative disease, with 50,000 new diagnoses each year, in the United States alone (National Parkinson Foundation, 2011). With an aging population, this disease represents a highly relevant area of research. Its namesake, James Parkinson, first described the disorder in 1817, with his publication, *An Essay on the Shaking Palsy*. He described many of the motor hallmarks of the disease, which include resting tremor, muscle rigidity, akinesia, bradykinesia, hunched posture, and shuffling gait (Parkinson, 1817). The disease is also associated with several non-motor symptoms, including depression, cognitive impairment, dementia, and sleep disturbances. Examination of brain tissue from PD patients shows further hallmarks, including alpha-synuclein aggregates, formation of Lewy bodies, and most importantly, degeneration of the pigmented dopaminergic neurons in the substantia nigra, which project to the striatum (for review see Davie, 2008). While less studied, it has long been known that the neurodegeneration in PD extends beyond the dopaminergic system, affecting serotonergic and noradrenergic systems as well (Scatton et al., 1983; Jellinger, 1991)

The cause of human PD is not known, but it likely involves both genetic and environmental factors. Several specific mutations have been identified that can cause familial, heritable forms of PD (for review see Rochet et al., 2012), but these only account for a very small proportion of all PD cases. No cure exists for this disease, and potential preventative strategies are hampered by a lack of early biomarkers for the disease; a majority of dopaminergic neurons have already degenerated by the time motor symptoms arise. Only symptomatic treatments exist, and these have debilitating side effects (Smith et al., 2012).

### 1.6.1 Imbalanced activity of direct and indirect pathways in Parkinson's disease

Imbalanced activity between the indirect and direct striatofugal pathways is one of the key pathophysiological features of Parkinson's disease. In patients with PD, degeneration of the nigrostriatal dopaminergic projection oppositely changes the level of activity in "direct" vs. "indirect" striatal MSNs, due to their differential expression of dopamine receptors. D1-containing direct pathway neurons, which are normally excited by dopamine, decrease their activity, whereas D2-containing indirect pathway MSNs, normally inhibited by dopamine, display an increased activity in PD. The increased striatal GABAergic outflow to the GPe reduces inhibitory pallidal influences on the STN which, in turn, provides an increased glutamatergic drive to the output nuclei. Together with the decreased inhibition from the direct pathway, this increased glutamatergic drive from the STN leads to an overactive inhibitory basal ganglia outflow to thalamocortical neurons, thereby contributing to reduced motor cortex activity and inhibition of voluntary movements.

This scheme is commonly referred to as the "rate model" of Parkinson's disease, and it has been highly useful in understanding PD pathology. However, not all experimental observations agree with the rate model. For example, lesions of the thalamus or GPe do not cause parkinsonism, as would be predicted by the rate model (Canavan et al., 1989; Soares et al., 2004). It is now believed that changes in other aspects of basal ganglia activity, such as firing patterns (see next section), also play an important role in parkinsonian pathophysiology.

Morphological changes in direct and indirect pathway MSNs may also contribute to their pathological activity in parkinsonism. In human parkinsonians and animal

models of PD, the depletion of striatal dopamine is accompanied by a significant loss of striatal spines, the main recipient of glutamatergic and dopaminergic inputs in the striatum. Although some authors have suggested that this loss of spines is selective for D2-containing neurons in rodents (Day et al., 2006), these observations have not been confirmed in the nonhuman primate model of parkinsonism nor patients with PD (Villalba et al., 2009).

### 1.6.2 Firing pattern abnormalities in Parkinson's disease

Alterations in firing rates among various nuclei, as discussed above, are not the only important abnormalities in basal ganglia activity in Parkinson's disease. Aberrant firing patterns also seem to play an important role in basal ganglia pathophysiology. Abnormal oscillations in neuronal firing have been identified in the STN, GPi, and SNr in animal models, as well as in PD patients (See Brown, 2007 for review). These oscillations have a characteristic frequency in the β range (10-30 Hz), and they disappear with antiparkinsonian medication or high frequency stimulation of the STN (Kühn et al., 2006; Wingeier et al., 2006).

Abnormal neuronal synchrony has also been observed in the parkinsonian basal ganglia. The basal ganglia circuitry is organized in functionally segregated loops, and this segregation is maintained at the cellular level, such that neighboring neurons often fire independently from each other. Under parkinsonian conditions, neuronal firing becomes widely synchronized across many basal ganglia neurons, likely disrupting the proper flow of information and the encoded functional specificity (for review see Hammond et al., 2007).

In addition, increases in burst firing have been described in the parkinsonian basal ganglia, especially in the pallidum and STN (Bergman et al., 1994; Wichmann et al., 1999; Soares et al., 2004). After dopamine depletion, burst firing becomes more frequent, and bursts become longer, both in PD patients and animal models (Hutchison et al., 1994; Magnin et al., 2000; Wichmann and Soares, 2006).

## 1.7 Animal models of Parkinson's disease

### 1.7.1 Acute and reversible models of PD

There are two pharmacological agents that are commonly used to achieve temporary parkinsonism in rodents: reserpine and haloperidol. Reserpine is an irreversible blocker of the vesicular monoamine transporter (VMAT), which is required for packaging of the monoamines including dopamine, serotonin, and norepinephrine into synaptic vesicles (Henry and Scherman, 1989). Once the existing pool of synaptic vesicles is exhausted, animals enter a state of catalepsy caused by the lack of dopamine release. The effects of reserpine can last for days, as new VMATs must be synthesized to replace those that were irreversibly blocked. Animals with reserpine-induced catalepsy can be used to test the efficacy of potential antiparkinsonian drugs; this model was instrumental in the discovery of the antiparkinsonian effects of levodopa (Carlsson et al., 1957). The fact that reserpine affects monoamine systems other than dopamine was originally viewed as a weakness, but after the realization that serotonergic and noradrenergic systems are affected in PD (Scatton et al., 1983; Jellinger, 1991), the validity of this model was reinforced.

Haloperidol is a long-acting antagonist of dopamine receptors that was originally used as an antipsychotic medication (Granger and Albu, 2005). When injected into rodents, the resulting blockade of dopaminergic transmission causes the animal to enter a rigid, cataleptic state, which can be reversed by antiparkinsonian drugs (Sanberg, 1980). While catalepsy is not exactly a symptom of PD, this condition is likened to the rigidy and inability to initiate movement that is associated with the disease.

Both of these models have similar benefits and drawbacks for modeling PD. They represent easy and inexpensive methods of generating an acute animal model of PD. They also may be considered more humane options compared to other models of PD, due to their temporary nature. However, the transient nature of dopamine depletion in these models means they cannot be used in studies requiring chronic parkinsonism. Also, these models are useless for studying the degenerative process of Parkinson's disease, or potential neuroprotective treatments, as little to no neurodegeneration occurs, along with all of the neuroanatomical and neurochemical changes that follow.

### 1.7.2 The 6-hydroxydopamine (OHDA)-treated rat model of Parkinson's disease

6-hydroxydopamine (6-OHDA) treatment of rats can be used to generate what is probably one of the most reliable, toxin-based rodent models of PD. This toxin is selectively taken up into dopaminergic and noradrenergic (can be prevented with the norepinephrine transporter blocker desipramine) neurons, which it kills through mitochondrial respiratory dysfunction and oxidative stress. When injected in the medial forebrain bundle or in the substantia nigra, 6-OHDA induces a loss of nigrostriatal dopaminergic neurons and leads to behavioral motor signs resembling those seen in

parkinsonism. This model has been used to test the efficacy of antiparkinsonian compounds, as well as to test potential neuroprotective treatments.

However, this model also has drawbacks. First, it is a relatively difficult model to achieve. As 6-OHDA does not cross the blood-brain barrier, it must be stereotactically injected into either the medial forebrain bundle or the substantia nigra itself, which are small targets. Dopaminergic lesions caused by 6-OHDA are often quite severe, so they are usually only induced unilaterally in order to avoid mortality. However, partial bilateral lesions have been generated by injection of the toxin directly into the dorsolateral striata (Amalric et al., 1995).

### 1.7.3 The MPTP-treated monkey model of Parkinson's disease

The MPTP-treated monkey model of PD, used in this dissertation, is considered the gold-standard animal model of PD for several reasons. First, monkeys are evolutionarily very closely related to humans, and they have very similar anatomy and physiology. This means that the validity of studying human diseases in these monkeys is improved, as compared with other commonly studied species, like rodents. Compared to human PD patients, MPTP-treated monkeys display very similar motor symptoms, show some of the non-motor symptoms (McDowell and Chesselet, 2012), undergo nearly identical cellular damage in the midbrain, and respond to antiparkinsonian drugs in a very similar manner, including the progressive development of motor side-effects. The basal ganglia circuit of the MPTP-treated monkey also shows many of the pathophysiological changes that occur in PD patients, such as altered firing rates and patterns, increased oscillatory activity, and aberrant neuronal synchrony (Nini et al., 1995; Raz et al., 2000; Wichmann and Delong, 2003; Meissner et al., 2005; Leblois et al., 2007). MPTP has

also been extensively used to induce midbrain dopaminergic neurodegeneration in mice. This model of PD has been helpful in understanding the neurodegenerative process, but behavioral parkinsonism in these animals is hard to observe (see Bové and Perier, 2012 for review).

The main drawback for MPTP is its danger to humans. It can enter the system trans-cutaneously or through inhalation of vapors, and causes degeneration of dopaminergic neurons in humans (Przedborski et al., 2001). Another drawback is that this model does not necessarily reproduce the slow development of PD. While the MPTP model is better than most in this respect (it can be given in low doses over long periods of time to slowly generate a dopaminergic lesion), human PD develops over a period of several years, which is not a practical time period for generating experimental animals. The following sections describe the discovery and mechanism of action of this neurotoxin.

*1.7.3.1 The discovery of MPTP*

MPTP was first synthesized in the 1940s in a search for novel analgesic drugs (Lee et al., 1947). However, the toxic nature of the molecule would not be recognized for many years, even though it was commonly used as a chemical intermediate in the synthesis of other molecules. In fact, in a case of true irony, the compound was even tested as a potential treatment for PD (Langston and Palfremann, 1995).

The compound's toxicity was nearly discovered in the late 1970s when a chemistry graduate student in Maryland botched the synthesis of a meperidine (Demerol) analog, producing MPTP as a major byproduct. He injected the resulting mixture of chemicals and rapidly developed severe parkinsonism, which was treated successfully

with levodopa. Investigators found MPTP, along with several other chemicals, in the man's lab, but they were unable to identify it as the agent responsible for his parkinsonism. When the man died 18 months later from cocaine overdose, autopsy showed that he had damage to the dopaminergic cells of the substantia nigra (Davis et al., 1979).

It wasn't until the early '80s that the full potential of MPTP was discovered. In 1982, a chemist in northern California again botched the synthesis of a meperidine analog and distributed the product. Over the following weeks, hospitals in the area saw an outbreak of cases of rapid-onset, advanced Parkinson's disease in young drug users. Analysis of the patients' leftover drugs revealed that MPTP was present. Shortly thereafter, scientist Bill Langston showed that when given to monkeys, MPTP induces behavioral symptoms that closely resemble human parkinsonism, which could be treated with levodopa. At the pathological level, MPTP induced the death of the same midbrain dopaminergic neurons that die in PD (Langston et al., 1984). This series of events, which led to the birth of the gold-standard animal model of PD, is an interesting example of a rather unfortunate situation serendipitously leading to a discovery that has greatly advanced our understanding of a crippling disease.

*1.7.3.2 Mechanism of action of MPTP*

MPTP itself is actually not toxic, but its lipophilic properties allow it to cross the blood-brain barrier. Once in brain, the chemical is converted into its active (toxic) metabolite 1-methyl-4-phenylpyridinium (MPP+) in astrocytes by monoamine oxidase B. MPP+ has affinity for the dopamine transporter, through which it is selectively taken up into dopaminergic terminals in the striatum, where it interferes with complex I of the

electron transport chain inside of mitochondria. This leads to free-radical production and ultimately death of the cell. MPTP intoxication is also known to cause damage to the other monoaminergic systems, including serotonergic and noradrenergic cells (Nayyar et al., 2009; Ansah et al., 2011; Masilamoni et al., 2011), as is seen in PD (Scatton et al., 1983; Jellinger, 1991).

## 1.8 Dopamine replacement therapy in PD

Remarkably, since the discovery half a century ago that L-DOPA administration can alleviate the symptoms of parkinsonism, dopamine replacement therapy remains the gold-standard pharmacotherapy for Parkinson's disease, despite the unfortunate fact that this treatment strategy often causes debilitating side effects. Common dopamine replacement therapies, such as the dopamine precursor levodopa and direct dopamine receptor agonists, can cause motor side effects, such as abnormal involuntary movements (dyskinesias) and "wearing off" of motor benefit, as well as non-motor side effects including hallucinations, sleep disturbances, psychosis, and compulsive behaviors (Smith et al., 2012).

Research has suggested that the non-physiological, pulsatory delivery of oral dopaminergic agents contributes to the development of motor side effects (Olanow et al., 2006; Antonini and Odin, 2009). As a result, several treatment strategies have been tested to deliver more constant levels of dopamine replacement. Dopamine receptor agonists with very long biological half-lives, such as cabergoline, have been used to this effect (Bracco et al., 2004), but like other dopamine agonist treatments, the efficacy declines as the disease progresses, and levodopa treatment is often eventually needed.

Strategies to constantly deliver shorter-acting dopaminergic agents via alternative routes, such as intra-intestinal or subcutaneous administration (Hughes et al., 1993; Annic et al., 2009; Westin et al., 2011), have seen some success. However, these methods are invasive, and complications with cannula displacement and inflammation at infusion sites are a problem.

Another interesting but invasive dopamine replacement strategy involves inducing cellular dopamine production in the striatum. This can be achieved by several means, including transplantation of extrinsic cells or gene therapy. Intrastriatal transplantation of grafts of human embryonic dopaminergic neurons has been tested in multiple studies (Freed et al., 2001; Brundin et al., 2010). Unfortunately, the efficacy of this treatment was found to be negligible, and in some patients the grafts induced drug-independent dyskinesias (Olanow et al., 2003). A second approach, which has yet to reach the point of testing in humans, is to transplant stem cells, destined to become dopaminergic cells, into the striatum (Hargus et al., 2010). This strategy carries major safety concerns, as the desired cellular differentiation isn't always guaranteed, and stem cells have the potential to proliferate in the brain, inducing tumor formation. A third method, which does not involve cellular transplantation, is to use gene therapy by means of viral vector-mediated delivery of genetic material encoding enzymes necessary for the production of dopamine or L-DOPA into intrinsic striatal cells (Christine et al., 2009; Jarraya et al., 2009). Clinical trials testing these treatments are underway, but there is some uncertainty about how striatal neurons might release dopamine, as they do not express the vesicular monoamine transporter, which is required for packaging of dopamine into synaptic vesicles. As such, there is concern that buildup of cytosolic dopamine in transfected

striatal neurons could lead to oxidative stress or even death of these cells (Chen et al., 2008). All three of the above-mentioned cellular therapies carry the double-edged sword of their irreversibility. While any observed antiparkinsonian benefit has the potential to be permanent and medication-independent, the same applies to any unwanted side effects.

In summary, while many improvements have been made to dopamine replacement therapy over the years, many of the resulting treatments have serious drawbacks, and the development of dyskinesia is often a persistent problem. For this reason, research into non-dopaminergic PD therapies remains a relevant and active field of study.

## 1.9 Non-dopaminergic antiparkinsonian drug targets

Surely the best way to avoid dyskinesias and other debilitating dopaminergic side effects is to simply avoid the use of dopaminergic drugs. Unfortunately, after decades of research, no non-dopaminergic pharmacotherapy has been discovered that is able to match the efficacy of dopamine replacement drugs. However, the search for non-dopaminergic treatments is an active field of research, and several targets for potential antiparkinsonian agents have been identified, some of which have promise. Furthermore, a compound does not necessarily need to be as efficacious as levodopa in order to be valuable. If a newly discovered drug could do so much as to potentiate the effect of dopaminergic agents, it would be highly useful as an adjunct treatment. Such an adjunct could allow for a reduction in the required dosage of dopaminergic agents and thereby decrease, delay, or maybe even prevent the development of dopaminergic side effects.

Additionally, when they are combined, different non-dopaminergic treatments may be able to enhance the efficacy of one another. Some of the non-dopaminergic targets that have received significant consideration are now discussed.

### 1.9.1 Cholinergic receptors

Anticholinergic agents were the very first pharmacotherapy for PD, dating all the way back to the use of herbal alkaloids in the 1800s. In fact, this class of drugs was essentially the only pharmacotherapy available for PD until the advent of dopamine replacement therapy in the 1960s. Interestingly, after over a century of use, the antiparkinsonian mechanism of action of these drugs is not completely understood. However, it is apparent that anticholinergic agents are more effective at treating tremor than the other motor symptoms of PD (Koller, 1986). Nowadays, this class of drug is rarely used to treat PD, mostly due to a myriad of adverse side effects, including confusion, cognitive impairment, constipation, and blurred vision. Additionally, anticholinergics are poorly tolerated in elderly patients (Feinberg, 1993), so the best candidates for anticholinergic therapy are young patients with problematic tremor. As a rare example of a beneficial side effect, anticholinergic agents can treat drooling, which is sometimes seen in PD, due to their peripheral activity as antisialagogues (Hyson et al., 2002). Recent research into new anticholinergic drugs that act selectively at specific subtypes of cholinergic receptors (Conn et al., 2009; Weaver et al., 2009; Digby et al., 2010) may be able to provide tremorolytic benefit with fewer peripheral side effects.

### 1.9.2 Glutamate receptors

The discoveries of overactive glutamatergic transmission at corticostriatal and subthalamofugal synapses (Fig. 1.1) have generated much interest in anti-glutamatergic

agents as potential therapeutics for PD. The main idea behind these treatments is to return the parkinsonian basal ganglia to a more normal state of activity by modulating glutamate (and sometimes GABA) transmission which has been altered by dopamine depletion. There are two major classes of glutamate receptors: ionotropic and metabotropic receptors. Potential treatments targeting both of these classes of glutamate receptor are discussed below.

*1.9.2.1 Ionotropic glutamate receptors*

Antagonists of ionotropic receptors were among the first anti-glutamatergic treatments to be tested, but serious non-motor side effects and poor efficacy have prevented most of these from being useful in humans (for review see Smith et al., 2012). Glutamate is the most abundant neurotransmitter in the brain, and ionotropic glutamate receptors are central to normal fast excitatory neurotransmission throughout the nervous system (Blandini and Greenamyre, 1998). Thus, it is not hard to imagine that blocking these receptors would cause far-reaching effects, well beyond modulation of the basal ganglia circuitry. Ionotropic glutamate receptors are classified into three subtypes, named for the agonists which aided in their discovery: α-amino-3-hydroxy-5-methyl-4-isoxazole-propionic acid (AMPA) receptors, kainate receptors, and N-methyl-D-aspartate (NMDA) receptors.

Preclinical investigation of the antiparkinsonian effects of AMPA receptor antagonists have yielded encouraging results in rat and monkey models of PD (Klockgether et al., 1991; Loschmann et al., 1992; Wachtel et al., 1992), but human studies were not so successful. Two studies of the AMPA receptor antagonist peramapanel found its antiparkinsonian effects to be no different than placebo (Eggert et

al., 2010; Lees et al., 2012). Other trials of the AMPA receptor antagonists talampanel and topiramate were terminated before completion, due to lack of efficacy.

Various NMDA receptor antagonists have been tested for antiparkinsonian effects in different animal models of PD (for review see (Johnson et al., 2009)), with varying degrees of success. Nonetheless, only one NMDA receptor antagonist, amantadine, has been approved for use in PD patients. Clinical trials with amantadine have shown that it attenuates levodopa-induced dyskinesias and motor fluctuations (Verhagen Metman et al., 1998), and may delay the onset of dementia (Inzelberg et al., 2006). Then again, amantadine also has anticholinergic effects (Warnick et al., 1982; Matsubayashi et al., 1997), so it isn't entirely clear if these effects are solely due to inhibition of NMDA receptors. Serious side effects of NMDA inhibitors, such as hallucinations, confusion, agitation, nightmares, catatonia, ataxia, and deficits in learning and memory raise questions about the usefulness of this class of drugs in humans. However, recent research into antagonists selective for the NR2B subunit of NMDA, which is enriched in striatal MSNs (Landwehrmeyer et al., 1995), may be able to treat PD with fewer side effects. Still, clinical trials with NR2B-selective agents have shown they can attenuate dyskinesias (Nutt et al., 2008), but do not confer any significant antiparkinsonian benefit (Montastruc et al., 1992; Addy et al., 2009).

Antagonists of AMPA and NMDA receptors also represent a good example of a potential non-dopaminergic combination treatment in PD, as they show synergy in their anti-dyskinetic effects when combined, in 6-OHDA-treated rats and MPTP-treated monkeys (Bibbiani et al., 2005; Kobylecki et al., 2011). Additionally, the

antiparkinsonian effect of NMDA antagonist can be potentiated by combination with an antagonist of metabotropic glutamate receptor 5 (Turle-Lorenzo et al., 2005).

*1.9.2.2 Metabotropic glutamate receptors*

Metabotropic glutamate receptors are divided into three major groups, comprised of eight different subtypes, based on their structure, pharmacology, and coupling to second messenger systems. Group I mGluRs include mGluR1 and mGluR5, which are coupled to the $G_q$ second messenger system that stimulates neurons through phospholipase C activation and release of calcium from internal stores. Group II mGluRs (mGluR2 and mGluR3), as well as group III mGluRs (mGluR4, mGluR6, mGluR7, and mGluR8) are coupled to the $G_i$ second messenger system, which inhibits neuronal activity through inhibition of adenylyl cyclase.

Metabotropic glutamate receptors are better targets for modulation of glutamatergic transmission than ionotropic receptors for several reasons (Niswender and Conn, 2010). First, they have slower, more modulatory effects on cellular excitability than do ionotropic receptors. Think of ionotropic receptors as a standard light switch and metabotropic receptors as a dimmer switch. This property allows neuronal excitability to be more subtly modulated, and any effects outside of the desired brain structure will likely be gentler. Second, mGluRs have more restricted patterns of localization in the brain than do ionotropic receptors. For example, whereas AMPA and NMDA receptors are found at high levels throughout the brain (Wenzel et al., 1997; Beneyto and Meador-Woodruff, 2004), mGluR5 expression is more heavily concentrated in the striatum and hippocampus than other structures (Shigemoto et al., 1993; Testa et al., 1994). Because research has generated selective compounds for many of the specific mGluR subtypes,

glutamatergic transmission can be modulated more selectively within the structures that are enriched in specific mGluR subtypes, minimizing off-target effects.

mGluR4 and mGluR5 in particular have garnered much attention as potential therapeutic targets for PD. These two receptors are the subject of research described in Chapters 2, 3, and 4 of this dissertation, and both are introduced below.

1.9.2.2.1 mGluR4

The metabotropic glutamate receptor 4 is a group III mGluR, which is generally found in axon terminals, where it inhibits neurotransmitter release. This receptor is expressed in many brain areas, but is particularly enriched in the rat striatum, globus pallidus (GP), entopeduncular nucleus, and SNr; the origin and major targets of striatal MSNs. At the EM level, mGluR4 is located in putative GABAergic axon terminals in the rat GP and SNr, as well as in pre- and postsynaptic structures in the striatum (Bradley et al., 1999; Corti et al., 2002), supporting strong expression of the receptor in striatal MSNs. Within the rat striatum, mGluR4 is located in inhibitory terminals, as well as in putative glutamatergic terminals (Corti et al., 2002), which likely originate in the cortex. Whether this pattern of localization holds true in primates was unknown, until publication of the research in chapter 4 of this dissertation confirmed that it does. These anatomical findings highlight two specific locations whereby activation of the inhibitory mGluR4 might be useful in normalizing neural activity in the parkinsonian basal ganglia: the striatopallidal terminals and corticostriatal terminals, both of which are thought to be overactive in the parkinsonian state.

Indeed, electrophysiological data support the feasibility of mGluR4-mediated modulation of striatopallidal and corticostriatal transmission. Recordings in rat GP slices

have shown that activation of mGluR4 can attenuate inhibitory postsynaptic currents induced by striatal stimulation (Matsui and Kita, 2003; Valenti et al., 2003; Beurrier et al., 2009). Furthermore, group III mGluR activation in rat striatal slices attenuates both excitatory and inhibitory postsynaptic potentials (Cuomo et al., 2009), in agreement with anatomical data showing the receptor in both types of terminal. The electrophysiological responses of primate striatal and pallidal neurons to local group III or selective mGluR4 activation was unknown, until described in chapter 4 of this dissertation.

Behavioral experiments also strengthen the idea that mGluR4 activation has potential as an antiparkinsonian treatment strategy. Intrapallidal, intrastriatal, intracerebroventricular, or systemic infusion of group III or mGluR4 agonists alleviates parkinsonism in rat models of PD (Marino et al., 2003; Valenti et al., 2003; MacInnes et al., 2004; Marino et al., 2005; Konieczny et al., 2007; Lopez et al., 2007; Beurrier et al., 2009; Cuomo et al., 2009). The behavioral effects of mGluR4 activation in primates remain unknown, but the development of mGluR4 allosteric potentiators with favorable pharmacokinetic properties and efficient brain penetration has laid the foundation for trials of mGluR4-active PD pharmacotherapeutics (Niswender and Conn, 2010; Engers et al., 2011; Smith et al., 2012).

1.9.2.2.2 mGluR5

The metabotropic glutamate receptor 5 is a group I mGluR, which is commonly found in postsynaptic elements, where it mediates slow excitatory effects in response to glutamate. This receptor is expressed throughout the brain, but it is most enriched in the striatum and hippocampus (Shigemoto et al., 1993; Testa et al., 1994). At the EM level, mGluR5 is located postsynaptically in neurons of multiple basal ganglia nuclei (Hanson

and Smith, 1999; Paquet and Smith, 2003; Hubert and Smith, 2004), putting it in ideal position to regulate glutamatergic transmission throughout the circuit, most pertinently at corticostriatal and subthalamofugal synapses, which are overactive in parkinsonism.

Antagonists of mGluR5 have been tested for antiparkinsonian effects in several behavioral studies, having the most success in rodent, rather than monkey models of PD. Blockade of mGluR5 has been shown to alleviate parkinsonian motor signs in 6-OHDA-lesioned rats (Breysse et al., 2002; Breysse et al., 2003), haloperidol-treated rats (Spooren et al., 2000; Ossowska et al., 2002; Ossowska et al., 2005; Dekundy et al., 2006), and reserpine-treated mice (Kachroo et al., 2005). Evidence from one of these studies suggests the antagonist treatment is more effective after chronic administration (Breysse et al., 2002). Despite all of these positive findings in rodents, essentially all subsequent studies in primates have found that mGluR5 antagonists have no significant antiparkinsonian benefit (Morin et al., 2010; Rylander et al., 2010; Berg et al., 2011; Gregoire et al., 2011), or that they even decrease the effectiveness of levodopa (Johnston et al., 2010). However, all of these primate studies were also designed to test the anti-dyskinetic properties of mGluR5, and as such, they used monkeys (or humans) with relatively severe nigrostriatal dopaminergic lesions that had also undergone the neurological changes underlying chronic levodopa treatment and dyskinesia development. The development of dyskinesia is known to be associated with abnormal basal ganglia glutamatergic transmission (Picconi et al., 2002; Calon et al., 2003; Picconi et al., 2003; Picconi et al., 2004; Robelet et al., 2004) and alterations in striatal mGluR5 expression (Samadi et al., 2008; Ouattara et al., 2010; Ouattara et al., 2011). In chapter 2 of this dissertation, we have revisited this issue and shown that mGluR5 antagonist can

potentiate the antiparkinsonian effect of a D2LR agonist in moderately MPTP-lesioned, dopaminergic drug-naïve monkeys.

As mentioned above, mGluR5 has also received much attention as a possible anti-dyskinetic target. Several studies have shown the anti-dyskinetic effects of mGluR5 antagonism in parkinsonian rodents (Dekundy et al., 2006; Mela et al., 2007; Gravius et al., 2008; Levandis et al., 2008; Rylander et al., 2009; Yamamoto and Soghomonian, 2009), monkeys (Johnston et al., 2010; Morin et al., 2010; Rylander et al., 2010; Gregoire et al., 2011), and humans (Berg et al., 2011). In addition, mGluR5 antagonism has been shown to protect dopaminergic, noradrenergic, and serotonergic neurons against MPTP- or 6-OHDA-induced degeneration in monkey and rodent models of PD (Battaglia et al., 2004; Aguirre et al., 2005; Armentero et al., 2006; Vernon et al., 2007; Masilamoni et al., 2011; Hsieh et al., 2012). With antiparkinsonian, anti-dyskinetic, and neuroprotective properties, mGluR5 has good potential as a non-dopaminergic target for future PD pharmacotherapeutics.

### 1.9.3 Adenosine $A_{2A}$ receptors

The adenosine $A_{2A}$ receptor is a metabotropic receptor coupled to the $G_s$ second messenger system, which excites neurons via activation of adenylyl cyclase. Multiple studies using various methods have described high levels of $A_{2A}R$ expression in the striatum and external globus pallidus, with lower levels elsewhere in the brain (Martinez-Mir et al., 1991; Schiffmann et al., 1991b; Dixon et al., 1996; Peterfreund et al., 1996; Svenningsson et al., 1997; Rosin et al., 1998; Svenningsson et al., 1998; Kaelin-Lang et al., 2000; Calon et al., 2004). An EM study in rats showed that $A_{2A}R$ is located mainly in dendrites and spines as well as putative glutamatergic and GABAergic terminals in the

striatum (Hettinger et al., 2001). Research described in chapter 2 of this dissertation showed a similar pattern of $A_{2A}R$ localization in the monkey striatum.

Research into $A_{2A}R$ accelerated rapidly when it was discovered that the receptor was expressed selectively in indirect pathway striatal MSNs, and not in direct pathway MSNs (Schiffmann et al., 1991a; Fink et al., 1992; Schiffmann and Vanderhaeghen, 1993; Augood and Emson, 1994; Svenningsson et al., 1998; Quiroz et al., 2009). This selective localization offered an attractive strategy to normalize the imbalance of activity between the two striatal output pathways. Specifically, antagonism of $A_{2A}R$ could decrease the excitability of the overactive indirect pathway striatal MSNs without further inhibiting the underactive direct pathway neurons.

As hypothesized, behavioral experiments showed that $A_{2A}R$ antagonists have antiparkinsonian effects in multiple animal models of PD, including 6-OHDA-treated rats (Morelli and Pinna, 2001; Coccurello et al., 2004; Pinna et al., 2007), reserpine-treated mice (Kanda et al., 1994; Tanganelli et al., 2004), and MPTP-treated monkeys (Grondin et al., 1999; Kanda et al., 2000; Bibbiani et al., 2003; Hodgson et al., 2010). Despite success in preclinical research, $A_{2A}R$ antagonists have not been as effective in human trials. However, trials of istradefylline, the first $A_{2A}R$ antagonist to go to clinical trial, as an adjunct to dopaminergic therapy showed that the drug provides small, but significant, beneficial effects, which were long-lasting (Factor et al., 2010), such as increasing "on time" by about an hour, while decreasing "off time" by a similar amount (Hauser et al., 2003; LeWitt et al., 2008; Stacy et al., 2008). On the other hand, istradefylline was rarely reported to improve parkinsonian severity (Bara-Jimenez et al., 2003) and actually was found to slightly increase dyskinesia in one trial (Hauser et al., 2003). When used as a

monotherapy, the effects of istradefylline did not differ from placebo (Fernandez et al., 2010). Due to disappointing efficacy and reports of increased dyskinesia, the drug was not approved by the FDA to treat PD. A newer $A_{2A}R$ antagonist with better pharmacologic properties (Hodgson et al., 2009), preladenant, also produced marginal benefits in PD patients, decreasing "off time" by a small amount (Hauser et al., 2011). In light of these modest effects in PD patients, perhaps combining an $A_{2A}R$ antagonist with a second non-dopaminergic drug, like an mGluR5 antagonist, is the key to achieving better antiparkinsonian efficacy. Because $A_{2A}R$, mGluR5 and D2 dopamine receptors display important physical and functional interactions in the striatum (see below), combination therapies that could take advantage of these interactions may have some benefit in PD.

### 1.9.4 mGluR5-$D_2R$-$A_{2A}R$ interactions

The mGluR5, $D_2R$, and $A_{2A}R$ are all expressed at high levels in the dendrites and spines of striatal indirect pathway MSNs. Early experiments using co-immunodetection, co-immunoprecipitation, and resonance energy transfer techniques showed physical interactions between $A_{2A}R$ and $D_2R$ (Canals et al., 2003; Ciruela et al., 2004), and $A_{2A}R$ and mGluR5 (Ferre et al., 2002) in transfected HEK cells and striatal neurons. A more recent study eloquently used a combination of bioluminescence and fluorescence resonance energy transfer to directly show mGluR5-$D_2R$-$A_{2A}R$ heterotrimers in living cells (Cabello et al., 2009). This study also showed that all three receptors co-immunoprecipitate from rat striatal membrane preparations.

The physical interaction between these three receptors conveys interesting functional properties with important implications for striatal indirect pathway MSN

function. Namely, activation of mGluR5 or $A_{2A}R$ decreases the affinity of $D_2R$ for agonists, and simultaneous activation of mGluR5 and $A_{2A}R$ synergistically potentiates this effect (Ferre et al., 1999; Popoli et al., 2001). Thus, upon antagonism of mGluR5 and $A_{2A}R$, indirect pathway MSN excitability would not only be decreased through inhibition of excitatory glutamate and adenosine signaling, but also through an increase in activation of inhibitory $D_2Rs$.

This interaction has biochemical (Ferre et al., 2002; Nishi et al., 2003) and behavioral relevance. Combined antagonism of $A_{2A}R$ and mGluR5 results in potentiation of the ability of these molecules to counteract parkinsonism in rodent models of PD (Coccurello et al., 2004; Kachroo et al., 2005) and alcohol self-administration in rodent models of alcoholism (Adams et al., 2008). The synergy between $A_{2A}R$ and mGluR5 antagonists in their ability to counteract parkinsonism has never been tested in primates. While $A_{2A}R$ and mGluR5 antagonists each provide small, but significant, antiparkinsonian effects, taking advantage of the synergy between these two receptors and $D_2R$ may be the key to development of effective non-dopaminergic adjunct treatments for PD. Combined $A_{2A}R$/mGluR5 antagonism with D2LR agonism surely warrants future investigation.

## 1.10 Research Summary

mGluR4, mGluR5, and $A_{2A}R$ all show promise as potential targets for non-dopaminergic antiparkinsonian drugs. Compounds acting at these receptors may be able to potentiate the effect of dopamine replacement therapy, thereby possibly decreasing

dosing and side effects of dopaminergic agents. Additionally, by combining drugs and taking advantage of receptor interactions among mGluR5, $A_{2A}R$, and $D_2R$, the efficacy of these treatments may be enhanced. In order to further advance knowledge in the development of new non-dopaminergic therapies in parkinsonism, the work presented in this thesis achieves the following specific aims:

**1.10.1 Specific Aim 1:** To examine the antiparkinsonian effects of combined dopamine D2-like receptor (D2LR) agonism/metabotropic glutamate receptor 5 antagonism in MPTP-treated monkeys.

D2LR agonists are a good frontline therapy for PD, but their efficacy decreases with chronic treatment, and side effects eventually appear. Due to receptor-receptor interactions in the striatum, the use of mGluR5 antagonist as an adjunct to D2LR agonist represents an interesting strategy to improve antiparkinsonian efficacy and decrease the dosage of dopaminergic agent required for motor benefits, potentially decreasing or delaying side effects. Through the use of a rating scale of parkinsonian motor symptoms and quantitative methods to assess the amount of body part movements and eye blinks, as well as an infrared beam breaks, our behavioral studies examine the ability of the mGluR5 antagonist MTEP to potentiate the antiparkinsonian effects of low doses of the D2LR agonist pramipexole. This research is described in Chapter 2.

**1.10.2 Specific Aim 2:** To characterize adenosine $A_{2A}$ receptor localization and co-localization with metabotropic glutamate receptor 5 at the ultrastructural level in the monkey basal ganglia.

As discussed above, $A_{2A}R$ is another attractive target for novel non-dopaminergic antiparkinsonian drugs. Knowing the subcellular/ultrastructural localization of $A_{2A}R$ in

the monkey basal ganglia would lay the foundation for a deeper understanding of the receptor's function, physiological properties, and mechanisms of activation in primates. Thus, in order to address this issue, we have used immunoperoxidase and immunogold labeling for $A_{2A}R$, combined with electron microscopy, to characterize the receptor's subcellular and subsynaptic localization in the monkey striatum, GPe, and SNr.

Combined $A_{2A}R$/mGluR5 antagonism with D2LR agonism represents an intriguing strategy to improve the efficacy, and possibly reduce the unwanted side effects, of these potential antiparkinsonian agents, by taking advantage of the three receptors' physical interactions and functional synergy. Examining the colocalization between $A_{2A}R$ and mGluR5 would provide valuable information on anatomical sites for possible interactions between the receptors in primates. Thus, we have used immunoperoxidase/immunogold double-labeling in combination with electron microscopy to determine the degree and subcellular sites of co-localization between $A_{2A}R$ and mGluR5 in the monkey striatum. This research is described in Chapter 3.

**1.10.3 Specific Aim 3:** To characterize the subcellular localization of metabotropic glutamate receptor 4, and examine the electrophysiological effects of local infusion of group III or mGluR4 agonists on firing rates and patterns of neurons in the MPTP-treated monkey GPe and putamen.

Evidence in rodents suggests that activation of mGluR4 represents another promising non-dopaminergic antiparkinsonian therapy and that mGluR4 agonists may exert antiparkinsonian effects by modulating glutamatergic and/or GABAergic transmission in the striatum or pallidum. However, the efficacy of these drugs is unknown in primate models of PD. As a first step towards the development of such

therapeutic assays, knowing the anatomical localization of mGluR4 and the electrophysiological effects of mGluR4 agonists in the monkey striatopallidal complex would provide valuable information about their mechanism of action and potential as an antiparkinsonian treatment in primates. Thus, in order to fill this knowledge gap, we examined the subcellular localization of mGluR4 in the striatum and GPe, using immunoperoxidase labeling with electron microscopy. Furthermore, in order to examine how mGluR4 activation affects the firing rates and patterns of striatal and pallidal neurons, we performed local injections of Group III agonist or selective mGluR4 allosteric potentiator, with simultaneous extracellular recordings in awake parkinsonian monkeys. These experiments are described in Chapter 4.

# Chapter 2

## *Specific Aim 1*

To examine the antiparkinsonian effects of combined dopamine D2 receptor agonism/metabotropic glutamate receptor 5 antagonism in MPTP-treated monkeys.

Bogenpohl JW, Patel L, Masilamoni GJ, Alagille D, Tamagnan G, Wichmann T, Smith Y. Metabotropic glutamate receptor 5 antagonist potentiates the antiparkinsonian effects of dopamine D2-like receptor agonist in MPTP-treated monkeys. 2013. In preparation.

## 2.1 Abstract

Although dopamine replacement therapy remains the first line of symptomatic treatment for Parkinson's disease (PD), the long term use of dopaminergic agents is significantly hampered by the development of motor and non-motor side effects. Because of this challenge, the search for non-dopaminergic drugs that could be used as monotherapy, or in combination with low doses of dopaminergic agents, has been at the forefront of PD pharmacotherapeutic research for decades. In recent years, the metabotropic glutamate receptor 5 (mGluR5) has been recognized as a highly relevant non-dopaminergic target for PD therapies, primarily because of its antidyskinetic, and neuroprotective properties. In this report, we demonstrate that the mGluR5 antagonist 3-((2-Methyl-4-thiazolyl)ethynyl)pyridine (MTEP) has modest antiparkinsonian effects when used as monotherapy and increases the number of movements induced by low doses of the dopamine D2-like receptor (D2LR) agonist pramipexole, in MPTP-treated parkinsonian monkeys. Thus, in addition to their anti-dyskinetic and neuroprotective properties, mGluR5 antagonists appear to have some antiparkinsonian benefits when used alone or combined with low doses of D2LR agonists. This finding further enhances the therapeutic relevance of mGluR5-related drugs for PD.

## 2.2 Introduction

Half a century after the discovery that levodopa can alleviate the motor signs and symptoms of Parkinson's disease (PD), dopamine replacement therapy remains the standard treatment for this disorder. Unfortunately, dopaminergic drugs often induce the development of involuntary movements (dyskinesias) and other debilitating non-motor side effects, which limits the long-term usefulness of these medications (for a review, see (Smith et al., 2012)). Therefore, the discovery of non-dopaminergic pharmacotherapeutics for PD is a highly relevant goal, as they represent a strategy to limit or even replace dopaminergic therapy in an effort to reduce troubling side effects.

Advances in our understanding of the pathophysiology of the basal ganglia circuitry in PD has led to the characterization of various non-dopaminergic targets that display promising anti-parkinsonian, anti-dyskinetic, and in some cases, neuroprotective therapeutic properties. Among these are the metabotropic glutamate receptors (mGluRs), a group of G-protein-coupled receptors. Because of their restricted pattern of expression in the basal ganglia, modulatory effects on neuronal excitability, and favorable pharmacologic properties, the mGluRs have become attractive targets for the treatment of PD and other neurological disorders (Niswender and Conn, 2010; Nicoletti et al., 2011).

The mGluR5, in particular, has shown much promise as a PD drug target. This excitatory ($G_q$-coupled) group I mGluR is expressed postsynaptically at high levels in all basal ganglia nuclei (Shigemoto et al., 1993; Testa et al., 1994; Hanson and Smith, 1999; Paquet and Smith, 2003; Hubert and Smith, 2004). Previous studies in rodent models of PD have shown that mGluR5 antagonists can improve parkinsonism (Breysse et al., 2002; Ossowska et al., 2002; Kachroo et al., 2005; Ossowska et al., 2005; Dekundy et al.,

2006). On the other hand, more recent findings in MPTP-treated monkeys (Johnston et al., 2010; Morin et al., 2010; Rylander et al., 2010; Gregoire et al., 2011) and PD patients (Berg et al., 2011) did not show antiparkinsonian effects of mGluR5 antagonists when used alone or in combination with levodopa. However, both nonhuman primate and rodent studies (Mela et al., 2007; Gravius et al., 2008; Levandis et al., 2008; Rylander et al., 2009; Yamamoto and Soghomonian, 2009; Johnston et al., 2010; Morin et al., 2010; Rylander et al., 2010; Gregoire et al., 2011) have shown that mGluR5 antagonists have significant anti-dyskinetic properties, which led to a recent clinical trial to assess the efficacy of the mGluR5 antagonist AFQ056 as an anti-dyskinetic agent in PD patients chronically treated with levodopa (Berg et al., 2011). This trial found that AFQ056 significantly decreased dyskinesia without changing the antiparkinsonian efficacy of levodopa.

D2-like dopamine receptor (D2LR) agonists, such as pramipexole, have good antiparkinsonian effects and very low dyskinetic potential in early stage PD (Group, 2000b; Group, 2000a; Holloway et al., 2004; Constantinescu et al., 2007; Group, 2009). These agents are often used as first-line treatment of patients with early-stage PD instead of levodopa, which is believed to be more prone to causing dyskinesia (Smith et al., 2012). However, dopamine receptor agonists are not as effective as levodopa, and have a significant liability to produce debilitating psychiatric and autonomic side effects, particularly when used at high doses (Stowe et al., 2008). Thus, the discovery of an adjunct treatment which enhances the efficacy of D2LR agonists could decrease or delay the need for dosage escalation and the resulting induction of side effects. In this study, we show for the first time that the mGluR5 antagonist, 3-((2-Methyl-4-

thiazolyl)ethynyl)pyridine (MTEP), significantly potentiates some of the antiparkinsonian effects of the D2LR agonist, pramipexole, in the MPTP-treated monkey model of PD.

## 2.3 Methods

### 2.3.1 Animals

Eight adult female rhesus macaques (14-17 years old) were used in this study. All experiments were performed in accordance with the National Institutes of Health's Guide for the Care and Use of Laboratory Animals (Garber et al., 2010) and the United States Public Health Service Policy on Humane Care and Use of Laboratory Animals. Five monkeys were treated with weekly intramuscular injections of 1-methyl-4-phenyl-1,2,3,6-tetrahydropyridine (MPTP; 0.2-0.8 mg/kg/week; Sigma, St. Louis, MO; total cumulative doses ranged from 4.2 to 33 mg/kg, total treatment time ranged from 3 to 16 months) until moderate parkinsonian motor signs were observed. Animals were allowed a minimum of 6 weeks stabilization after the last injection of MPTP (tested with the behavioral rating methods mentioned below) before they were used in the drug testing studies. Three monkeys went untreated and were only used as control animals for tyrosine hydroxylase (TH) immunostaining.

### 2.3.2 TH immunolabeling

One of the MPTP-treated monkeys used for behavioral experiments and three control monkeys were deeply anesthetized with pentobarbital (100 mg/kg i.v.) and transcardially perfused with cold oxygenated Ringer's solution, followed by a fixative containing 4% paraformaldehyde and 0.1% glutaraldehyde in a phosphate buffer solution. After perfusion, brains were removed from the skull, sliced coronally into thick (~1 cm)

blocks, and post-fixed overnight in 4% paraformaldehyde. These thick blocks were then cut into 60 μm-thick coronal sections using a vibrating microtome.

To assess the extent of MPTP-induced degeneration to the dopaminergic nigrostriatal system, sections at the level of striatum and substantia nigra of control and MPTP-treated monkeys were immunostained with mouse anti-tyrosine hydroxylase antibodies (Millipore, Temecula, CA, USA; Catalog number 318) at a dilution of 1:1000. The immunoperoxidase avidin-biotin complex method with diaminobenzidine as chromogen was used to localize the dopaminergic system according to procedures described in previous studies (Smith and Bolam, 1991). The sections were mounted on gelatin-coated slides, dehydrated in alcohol, immersed in toluene, and a coverslip was applied with Cytoseal XYL (Richard-Allan Scientific, Kalamazoo, MI). Then, slides were digitized with an Aperio Scanscope CS (Aperio Technologies, Vista, CA), and macroscopic images were acquired using Imagescope viewer software (Aperio Technologies), at 0.5× magnification. The images were then imported into ImageJ (National Institutes of Health, nih.gov) for further analysis.

For optical density measurements, the images were converted into 16-bit grayscale format and inverted. The functional striatal territories were delineated as described in our previous study (Masilamoni et al. 2011). For each animal, density measurements throughout the rostrocaudal and mediolateral extent of the caudate nucleus (n=9), putamen (n=15), and nucleus accumbens (n=3) were performed. Two measurements were also made in the internal capsule to assess background labeling. To control for differences in background staining, the average optical density measurement

in the internal capsule of each animal was subtracted from that obtained in the different striatal regions.

**2.3.3 Drug administrations**

MTEP was prepared by one of the authors (GT), dissolved in sterile saline and injected intramuscularly. Standard commercially available pramipexole tablets (Actavis Pharma Manufacturing, Alathur, India) were administered orally.

Due to variability in different animals' responses to antiparkinsonian drugs, a (cursory) dose-response curve for each of these drugs was generated in each animal. This allowed us to find customized threshold and optimal dosages of the two drugs for each monkey, while avoiding obvious side effects. The only side effects we observed occurred in response to high doses of MTEP ($\geq$ 30 mg/kg). These included stereotyped behaviors, including continuous rapid eye movements, staring at the ceiling, and reactions to nonexistent stimuli (grimacing, withdrawal). High drug doses that induced side effects were not included in the study.

Each animal underwent three trials with each of five different drug treatments, given in pseudorandom order: MTEP, low-dose pramipexole, high-dose pramipexole, MTEP/low-dose pramipexole combination, and saline. The chosen doses were individualized for each animal, based on the dose-response experiments mentioned above. The MTEP dose was selected as the most effective dose that did not induce visible side effects (doses ranged from 5-30 mg/kg, mean 13 mg/kg). The 'low dose' of pramipexole was selected as the lowest dose that reliably induced mild behavioral activation, mainly observed as a decrease in akinesia (these doses ranged from 0.125-0.25 mg, mean 0.2 mg). The 'high dose' of pramipexole was selected as the lowest dose that

resulted in maximal relief of parkinsonian motor signs (these doses ranged from 0.5-1 mg, mean 0.9 mg). Animals were given at least 48 hours of washout after each pramipexole experiment, in order to avoid carryover of antiparkinsonian effects from the previous experiment. No washout was given for MTEP, because it is rapidly cleared (Johnston et al., 2010).

Prior to any of the drug injections, the animals were acclimated to a standard observation cage which was used for all of the subsequent experiments. All studies were conducted in the early afternoon of experiment days. On each of the days, the animal was transferred to the observation cage and allowed to acclimate for 30-60 minutes. Then, a 15 min pre-drug baseline observation was conducted (see description below), followed immediately by drug administration (then sometimes a delay followed by administration of the second drug). For experiments in which both MTEP and pramipexole were administered, pramipexole was given 30 minutes prior to MTEP, in order to align the peak effects of both drugs, based on our empirical observations as well as pharmacokinetic data (Wright et al., 1997; Johnston et al., 2010). The animal was then observed and recorded for alternating 15 min periods (15-30 min, 45-60 min, 75-90 min, etc.), out to 180 min.

**2.3.4 Quantitative Assessment of Parkinsonism**

The parkinsonian motor signs in each monkey were quantified using 4 independent measures: quantification of movements, automated counting of infrared beam breaks in the activity monitoring cage, scoring of parkinsonian motor signs with a parkinsonism rating scale for non-human primates, and determination of the animal's eye blink rate.

*2.3.4.1 Quantification of movements*

For each experiment, an observer watched live video of the animal to quantify the number of movements made by the animal, using a keypad with eight buttons corresponding to different body parts (left and right arms and legs, head, and torso). Movement counts of all body parts were summed together to generate the total number of movements for each session. For each drug administration trial, the number of movements made during five 15-min post-drug observations was summed, beginning with the 15-30 min post-injection observation for MTEP and combination experiments, or the 45-60 min post-injection observation for pramipexole experiments. This assured that similar periods were analyzed in the monotherapy experiments as were used in the drug combination experiments, when pramipexole was given 30 min prior to MTEP. The mean summed movement counts of the three trials for each drug treatment were divided by the mean response to saline for each animal, in order to normalize the data. These normalized data from the five animals were statistically compared using one-way repeated measures ANOVA with Newman-Keuls post-hoc analysis. Individual animal data for responses to MTEP vs. saline were compared using paired t-tests.

*2.3.4.2 Counting of infrared beam breaks*

The observation cage was equipped with eight infrared beams, crossing the cage in two horizontal planes. The total number of beam breaks made during the five 15-min post-drug observations was normalized to each animal's response to saline, and analyzed as described above for the quantification of movements.

*2.3.4.3 Parkinsonism rating scale*

Videos of the "pre-drug baseline" session and the fifth "drug effect" session (during plateau of drug effect) of each experiment were scored off-line, independently by two observers, who were blinded to the drug treatment. Scores of 0-3 were given in each of 7 categories (bradykinesia, range of motion of individual extremities, freezing episodes, tremor, quantity of movements, balance, posture), for a maximum score of 21. The two observers' scores were averaged for each video, and the baseline score for each experiment was subtracted from the drug effect score to calculate the change in parkinsonism score for that experiment. Data from the three trials of each treatment were used to calculate mean changes in parkinsonism score for each animal. The mean changes in score for each of the five animals were averaged, and statistical comparisons were made using one-way repeated measures ANOVA with Newman-Keuls post-hoc analysis.

*2.3.4.4 Eye blink rate*

Decreased eye blink rate is a well-characterized symptom of PD (Karson et al., 1984; Deuschl and Goddemeier, 1998; Kaneko and Sakamoto, 2001; Agostino et al., 2008) that is improved with levodopa or STN stimulation (Bologna et al., 2012). By video observation, the number of eye blinks occurring in 1 min was recorded for the "pre-drug baseline" and fifth "drug effect" segment of each drug administration trial. The baseline eye blink rate was subtracted from the drug effect blink rate to calculate the change in blink rate for each experiment. Mean changes in eye blink rate were calculated and analyzed as described above for parkinsonism rating scale data.

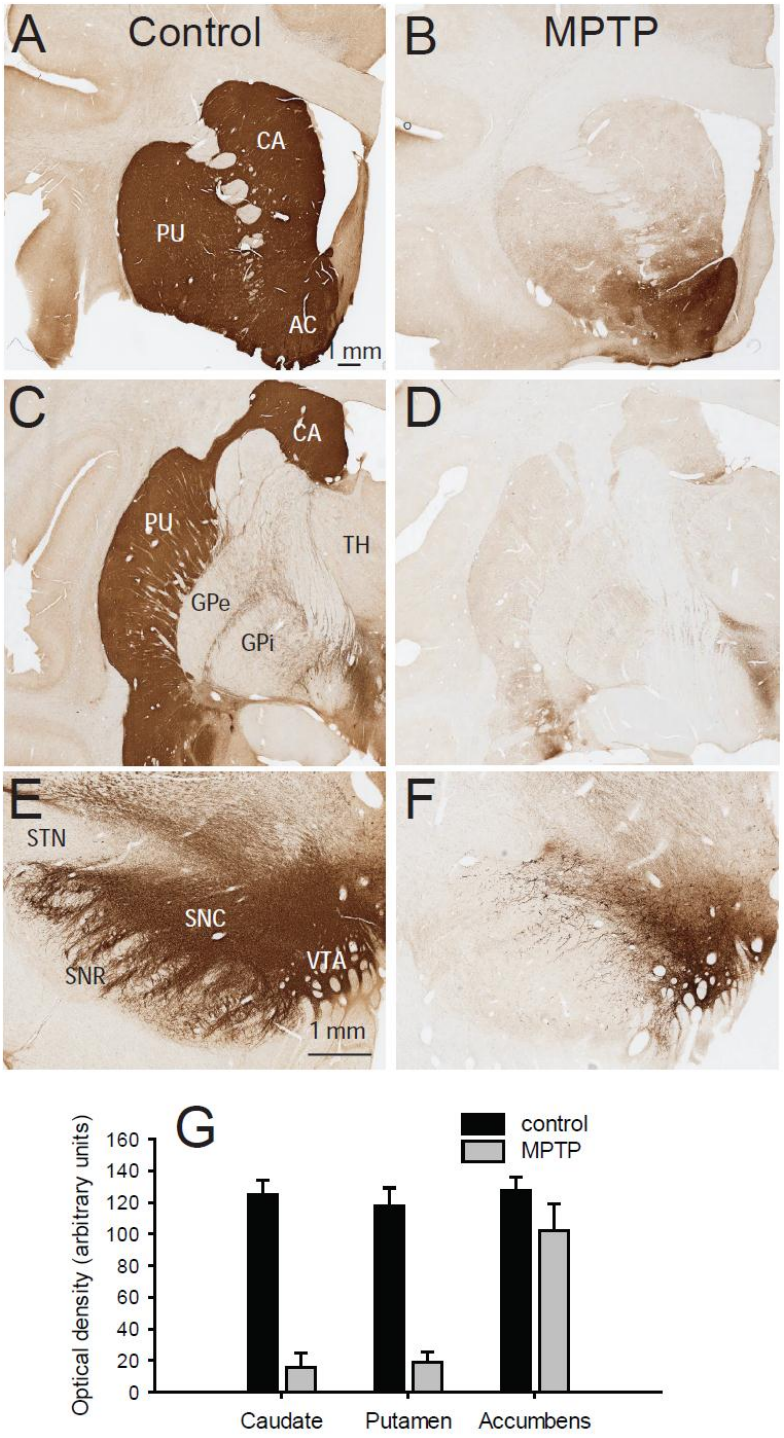


**Figure 2.1** TH immunolabeling in control and MPTP-treated monkeys. Immunoperoxidase labeling for TH is shown in the anterior and posterior striatum and the substantia nigra of untreated (A,C,E) and MPTP-treated (B,D,F) monkeys. Optical density measurements from the caudate nucleus (n=9 per animal), putamen (n=15 per animal), and nucleus accumbens (n=3 per animal) are shown in G. Values represent mean±standard deviation. n=3 control monkeys, 1 MPTP-treated.

## 2.4 Results

### 2.4.1 TH immunolabeling

MPTP treatment induced a marked loss of TH immunolabeling in the caudate and putamen, where optical density values were 12.4% and 15.9% of those acquired from control monkeys (Fig. 2.1). The nucleus accumbens was comparatively much less depleted, with optical density measurements reaching 80.1% of those measured in control monkeys. The substantia nigra of the MPTP-treated monkey also showed substantial loss of TH immunolabeling, as compared to control monkeys (Fig 2.1E,F).

### 2.4.2 Quantification of movements

Analysis of variance confirmed statistical differences between the four drug treatments ($p=0.003$; $F=8.142$). Compared with the saline treatment, administration of MTEP or low-dose pramipexole induced 2.7±0.8 (mean±SEM) and 2.1±0.2 times more movements, respectively (Fig. 2.2A). Looking at the un-normalized raw data, as a group, the response to MTEP monotherapy was not statistically significant from that of vehicle injections (paired t-test, $p>0.05$). However, it is worth noting that in 3 of the 5 animals, the MTEP trials generated significantly more movements than did the saline trials (paired t-tests, $p<0.05$). The combination of MTEP with low-dose pramipexole elicited 4.0±0.7 times the number of movements as did saline, significantly more than the same dose of pramipexole alone (Newman-Keuls, $p=0.045$). High-dose pramipexole elicited 5.2±1.1 times the number of movements as saline, an effect that was statistically greater than low-dose pramipexole (Newman-Keuls, $p=0.003$) and MTEP ($p=0.009$) monotherapies, but not statistically different from the response to the MTEP/low-dose pramipexole combination ($p>0.05$).

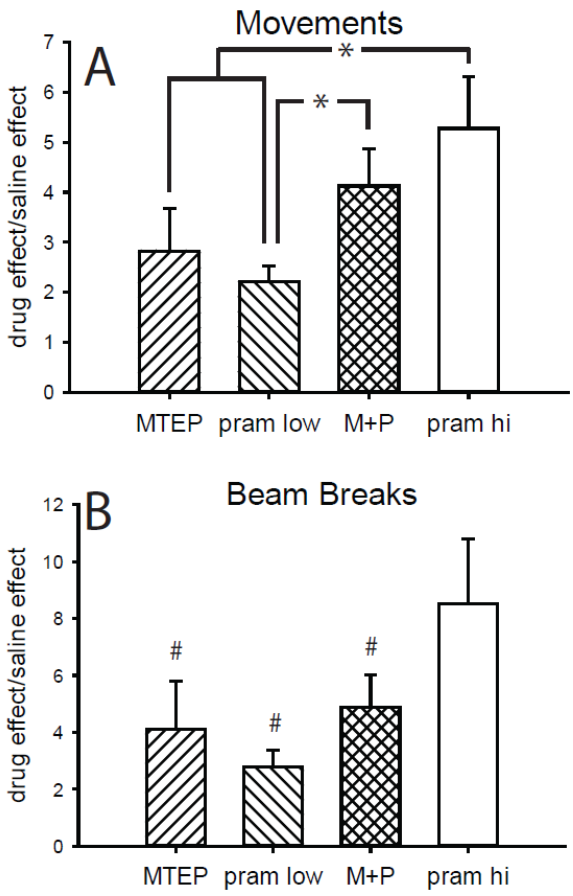


**Figure 2.2** The effect of drug treatments on quantity of movements (A) and infrared beam break counts (B). Each animal's mean number of movements or beam breaks induced by the drug treatments MTEP, low-dose pramipexole (pram lo), MTEP/low-dose pramipexole combination (M+P), and high-dose pramipexole (pram hi) were divided by each animal's response to saline to get the drug effect/saline effect ratio. Values represent mean±SEM; N=5 monkeys; *p<0.05, ANOVA with Newman-Keuls. #p<0.05 vs. pram hi, ANOVA with Newman Keuls.

### 2.4.3 Infrared beam breaks

Analysis of variance confirmed statistical differences between the four drug treatments (p=0.010; F=5.986). Given alone, MTEP and low-dose pramipexole induced 4.0±1.8 and 2.6±0.5 times the number of beam breaks as did saline, respectively (Fig 2.2B). The MTEP/pramipexole combination elicited 4.6±1.1 times the number of beam breaks as did saline. While the beam break data followed the same trend as the movement quantification data, the drug combination did not produce significantly more beam breaks than the same dose of pramipexole alone (Newman-Keuls, p>0.05). High-dose pramipexole administration resulted in 8.2±2.4 times the number of beam breaks as did saline, which was statistically different from all other treatments (Newman-Keuls, p<0.05).

### 2.4.4 Parkinsonism Rating Scale

Analysis of variance confirmed statistical differences between the five treatments ($p=0.011$; $F=4.638$). The mean pre-drug baseline parkinsonism score for all experiments, across all monkeys was 7.5±0.24. Saline injection caused very little change in this score (+0.04±0.43; Fig 2.3A). MTEP injection, on the other hand, induced a drop in the score (-3.6±1.1), which was statistically different from the saline response (Newman-Keuls, $p=0.017$). Low-dose pramipexole and the low-dose pramipexole/MTEP combination also caused decreases in the parkinsonism score (-2.6±1.2, and -3.8±0.72, respectively) that were significantly different than response to vehicle (Newman-Keuls, $p=0.038$ and $p=0.020$, respectively). Administration of high-dose pramipexole lead to a large decrease in the parkinsonism score (-4.4±0.86) which was statistically different from vehicle (Newman-Keuls, $p=0.010$). While they followed the same trend as the beam break and movement quantification data, none of the four drug treatments were significantly different from one another, as measured with the parkinsonism rating scale.

### 2.4.5 Eye blink rate

While the data followed a similar trend as the other methods of quantifying parkinsonism (drug combination > drug monotherapies), analysis of variance found no significant differences among the different drug treatments, as measured by eye blink rate ($p=0.254$, $F=1.483$). The mean number of eye blinks/min for all baseline sessions was 10.5±0.8. Saline injection caused little change in the rate of eye blinks (+0.73±0.29; Fig 2.3B). MTEP and low-dose pramipexole monotherapies both induced increases in eye blinks/min, but with large amounts of variability (+3.6±2.5 and +4.5±2.6, respectively).

The drug combination induced the largest increase in eye blink rate (+6.5±1.4), and high-dose pramipexole induced an increase of 4.7±1.5 eye blinks/min.

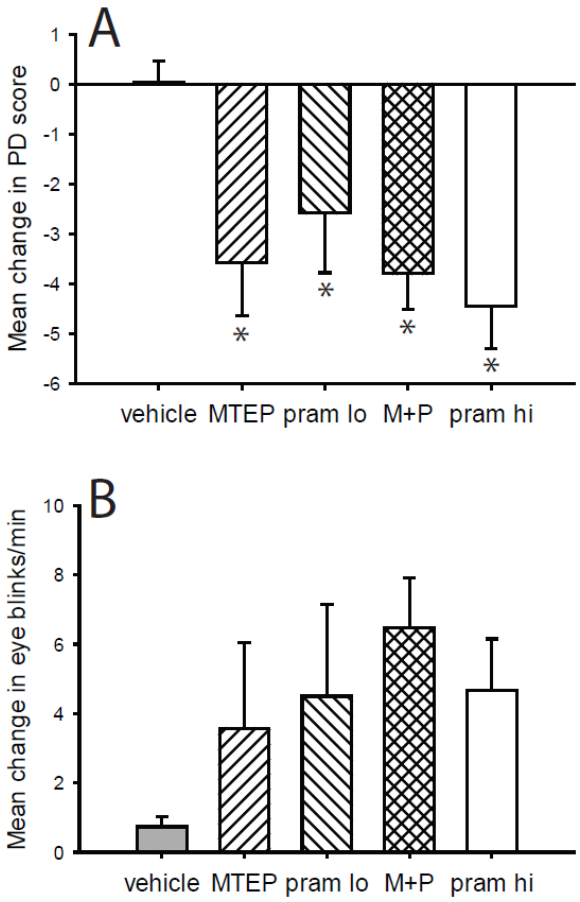


**Figure 2.3** The effect of drug treatments on parkinsonism (PD) score (A) and eye blink rate (B). Each animal's pre-drug baseline parkinsonism scores or eye blink rates were subtracted from its post-drug values to calculate the change in parkinsonism score or eye blink rate for each experiment. Mean±SEM values for these measures are presented for saline (vehicle), MTEP, low-dose pramipexole (pram lo), MTEP/low-dose pramipexole combination (M+P), and high-dose pramipexole (pram hi). Values represent mean±SEM; N=5 monkeys; *p<0.05 vs. vehicle, ANOVA with Newman-Keuls.

## 2.5 Discussion

In this study, we have shown that the mGluR5 antagonist MTEP has modest antiparkinsonian effects when used alone, and potentiates some of the antiparkinsonian effects of the D2LR agonist pramipexole in MPTP-treated monkeys. These results suggest that mGluR5 antagonist may be useful as an adjunct to low doses of D2LR agonist treatment in early PD, a therapeutic strategy that may help reduce the development of non-motor side effects frequently seen in patients chronically treated with D2LR agonists.

### 2.5.1 mGluR5 antagonist as an antiparkinsonian monotherapy

When given alone, mGluR5 antagonists have been shown to alleviate parkinsonism in rodent models of PD, including 6-OHDA-lesioned rats (Breysse et al., 2002; Breysse et al., 2003), haloperidol-treated rats (Spooren et al., 2000; Ossowska et al., 2002; Ossowska et al., 2005; Dekundy et al., 2006), and reserpine-treated mice (Kachroo et al., 2005). However, most studies in MPTP-treated monkeys did not reveal significant antiparkinsonian effects of mGluR5 antagonists when given alone or with levodopa (see next section). Our findings are partly in line with previous studies because they showed that the antiparkinsonian effects of MTEP monotherapy were modest and inconsistent across the different quantitative measurements of parkinsonian motor signs used in our study. For example, although MTEP induced a significant decrease in average parkinsonism score that was statistically equivalent to the maximally effective dose of pramipexole, it did not significantly increase eye blink rate. Also, three out of five individual animals responded to MTEP with significant increases in the number of movements, but as a group, the effect was not significant.

It is not entirely clear why mGluR5 antagonist monotherapy is apparently more effective in rodents than in primates. This may be indicative of a species difference of unknown nature between rodents and primates. Alternatively, this discrepancy may be due to differences in the 6-OHDA, haloperidol, and reserpine PD models, as compared to the MPTP model. Another important dissimilarity between previous rodent and primate studies is that the primates had undergone chronic levodopa treatment and dyskinesia development (which is known to cause altered glutamatergic transmission and mGluR5

expression (Picconi et al., 2002; Calon et al., 2003; Picconi et al., 2003; Picconi et al., 2004; Robelet et al., 2004; Samadi et al., 2008; Ouattara et al., 2010; Ouattara et al., 2011)), whereas the rodents had not. The suggestion that these changes underlie the discrepancy is supported by the fact that mGluR5 antagonist was slightly more effective in our monkeys, which were levodopa-naïve, than in the monkeys used in previous studies.

### 2.5.2 Potentiation of dopamine receptor-mediated antiparkinsonian effects by mGluR5 antagonist: Differences between L-DOPA and D2-like receptor agonists

In this report, we demonstrate that the mGluR5 antagonist MTEP can significantly potentiate some of the antiparkinsonian effects of low doses of the D2LR agonist pramipexole. As shown by our movement quantification data, adding MTEP to a low dose of pramipexole potentiated the antiparkinsonian effect to a level that was statistically equivalent to a maximally effective dose of pramipexole. In fact, in all four methods that we used to quantify parkinsonism, the data showed a trend of the drug combination being more effective than either monotherapy, although the data did not reach statistical significance for most of the behavioral measures, most likely due to the small number of animals used and inter-individual variability in their responses to antiparkinsonian agents. This result is partly different from those of recent studies showing that mGluR5 antagonists do not potentiate the antiparkinsonian effects of chronic levodopa (Johnston et al., 2010; Morin et al., 2010; Rylander et al., 2010; Berg et al., 2011; Gregoire et al., 2011). Although the source of this difference remains to be established, it is reasonable to believe that the specificity of interactions with dopamine receptors offered by the two different dopamine replacement strategies may be important.

L-DOPA administration most likely leads to activation of D1-like and D2-like receptors, while pramipexole acts predominately on D2LRs (Newman-Tancredi et al., 2002; Kvernmo et al., 2006). It is noteworthy that the specific usefulness of a combination of D2LR agonists and mGluR5 receptor agents is also suggested by the known physical interaction and functional synergy between $D_2$Rs and mGluR5 described in recent studies (see below). However, because our experiments do not address the mechanism of (inter)action of the two agents, it is possible that MTEP and pramipexole independently modulated different neural networks, and that their actions extended beyond the striatum.

### 2.5.3 Molecular interactions between mGluR5 and D2LRs

As stated above, the ability of the mGluR5 antagonist MTEP to potentiate the antiparkinsonian effects of the D2LR agonist pramipexole may be in part due to physical and functional interactions between these receptors within the striatum. Previous studies have, indeed, shown that mGluR5 and the $D_2$ dopamine receptor subtype physically interact in the striatum (Ferre et al., 2002; Ferre et al., 2003; Cabello et al., 2009), and that this interaction functionally links the activity of the two receptors, so that mGluR5 activation can decrease the affinity of $D_2$ receptor for dopamine, and vice versa (Ferre et al., 1999; Popoli et al., 2001). Thus, antagonism of mGluR5 and activation of $D_2$ receptors may synergistically reduce the excitability of the $D_2$-receptor expressing indirect pathway striatal projection neurons, which are known to be hyperactive in parkinsonism.

The mGluR5 and $D_2$ receptors in striatal indirect pathway neurons also interact with the adenosine $A_{2A}$ receptor ($A_{2A}$R) (Ferre et al., 1999; Popoli et al., 2001; Cabello et al., 2009). Furthermore, mGluR5 and $A_{2A}$R show functional synergy in their ability to

modulate motor behavior and other $D_2$ receptor-mediated effects in rodents (Popoli et al., 2001; Ferre et al., 2003; Coccurello et al., 2004; Kachroo et al., 2005). These findings, in combination with our monkey data, warrant future experiments to examine the antiparkinsonian effects of combinations of mGluR5 antagonists, $A_{2A}$R antagonists and D2LR agonists.

### 2.5.4 mGluR5 antagonist/D2LR agonist combination as a potential treatment for early PD

We showed that blockade of mGluR5 may amplify the effects of D2LR agonist therapy. If similar effects were found in PD patients, it could allow for a reduction of the total dose of D2LR agents being used, while maintaining good antiparkinsonian efficacy. This could help to avoid psychiatric and autonomic side effects associated with D2LR agonist treatment in PD patients (Smith et al., 2012). Thus, in combination with other recent studies showing the robust anti-dyskinetic properties of mGluR5 antagonists in various animal models and PD patients chronically treated with L-DOPA (Johnston et al., 2010; Morin et al., 2010; Rylander et al., 2010; Berg et al., 2011; Gregoire et al., 2011), and the preclinical evidence for protection of dopaminergic, noradrenergic, and serotonergic neurons against MPTP- or 6-OHDA-induced degeneration in monkey and rodent models of PD (Battaglia et al., 2004; Aguirre et al., 2005; Armentero et al., 2006; Vernon et al., 2007; Masilamoni et al., 2011; Hsieh et al., 2012), the results of the present study further encourage the use of mGluR5 antagonist therapy in PD patients.

# Chapter 3

## *Specific Aim 2*

To characterize adenosine $A_{2A}$ receptor localization and co-localization with metabotropic glutamate receptor 5 at the ultrastructural level in the monkey basal ganglia.

Bogenpohl JW, Ritter SL, Hall RA, Smith Y. Adenosine $A_{2A}$ receptor in the monkey basal ganglia: ultrastructural localization and co-localization with the metabotropic glutamate receptor 5 in the striatum. Journal of Comparative Neurology. 2012; 520(3):570-89.

## 3.1 Abstract

The adenosine $A_{2A}$ receptor ($A_{2A}R$) is a potential drug target for the treatment of Parkinson's Disease and other neurological disorders. In rodents, the therapeutic efficacy of $A_{2A}R$ modulation is improved by concomitant modulation of the metabotropic glutamate receptor 5 (mGluR5). To elucidate the anatomical substrate(s) through which these therapeutic benefits could be mediated, pre-embedding electron microscopy immunohistochemistry was used to conduct a detailed, quantitative ultrastructural analysis of $A_{2A}R$ localization in the primate basal ganglia, and assess the degree of $A_{2A}R$/mGluR5 co-localization in the striatum. $A_{2A}R$ immunoreactivity was found at highest levels in the striatum and external globus pallidus (GPe). However, the monkey, but not the rat, substantia nigra pars reticulata (SNr) also harbored a significant level of neuropil $A_{2A}R$ immunoreactivity. At the electron microscopic level, striatal $A_{2A}R$ labeling was most commonly localized in postsynaptic elements (58±3% of labeled elements), while in the GPe and SNr, the labeling was mainly presynaptic (71±5%) or glial (27±6%). In both striatal and pallidal structures, putative inhibitory and excitatory terminals displayed $A_{2A}R$ immunoreactivity. Striatal $A_{2A}R$/mGluR5 co-localization was commonly found; 60-70% of $A_{2A}R$-immunoreactive dendrites or spines in the monkey striatum co-express mGluR5. These findings provide the first detailed account of the ultrastructural localization of $A_{2A}R$ in the primate basal ganglia, and demonstrate that $A_{2A}R$ and mGluR5 are located to functionally interact in dendrites and spines of striatal neurons. Together, these data foster a deeper understanding of the substrates through which $A_{2A}R$ could regulate primate basal ganglia function, and potentially mediate its therapeutic effects in parkinsonism.

## 3.2 Introduction

Adenosine is a ubiquitous neuromodulator that binds to at least four known G-protein-coupled receptors in the brain ($A_1$, $A_{2A}$, $A_{2B}$, and $A_3$). Because of its localization and functional interaction with dopamine D2 receptors (D2R), the $A_{2A}$ receptor has gained interest as a potential drug target for several diseases, including Parkinson's Disease (PD) (Pinna, 2009), drug addiction (Brown and Short, 2008), sleep disorders, pain (Ferre et al., 2007b), and psychiatric disorders (Cunha et al., 2008).

In situ hybridization experiments (Schiffmann et al., 1991b; Dixon et al., 1996; Peterfreund et al., 1996; Svenningsson et al., 1997; Svenningsson et al., 1998; Kaelin-Lang et al., 2000), radioligand binding studies (Martinez-Mir et al., 1991; Calon et al., 2004), and light microscopic (LM) immunohistochemical data (Rosin et al., 1998) have described high levels of $A_{2A}$R expression in the striatum, nucleus accumbens, external globus pallidus (GPe), and olfactory tubercle, with low expression levels elsewhere in the brain. Qualitative electron microscopic data have indicated that dendrites, spines, and terminals express $A_{2A}$R immunoreactivity in the rat striatum (Hettinger et al., 2001). Furthermore, double in situ hybridization studies (Schiffmann et al., 1991a; Fink et al., 1992; Augood and Emson, 1994; Svenningsson et al., 1998) and double-labeling immunohistochemistry (Quiroz et al., 2009) in the rat striatum have shown that $A_{2A}$R co-localizes with enkephalin and D2R, but not dopamine D1 recpetor, substance P, or somatostatin, indicating a preferential expression of $A_{2A}$R in indirect pathway (striatopallidal) medium spiny neurons (MSNs). These findings are also supported by tract-tracing studies showing a lack of $A_{2A}$R expression in rat striatonigral neurons (Schiffmann and Vanderhaeghen, 1993).

In cell culture, $A_{2A}$Rs physically interact with D2Rs (Ferre et al., 1997; Ferre et al., 1999; Franco et al., 2000; Ferre et al., 2001; Hillion et al., 2002; Canals et al., 2003; Ciruela et al., 2004) and the group I metabotropic glutamate receptor 5 (Ferre et al., 1999; Ferre et al., 2002; Cabello et al., 2009). In addition to their physical interactions, simultaneous activation of $A_{2A}$R and mGluR5 results in synergistic functional effects that can be seen in several downstream biological processes, including decreased affinity of D2R for dopamine (Ferre et al., 1999), increased striatal c-Fos expression (Ferre et al., 2002), and increased cyclic adenosine monophosphate (cAMP) formation and striatal dopamine- and cAMP-regulated neuronal phosphoprotein (DARPP-32) phosphorylation (Nishi et al., 2003). Most importantly, antagonists of $A_{2A}$R decrease parkinsonian motor signs in animal models of PD (Grondin et al., 1999; Kanda et al., 2000; Bibbiani et al., 2003; Tanganelli et al., 2004; Pinna et al., 2007; Hodgson et al., 2010) and decrease alcohol self-administration in rodent models of alcoholism (Thorsell et al., 2007); two effects that are synergistically potentiated by the concomitant administration of mGluR5 antagonist (Coccurello et al., 2004; Kachroo et al., 2005; Adams et al., 2008).

Although the exact sites of functional interactions between these two receptors in the central nervous system remain to be determined, both $A_{2A}$R and mGluR5 are heavily expressed in dendrites and spines of striatal MSNs, as revealed in single labeling immuno-electron microscopic studies in rats and monkeys (Hettinger et al., 2001; Paquet and Smith, 2003). However, despite low levels of presynaptic mGluR5 reported in ultrastructural studies of the rat and monkey striatum (Shigemoto et al., 1993; Paquet and Smith, 2003), synaptosomal fractionation and immunofluorescence techniques have identified a large proportion of "putative" axon terminals in the rodent striatum

(Rodrigues et al., 2005) and hippocampus (Tebano et al., 2005) that co-express $A_{2A}R$ and mGluR5.

In order to gain a better understanding of the primate adenosinergic system, and to characterize potential target sites where $A_{2A}R$ and mGluR5 antagonists could mediate their synergistic behavioral effects, we have conducted a detailed quantitative study of the ultrastructural localization of $A_{2A}Rs$ in the basal ganglia, and determined the degree of striatal $A_{2A}R$/mGluR5 co-localization in rhesus monkeys using single and double immunohistochemistry at the electron microscopic (EM) level.

## 3.3 Materials and Methods

### 3.3.1 Animals and tissue preparation

A total of four adult rhesus monkeys (2 males, 2 females; 8-18 years old) and four adult female Sprague-Dawley rats were used in this study. All procedures were approved by the animal care and use committee of Emory University and conform to the U.S. National Institutes of Health guidelines. For immunohistochemistry, animals were deeply anesthetized with pentobarbital (100 mg/kg i.v.) and transcardially perfused with cold oxygenated Ringer's solution, followed by a fixative containing 2% paraformaldehyde and 3.75% acrolein in a phosphate buffer (PB) solution. After perfusion, the brains were removed from the skull, coronally sliced into thick (~1 cm) blocks, and post-fixed overnight in 2% paraformaldehyde. These thick blocks were then cut into 60-μm-thick coronal sections using a vibrating microtome and stored at -20° C in an anti-freeze solution containing 30% ethylene glycol and 30% glycerol in PB. Prior to immunohistochemical (IHC) processing, sections were washed with phosphate buffered

saline (PBS; 0.01M, pH 7.4), treated with a 1% sodium borohydride solution for 20 minutes, and then washed in PBS again.

For Western blot studies, one rat and one monkey were deeply anesthetized with pentobarbital (100 mg/kg i.v.) and killed by decapitation. Brains were rapidly removed from the skull and dissected. Samples were taken from the cerebral cortex, hippocampus, caudate nucleus, putamen (or striatum in rat), cerebellum, and ventral midbrain (containing the substantia nigra) and flash frozen in liquid nitrogen. Frozen samples were stored at -80º C until needed.

**3.3.2 Antibody Characterization** (Table 3.1)

For the localization of the adenosine $A_{2A}$ receptor, a commercially available mouse monoclonal antibody (Millipore Corporation, Billerica, MA; catalog # 05-717, lot # 28777) was used. This antibody was raised against the full-length human adenosine $A_{2A}$ receptor and was epitope-mapped to the sequence SQPLPGER in the third intracellular loop of the receptor. The specificity of this antibody has been previously characterized via Western blot in rat brain (band at 45 kDa), slot blot, IHC in transfected cells, and antibody pre-adsorption with IHC in rat brain slices (Rosin et al., 1998). This antibody does not label tissue from $A_{2A}$R-knockout mice (Day et al., 2003). In the present study, Western blots show high specificity of the antibody for $A_{2A}$R in monkey tissue (Fig. 3.1B). Omission of the primary antibody from IHC processing of our monkey brain tissue resulted in the disappearance of immunostaining. When the primary antibody is pre-adsorbed with a synthetic peptide matching the epitope described above, there is a significant loss of neuropil staining, thereby providing further evidence for the antibody's specificity in monkeys.

For the localization of mGluR5, an affinity-purified polyclonal rabbit antibody (Millipore; catalog # 06-451) raised against a 21-residue synthetic peptide (K-SSPKYDTLIIRDYTNSSSSL) corresponding to the C-terminal of mGluR5 with a lysine added to the N-terminal was used at a dilution of 1:5,000. The specificity of this antibody has been characterized by immunoblot on homogenate from cells transfected with the receptor and from rat brain areas known to express the receptor (band at 140 kDa) (Marino et al., 2001). The antibody does not stain brain tissue from mGluR5 knockout mice (Kuwajima et al., 2004).

**Table 3.1** – Antibody information.

| Target protein | Antigen sequence | Source |
|---|---|---|
| adenosine $A_{2A}$ receptor | SQPLPGER | Millipore Corporation, Billerica, MA; catalog # 05-717, lot # 28777; raised in mouse, monoclonal |
| metabotropic glutamate receptor 5 | KSSPKYDTLIIR DYTNSSSSL | Millipore; catalog # 06-451; raised in rabbit, polyclonal |

### 3.3.3 Western Blots

HEK293T cells (ATCC**,** Manassas, VA) were maintained in DMEM GlutaMAX™ (Invitrogen, Carlsbad, CA), supplemented with 10% dialyzed fetal bovine serum (Invitrogen) and 1% Penicillin/Streptomycin (Thermo Scientific, Waltham, MA) in a humidified incubator at 37°C and 5% $CO_2$. Cells were transfected with plasmids encoding mock pcDNA3.1 (Invitrogen), human $A_1$, or human $A_{2A}$ receptor cDNAs (Missouri S&T cDNA Resource Center, Rolla, MO) using the lipofectamine transfection method (Lipofectamine 2000; Invitrogen). Following 24 hours of expression, cells were

washed twice with ice-cold PBS/$Ca^{2+}$ (phosphate buffered saline supplemented with calcium) and harvested in ice-cold harvest buffer containing 50 mM NaCl, 20 mM HEPES, 5 mM EDTA, 1 protease inhibitor cocktail tablet (Roche Applied Science, Basel, Switzerland), diluted with $dH_2O$ up to 50 ml, pH 7.4. Cell lysates were snap frozen at -80°C until needed.

To prepare brain tissue homogenates, monkey and rat brain tissue samples were thawed on ice, and each brain region was individually homogenized using a dounce homogenizer for 10 strokes in ice-cold harvest buffer on ice. Prepared tissue homogenates were aliquotted, snap frozen in liquid nitrogen, and stored at -80°C until needed.

After thawing HEK293T cell lysates and brain tissue homogenates on ice, bicinchoninic acid protein assays (Thermo Scientific) were performed to normalize protein across samples. Samples were then prepared for Western blotting by diluting with 6X Laemmli sample buffer to a final 1X concentration, followed by robust sonication on ice. Samples from the HEK293T cell lysates and brain tissue homogenates were loaded onto 4-20% Tris-Glycine gels and subjected to SDS-PAGE electrophoresis. Proteins were then transferred to nitrocellulose membranes and visualized with Ponceau stain. Membranes were subjected to Western blotting to probe for the $A_{2A}$ receptor and to test the specificity of the anti-$A_{2A}$R antibody. Following blocking for 30 minutes in "blot buffer" containing 2% non-fat milk, 50 mM NaCl, 10 mM HEPES, and 0.1% Tween-20 in $dH_2O$, membranes were incubated with the anti-$A_{2A}$R antibody diluted 1:2,000 in blot buffer for 1 hour at room temperature. After washing in blot buffer, membranes were probed with anti-mouse HRP-conjugated secondary antibody (diluted in blot buffer,

1:4,000) for 30 minutes. Bands were visualized using an enhanced chemiluminescence kit (Thermo Scientific) and membranes were exposed to films for various time-points. Membranes were then stripped using Restore Buffer (Thermo Scientific) and probed with anti-actin (Sigma, St. Louis, MO) to verify equal protein loading.

### 3.3.4 Single immunoperoxidase labeling for light microscopy

In order to map the expression pattern of $A_{2A}R$ immunoreactivity in the monkey brain, a total of 56 coronal brain sections from a single monkey, each separated by 300 μm, were simultaneously immunostained for $A_{2A}R$, covering a total brain area that extends from approximately interaural +28 to +3 in the rostrocaudal plane according to the Paxinos stereotaxic atlas (Paxinos et al., 2000). After sodium borohydride treatment, sections were incubated for 1 hour in PBS containing 10% normal horse serum (NHS) for $A_{2A}R$ localization or normal goat serum (NGS) for mGluR5 localization, 1% bovine serum albumin (BSA), and 0.3% Triton X-100. Then, the sections were incubated in the primary antibody solution containing a 1:2,000 dilution of $A_{2A}R$ antibody, 1% NHS or NGS, 1% BSA, and 0.3% Triton X-100 in PBS for 24 hours at room temperature. Sections were then rinsed three times in PBS and incubated in the secondary antibody solution containing 1% normal horse or goat serum, 1% BSA, 0.3% Triton X-100, and biotinylated horse anti-mouse or goat anti-rabbit IgGs (Vector Laboratories, Burlingame, CA) at a dilution of 1:200 for 90 minutes at room temperature. After three rinses in PBS, sections were incubated for 90 minutes in the avidin-biotin peroxidase complex (ABC) solution at a dilution of 1:100 (Vectastain standard ABC kit, Vector Laboratories) including 1% BSA and 0.3% Triton X-100. To reveal labeling, sections were first rinsed with PBS and Tris buffer (50 mM; pH 7.6), then incubated in a solution containing

0.025% 3,3'-diaminobenzidine tetrahydrochloride (DAB; Sigma), 10 mM imidazole, and 0.005% hydrogen peroxide in Tris buffer for 10 minutes. Then, sections were rinsed in PBS, mounted onto gelatin-coated slides, dehydrated, and then coverslipped with Permount™ (Fisher Scientific, Hampton, NH).

**3.3.5 Single immunoperoxidase labeling for electron microscopy**

Sections containing the striatum, GPe, or substantia nigra from three monkeys were processed for the electron microscopic immunoperoxidase localization of $A_{2A}R$. After sodium borohydride treatment, sections were transferred to a cryoprotectant solution containing 25% sucrose and 10% glycerol in PB (0.05M, pH 7.4) for 20 minutes and then placed in a -80°C freezer for 20 min to permeabilize cell membranes. Brain sections were then thawed through washes in decreasing concentrations of cryoprotectant solution until being put into PBS. The processing of sections was then identical to that used for light microscopy up to the point of DAB revelation, with two important differences: 1) Triton X-100 was omitted from all solutions and 2) sections were incubated in the primary antibody (1:1,000 dilution) solution for 48 hours at 4°C.

After DAB revelation, the tissue was rinsed in PB (0.1M, pH 7.4) and treated with 1% osmium tetroxide for 20 minutes. It was then rinsed with PB and dehydrated with increasing concentrations of ethanol. Uranyl acetate (1%) was added to the 70% EtOH dehydration solution and incubated for 35 minutes in order to increase the contrast of membranes in the electron microscope. After alcohol dehydration, sections were treated with propylene oxide and embedded in epoxy resin (Durcupan ACM; Fluka, Buchs, Switzerland) for at least 12 hours, mounted onto slides, and placed in a 60°C oven for 48 hours to cure the resin.

Small blocks of tissue from the motor putamen, GPe and substantia nigra pars reticulata (SNr) were cut out from the embedded sections and glued onto resin blocks for ultrathin sectioning with an ultramicrotome (Leica Ultracut T2). Sixty nanometer-thick sections were collected from the surface of the tissue block to ensure that antibody penetration was optimal in the tissue analyzed in the EM. Sections were mounted on single-slot pioloform-coated copper grids, stained for 5 minutes with lead citrate, and examined on a Zeiss EM-10C transmission electron microscope. Electron micrographs were captured and saved with a CCD camera (DualView 300W; Gatan, Inc., Pleasanton, CA) controlled by DigitalMicrograph software (version 3.11.1; Gatan, Inc.).

**3.3.6 Single pre-embedding immunogold labeling for electron microscopy**

Two tissue sections at the level of the striatum from each of the three monkeys were used for the immunogold localization of $A_{2A}R$. After having been pre-treated with sodium borohydride and cryoprotectant solutions, as detailed above, brain sections were incubated for 30 minutes in PBS containing 5% dry milk and then rinsed in TBS-gelatin (TRIS-buffered saline; 0.24% TRIS, 0.1% fish gelatin, pH 7.6) buffer. Sections were then exposed to the primary antibody solution containing 1% dry milk and mouse anti-$A_{2A}R$ primary antibody (1:1,000) in TBS-gelatin buffer for 24 hours at room temperature. After rinsing with TBS-gelatin, sections were exposed to the secondary antibody solution containing 1% dry milk and horse anti-mouse IgGs conjugated to 1.4-nm diameter gold particles (Nanoprobes, Yaphank, NY) at a concentration of 1:100 in TBS-gelatin for 2 hours at room temperature. After rinsing with TBS-gelatin and 2% sodium acetate buffer, gold particles were enlarged to 30-50 nm using the silver intensification method (HQ silver kit, Nanoprobes). Then, sections underwent osmification, dehydration, and

embedding as detailed above for immunoperoxidase experiments, but with two important differences: 1) exposure to 0.5% osmium tetroxide for 10 minutes instead of 1% for 20 minutes and 2) exposure to 1% uranyl acetate for 10 minutes instead of 35. Ultrathin sections were then cut and collected as described above.

### 3.3.7 Dual pre-embedding immunogold/immunoperoxidase method for striatal co-localization of $A_{2A}R$ and mGluR5

In order to determine the degree and pattern of co-localization of $A_{2A}R$ and mGluR5 in the motor putamen, two sections from each of the three monkeys used for electron microscopy studies were processed for the dual localization of mGluR5 and $A_{2A}R$ immunoreactivity using the pre-embedding immunogold and immunoperoxidase methods. To assess the extent of co-localization and avoid interpretation problems due to the differential sensitivity of the peroxidase- or gold-labeled antibodies for their respective antigens, two different reactions were performed on separate sets of striatal sections. In the first series of sections, $A_{2A}R$ was labeled with peroxidase and mGluR5 was revealed with gold, while in the second series of incubations, $A_{2A}R$ was labeled with gold and mGluR5 with peroxidase.

The incubation procedures and preparation of brain sections for these double labeling studies were similar to those used for the single pre-embedding immunogold and immunoperoxidase labeling, except that antibody solutions contained a cocktail of two different primary or secondary antibodies. $A_{2A}R$ primary antibody was used at a dilution of 1:1,000, and mGluR5 primary antibody was used at a dilution of 1:5,000. Following secondary antibody incubations, the tissue was processed for silver intensification of gold particles, rinsed with PBS, and then exposed to ABC and DAB as described above for the

single immunoperoxidase labeling procedure. After rinsing in PB, sections underwent osmification, dehydration, resin embedding, and ultrathin sectioning as described above.

### 3.3.8 Analysis of material

*3.3.8.1 Light microscopic analysis*

Brain sections mounted on glass slides were scanned at 20X using a ScanScope CS scanning light microscope system (Aperio Technologies, Vista, CA). Digital representations of these slides were saved and analyzed using ImageScope software version 10.0.36.1805 (Aperio Technologies).

*3.3.8.2 Electron microscopic analysis*

In most cases, the ultrathin sections analyzed on the EM were taken from at least two different tissue blocks per structure per animal, in order to increase the sampling of tissue analyzed. From single immunoperoxidase-labeled sections, 100 micrographs per structure per animal of randomly-encountered $A_{2A}$R-labeled neuronal elements were captured at 25,000X, giving a total of 1,162 μm² of tissue analyzed per structure per animal. Fifty micrographs per structure per animal were captured in the same manner for gold-labeled tissue, giving an area of 581 μm² analyzed. In double-labeled tissue, 100 micrographs per structure per animal of randomly-encountered $A_{2A}$R-labeled neuronal elements were captured at 25,000X, irrespective of the presence or absence of mGluR5 labeling in the same element. As a prerequisite to ensure that the double-labeled tissue examined contained optimal immunostaining for both $A_{2A}$R and mGluR5, micrographs were taken only from areas in which both the immunoperoxidase and immunogold deposits were visible. Dendrites and terminals were considered immunoreactive in gold-labeled tissue if they contained at least two gold particles, while because of their

relatively small surface area, spines and unmyelinated axons were categorized as immunoreactive if they were overlaid with a single gold particle or more. Using these selection criteria, the overall proportions of $A_{2A}$R-labeled spines and dendrites in the immunogold and immunoperoxidase material were closely related, thereby supporting the reliability of the quantitative data collected across immunoperoxidase and immunogold material. Contrast and sharpness of micrographs shown were adjusted to best show relevant aspects.

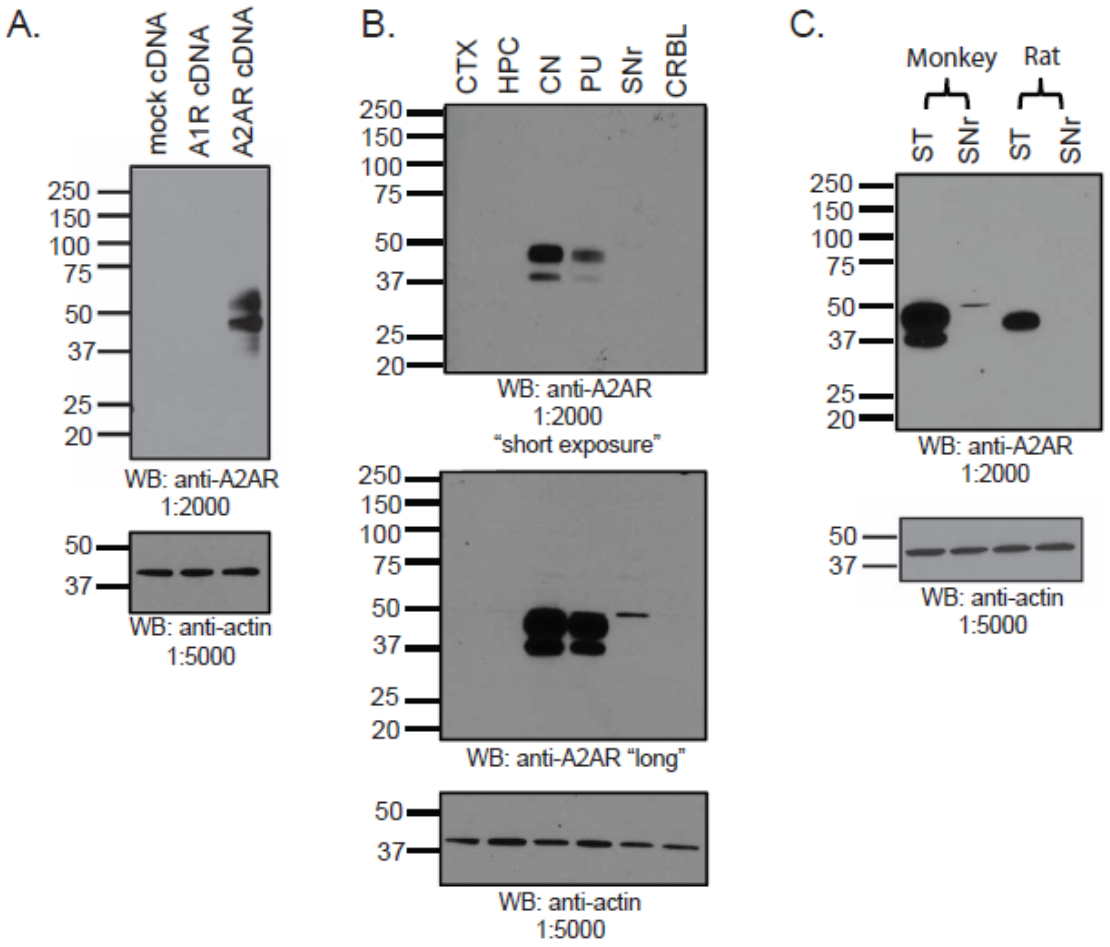


**Figure 3.1 –** Antibody characterization and Western blot detection of $A_{2A}R$ in the monkey and rat. **A)** 10 µg of HEK293T cell lysates transfected with mock pcDNA3.1, $A_1$, or $A_{2A}$ receptor cDNAs were subjected to SDS-PAGE and Western blotting with anti-$A_{2A}R$ antibody (1:2000). Two specific bands, probably representing the unmodified and glycosylated versions of the $A_{2A}$ receptor, were detected at approximately 45 and 55 kDa, respectively, in the $A_{2A}R$-transfected condition (top panel, lane 3) and not in mock- or $A_1R$-transfected cell lysates (top panel, lanes 1 and 2). Probing samples for actin confirmed equal protein loading (lower panel). **B)** 20 µg of macaque brain region samples were subjected to SDS-PAGE and Western blotting with the anti-$A_{2A}R$ antibody (1:2000). $A_{2A}R$ is enriched in the macaque striatum, with detection of $A_{2A}R$ at approximately 45 kDa, and a minor band that may represent an $A_{2A}R$ degradation product at approximately 37 kDa (top panel). Longer exposures of the same blot revealed that $A_{2A}R$ is most enriched in CN > PU > SNr (middle panel). Probing samples for actin confirmed equal protein loading (lower panel). **C)** 20 µg of macaque or rat brain regions were subjected to SDS-PAGE. Western blotting with the anti-$A_{2A}R$ (1:2000) revealed $A_{2A}R$ to be detectable in the macaque SNr but not the rodent SNr (top panel). Probing samples for actin confirmed equal protein loading (lower panel). CTX – cortex, CN – caudate nucleus, CRBL – cerebellum, HPC – hippocampus, PU – putamen, SNr – substania nigra pars reticulata, ST – striatum, WB – Western blot

## 3.4 Results

### 3.4.1 Western blots

To further demonstrate the specificity of the $A_{2A}R$ antibody, we performed a series of immunoblot experiments probing transfected cell lysates and brain tissue homogenates. Lysates from HEK293T cells transfected with pcDNA3.1 (mock), human adenosine $A_1$ receptor ($A_1R$), or human $A_{2A}R$ were immunoblotted for detection of $A_{2A}R$. Human receptors were used in order to provide further characterization of the antibody for use in immunohistochemistry of primate tissue, as well as to confirm adenosine receptor subtype specificity in our hands, as previously reported (Rosin et al., 1998). Corresponding with the predicted molecular weight of the $A_{2A}R$, a prominent band at around 45 kDa was detected only in the lysate expressing $A_{2A}R$, and not in the cell lysates expressing $A_1R$ or mock cDNA (Fig. 3.1A). The second band in the $A_{2A}R$ cell lysate, at about 55 kDa, presumably represents glycosylated $A_{2A}R$, as suggested in Rosin et al. (1998). Probing for actin showed equal protein loading from all cell lines. This demonstrates the specificity of the antibody, in agreement with Rosin et al. (1998).

Western blotting for detection of $A_{2A}R$ in the monkey cortex, hippocampus, caudate nucleus, putamen, midbrain, and cerebellum provided further evidence for the specificity of this antibody in monkey tissue. Short exposures of these blots revealed specific bands, only in the lanes for the caudate nucleus and putamen, at the expected molecular weight for $A_{2A}R$ (45 kDa), as well as a lighter minor band around 37 kDa, which may represent $A_{2A}R$ proteolytic degradation product, as suggested in Rosin et al. (1998) (Fig. 3.1B, top). However, longer exposures of the same blots revealed immunolabeling for $A_{2A}R$ in all structures sampled, the strongest of which (other than

caudate and putamen) was from the ventral midbrain (SNr, Fig. 3.1B, bottom). Blots probed with an anti-actin antibody demonstrated equal protein loading for all structures.

### 3.4.2 Immunoperoxidase $A_{2A}R$ labeling: Light microscopy

At the light microscopic level, immunoperoxidase labeling resulted in a dark brown deposit which, in most labeled structures, was predominantly associated with fine neuropil processes. The most strongly labeled structures in the monkey brain were the striatum and GPe (Fig. 3.2). Dense, homogeneous labeling invaded the whole extent of the caudate nucleus, putamen, nucleus accumbens and olfactory tubercle. Dense neuropil labeling in these structures precluded identification of labeled soma.

In the GPe, intense labeling was found in neuropil processes that invaded the whole extent of the structure. The dense immunoreactivity associated with the GPe stood out next to the very low level of labeling in the neighboring GPi (Fig. 3.2D-F).

Another basal ganglia nucleus that displayed a significant level of $A_{2A}R$ immunoreactivity was the SNr (Figs. 3.2G, H, I, 3.3D). Although not generally recognized as a major $A_{2A}R$-containing structure in rodents, the monkey SNr displayed moderate neuropil immunoreactivity along its whole rostrocaudal extent, which stood out next to the lightly labeled substantia nigra pars compacta (Fig. 3.2G, H).

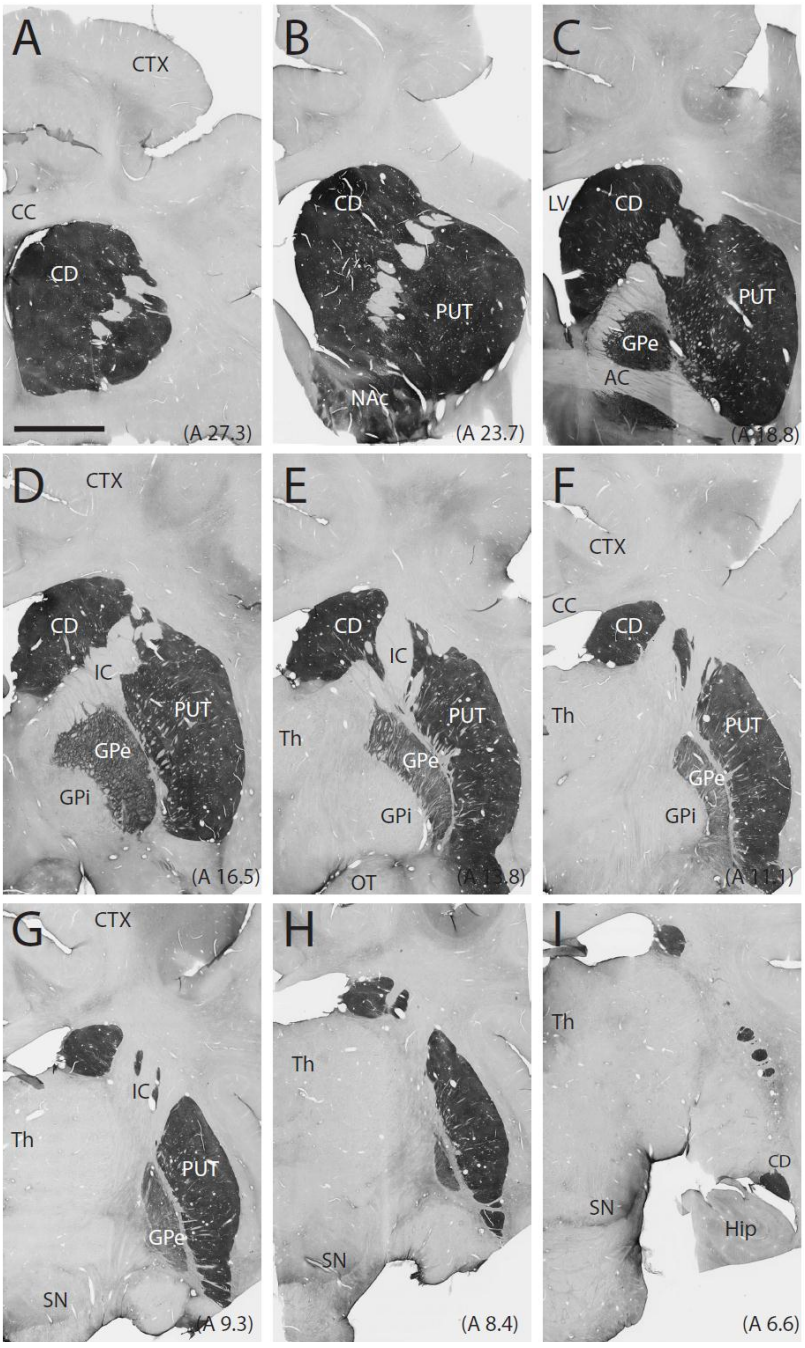


**Figure 3.2 –** Overall distribution of immunoperoxidase labeling for $A_{2A}R$ in the monkey basal ganglia. A series of low-power light micrographs of coronal brain sections (9 out of 56 shown) showing $A_{2A}R$ immunoreactivity throughout the rostrocaudal extent of the monkey basal ganglia. The interaural stereotaxic coordinate for each section is indicated at the bottom right of each panel (Paxinos et al., 2000). Scale bar: 5 mm (valid for A-I). AC – anterior commissure, CC – corpus collosum, CD – caudate nucleus, CTX – cortex, GPe – external globus pallidus, GPi – internal globus pallidus, Hip – hippocampus, IC – internal capsule, LV – lateral ventricle, NAc – nucleus accumbens, OT – optic tract, PUT – putamen, SN – substantia nigra, Th – thalamus.

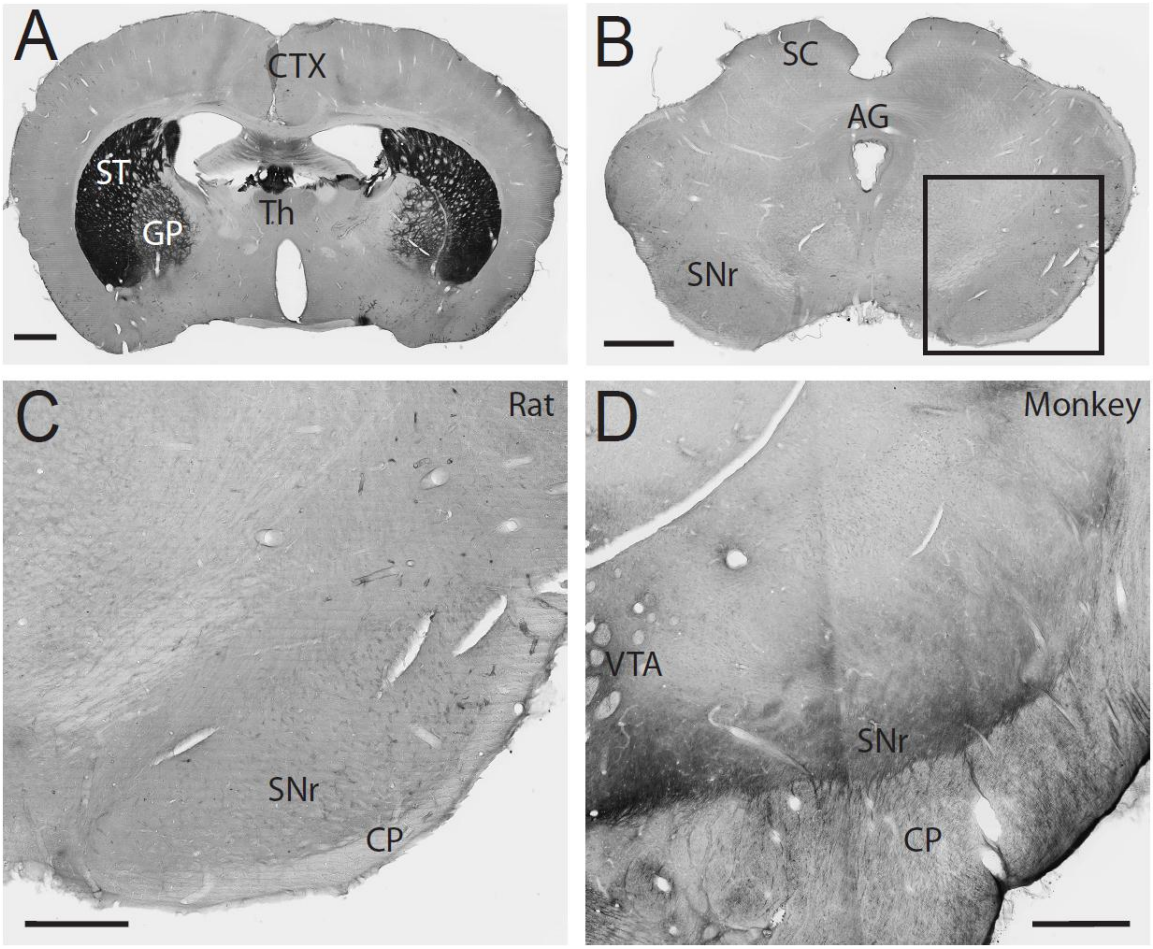


**Figure 3.3 –** $A_{2A}R$ immunolabeling in rat and monkey substantia nigra. A series of medium to high power micrographs depicting details of $A_{2A}R$ immunostaining in the rat (A-C) and monkey (D) basal ganglia. All sections in this figure were processed in the same immunohistochemical reaction. **A)** $A_{2A}R$ immunolabeling at the level of the rat striatum/GP. Note the strong immunoreactivity in the striatopallidal complex comparable with the pattern of labeling in monkeys (see Fig. 2). **B, C)** Lack of $A_{2A}R$ immunolabeling in the rat SNr. C is a higher magnification image of the boxed area in B. **D)** $A_{2A}R$ immunolabeling in the monkey SNr. Note the higher degree of neuropil $A_{2A}R$ immunoreactivity in the monkey than in the rat SNr. Scale bars= 1mm. AG – periaqueductal gray, CP – cerebral peduncle, CTX – cortex, GP – globus pallidus, SC – superior colliculus, SNr – substantia nigra pars reticulata, ST – striatum, Th – thalamus, VTA – ventral tegmental area.

Because previous immunohistochemical studies did not report the SNr as being enriched in $A_{2A}R$ immunoreactivity in the rat, we performed additional experiments in 3 rats to assess a possible species difference in the extent of $A_{2A}R$ immunoreactivity in the SNr between rodents and primates. When run together in the same antibody solutions

and processed during the same immunohistochemical reaction, striatal and GPe neuropil in both species displayed strong $A_{2A}R$ labeling, while significant $A_{2A}R$ immunoreactivity was evident in the monkey, but not the rat, SNr (Fig. 3.3). To confirm this species difference in nigral expression of $A_{2A}R$ between monkey and rat, a Western blot was run for detection of $A_{2A}R$ in the monkey and rat striatum and SNr. Although high levels of receptor proteins were detected in both the monkey and rat striatal tissue, $A_{2A}R$ was detected in the monkey, but not the rat, ventral midbrain samples containing the SNr (Fig. 3.1C). Also, the doublet of bands seen in monkey tissue representing whole $A_{2A}R$ and a proteolytic fragment was not evident in the rat striatum, in agreement with previous findings (Rosin et al., 1998). This may be due to a species difference in $A_{2A}R$ proteolytic processing, or a number of other factors beyond the scope of the present study. Blotting for actin showed equal protein loading from both species.

In addition to basal ganglia nuclei, all layers of the cerebral cortex contained light perikaryal labeling, with relatively denser labeling in the underlying white matter, which appeared to be mostly glial in nature (Fig. 3.2). Other brain areas that contained lower levels of $A_{2A}R$ immunoreactivity in the monkey brain included the thalamus, hippocampus, subthalamic nucleus, and claustrum (Fig. 3.2). Brainstem regions posterior to the substantia nigra were largely devoid of $A_{2A}R$ immunoreactivity.

### 3.4.3 Ultrastructural Localization of $A_{2A}R$

#### *3.4.3.1 Immunoperoxidase $A_{2A}R$ labeling*

While most of the $A_{2A}R$ labeling was found in the neuropil of basal ganglia nuclei, light microscopy does not provide a level of resolution high enough to categorize the neuronal and glial elements with which these receptors are associated. To address

this issue, we performed a quantitative electron microscopic analysis of the distribution of $A_{2A}R$ immunoreactivity in the monkey basal ganglia (Fig. 3.4). $A_{2A}R$-immunostained sections from the putamen, GPe, and SNr were examined in the electron microscope. At the electron microscopic level, the immunoperoxidase labeling for $A_{2A}R$ could be identified as a dark, electron dense, amorphous deposit associated with restricted compartments of neuronal and glial elements. The relative abundance of immunoreactive structures in each of these regions, identified based on specific ultrastructural features (Peters et al., 1991), was determined and plotted against each other in distribution histograms (Fig. 3.4E, F).

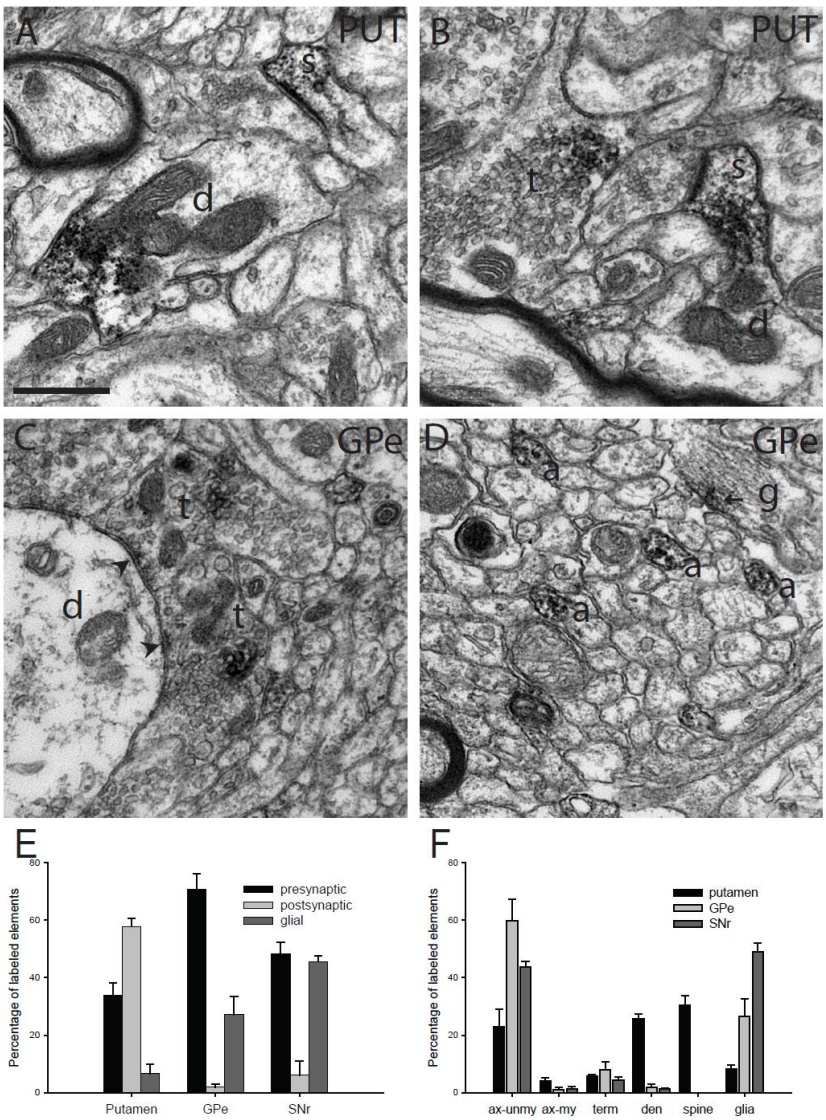


**Figure 3.4 –** Ultrastructural localization of $A_{2A}R$ in the monkey basal ganglia. Electron micrographs of neuronal elements immunolabeled for $A_{2A}R$ (A-D) and quantification of immunoperoxidase labeling in the postcommissural putamen, GPe, and SNr of rhesus monkeys (E, F). **A)** An $A_{2A}R$-labeled dendrite (d) and spine (s) in the sensorimotor putamen. **B)** A labeled spine (s) protruding from an unlabeled dendrite (d) in the putamen. A labeled terminal (t) is also visible. **C)** Two immunoreactive putative GABAergic terminals (t) form symmetric synapses on an unlabeled dendrite (d) in the GPe. **D)** Labeled unmyelinated axons (a) in the GPe. A lightly labeled (arrow) fibrous astrocytic process (g) is also seen. **E)** Quantification of the percentages of labeled elements categorized as neuronal (presynaptic versus postsynaptic) or glial in the monkey putamen and GPe. **F)** Breakdown of the percentages of each type of $A_{2A}R$-labeled element in different basal ganglia nuclei. Percentage values refer to the number of specific labeled neuronal or glial elements over the total number of labeled elements examined in that structure (+/- SEM). Scale bar: 0.5 µm (valid for A-D). Symmetric synapses are marked with arrowheads, and asymmetric synapses are marked with chevrons.

3.4.3.1.1 Putamen

The $A_{2A}R$ striatal labeling was mainly localized to postsynaptic elements including dendritic spines and shafts, which accounted for 58±3% of labeled elements in the putamen. On the other hand, 34±4% of labeled striatal elements were presynaptic in nature, the majority of which were unmyelinated axons, although immunoreactive terminals were also encountered. Seventeen of the 37 labeled terminals identified formed axo-dendritic symmetric synapses, 10 displayed asymmetric synapses, while the synaptic specialization of the remaining 10 boutons was not visible in the plane of section or not well preserved enough to be categorized as symmetric or asymmetric. Of the 10 $A_{2A}R$-labeled terminals forming asymmetric synapses, 8 were in contact with spines, while the other 2 formed synapses with dendritic shafts. Labeled glial processes were rare in the striatum (7±3% of labeled elements), but represented a larger proportion of labeled elements in other structures examined (Fig. 3.4E, F).

3.4.3.1.2 GPe

In the GPe, the bulk of labeling was expressed presynaptically (71±5% of labeled elements), largely in unmyelinated axons with more modest labeling of axon terminals forming either symmetric (47 of 76 labeled terminals) or asymmetric (6 of 76) synapses. The scarcity of labeled postsynaptic elements (2±1%) indicates that $A_{2A}R$ immunoreactivity in the GPe is largely confined to afferent axons and terminals. On the other hand, immunoreactive glial processes were commonly found in the GPe (27±6% of labeled elements). The glial immunoreactivity was associated either with large diameter processes of fibrous astrocytes (Fig. 3.4D) or with thinner glial processes in close contact with neuronal elements.

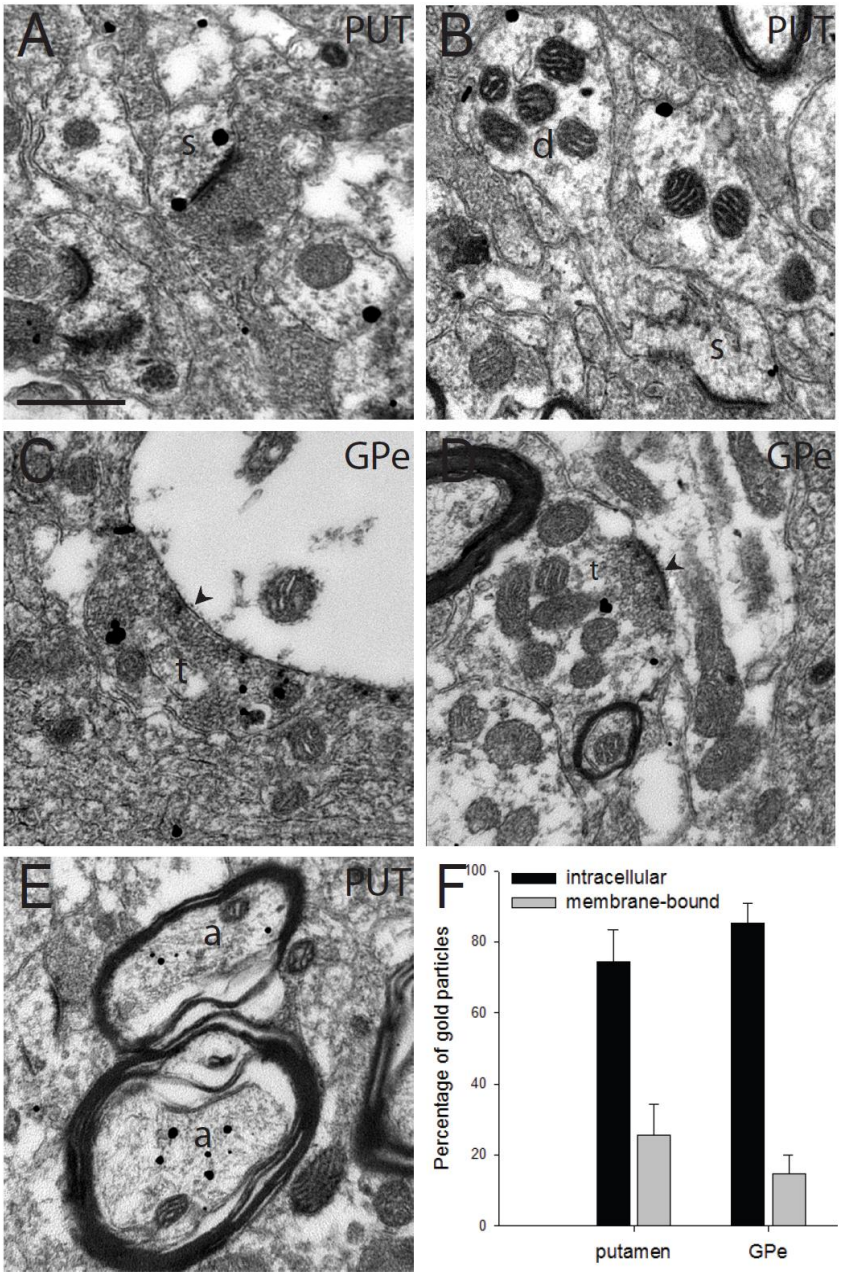


**Figure 3.5 –** EM immunogold labeling for A2AR. Electron micrographs of neuronal elements immunolabeled for A2AR (A-E) and quantification of immunogold labeling (F) in the putamen and GPe. A) Perisynaptic and intracellular labeling for A2AR in a striatal spine. B) A labeled spine protrudes from an immunoreactive dendrite (d) in the putamen. C) An A2AR-labeled putative inhibitory axon terminal (t) that forms a symmetric axo-dendritic synapse in the GPe. D) A labeled putative excitatory terminal (t) forming an asymmetric synapse with an unlabeled dendrite in the GPe. E) Two labeled myelinated axons (a) in the putamen. F) Quantification of intracellular vs. plasma membrane-bound A2AR immunogold labeling in the putamen and GPe. Scale bar: 0.5 µm (valid for A-E). Symmetric synapses are marked with arrowheads, and asymmetric synapses are marked with chevrons.

3.4.3.1.3 SNr

Like the GPe, $A_{2A}R$ labeling in the SNr was composed primarily of presynaptic elements (48±4% of labeled elements) with scarce postsynaptic immunoreactivity (6±5% of labeled elements). Labeled terminals in the SNr formed predominantly axo-dendritic symmetric synapses (17 of 33 labeled terminals). The remaining boutons either formed asymmetric synapses (4 of 33 labeled terminals) or did not establish clear synaptic junctions in the plane of section that was examined. The SNr contained a larger proportion of labeled glial elements (46±2% of labeled elements) than other basal ganglia nuclei.

*3.4.3.2 Immunogold $A_{2A}R$ labeling*

In order to further characterize the potential subsynaptic sites of action where adenosine could mediate its effects through $A_{2A}R$ activation in the striatopallidal complex, the immunogold method was used to provide a more accurate description of the subcellular and subsynaptic localization of $A_{2A}R$ in the post-commissural putamen and GPe (Fig. 3.5). The gold labeling in neuronal elements was divided into two major categories: intracellular versus plasma membrane-bound. The membrane-bound gold particles were further divided into three sub-categories: synaptic (within or directly apposed to the synaptic active zone), perisynaptic (<20 nm outside of active zone), or extrasynaptic (>20 nm from the synapse). In both the putamen and GPe, 75-85% of $A_{2A}R$-associated gold particles were found in the intracellular compartment (Fig. 3.5F). The difference between intracellular and membrane-bound gold particles was statistically significant in both structures (t-test, $p<0.05$). There was no statistical difference in the pattern of labeling (intracellular vs. membrane-bound) between the two structures (t-test,

p=0.355). Among membrane-bound gold particles, only 2.6% in the putamen and 1.5% in the GPe were found at synaptic and perisynaptic sites; the bulk of labeling was extrasynaptic in both nuclei. Glial gold labeling was not included in this analysis.

*3.4.3.3 $A_{2A}$R/mGluR5 co-localization*

Because $A_{2A}$R and mGluR5 have been shown to physically interact in the rat striatum, we performed double-labeling EM co-localization experiments in the monkey putamen to identify the subcellular compartments where these interactions could potentially occur in primates. The degree of co-localization of $A_{2A}$R and mGluR5 in the putamen was substantial, especially in postsynaptic elements (Fig. 3.6). When $A_{2A}$R was labeled with peroxidase and mGluR5 with gold, 68±5% of $A_{2A}$R-containing spines and 60±2% of dendrites also contained mGluR5 (N=717 $A_{2A}$R-immunoreactive elements). When $A_{2A}$R was labeled with gold and mGluR5 with peroxidase, 73±2% of $A_{2A}$R-containing spines and 62±1% of dendrites also contained mGluR5 (N= 904 $A_{2A}$R-immunoreactive elements). Co-localization in presynaptic elements was much less frequent; only 5-15% of $A_{2A}$R-containing axons and terminals also contained mGluR5, likely owing to the fact that mGluR5 is rarely found in presynaptic elements in the striatum (Paquet and Smith, 2003; Mitrano and Smith, 2007). Only 2-6% of all double-labeled elements observed were presynaptic in nature. There was no significant difference in the degree of co-localization in any type of element when $A_{2A}$R was labeled with peroxidase versus gold (t-test, $p>0.05$), which validates the reliability of our double labeling method.

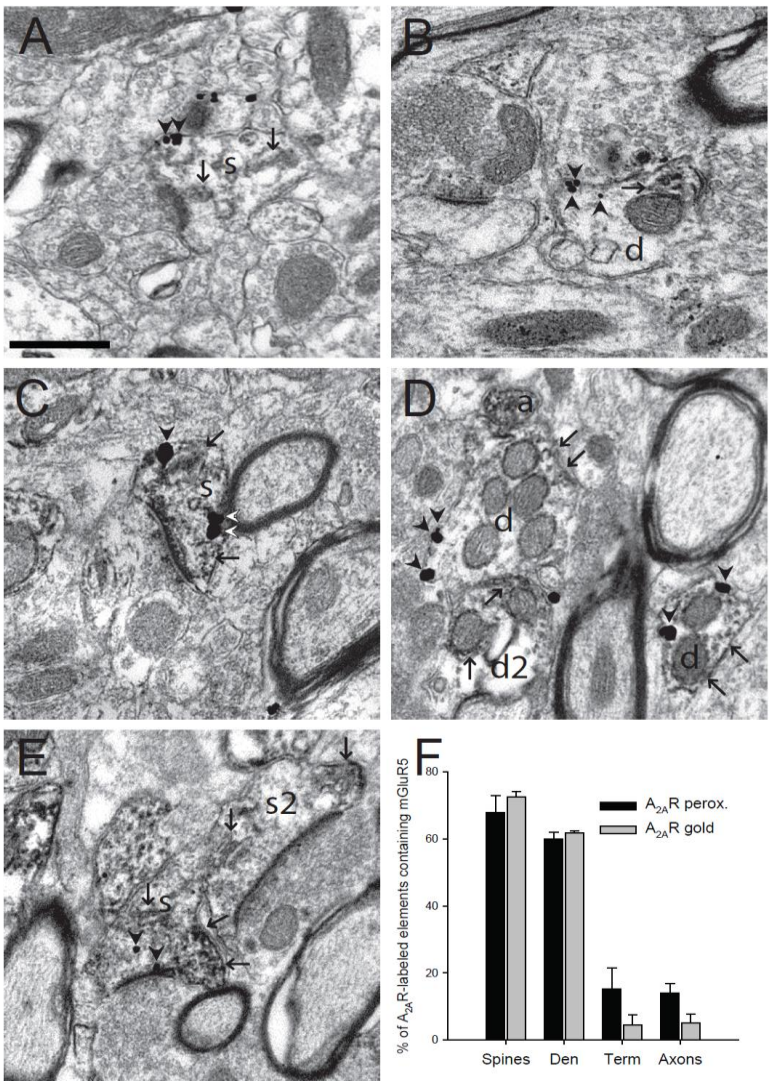


**Figure 3.6 –** $A_{2A}$R/mGluR5 double-labeling in the motor putamen. Electron micrographs of $A_{2A}$R/mGluR5 double-labeled neuronal elements in the monkey putamen (A-E) and quantification of co-localization (F). **A-E)** Examples of spines (s) and dendrites (d) co-labeled for both $A_{2A}$R and mGluR5 in the putamen. In each panel, arrows point at peroxidase deposits,arrowheads indicate immunogold labeling, and chevrons mark asymmetric synapses. In A and B, the immunoperoxidase deposit indicates $A_{2A}$R immunoreactivity, while mGluR5 is labeled with gold particles. In C-E, the reaction was reversed, i.e. peroxidase is used to localize mGluR5, while $A_{2A}$R is labeled with gold. A spine (s2) and dendrite (d2) single-labeled for mGluR5 are also visible in D and E, respectively. **F)** Quantification of the percentage of $A_{2A}$R-labeled neuronal elements that also express mGluR5 immunoreactivity in the motor putamen. Black bars represent the percentages of $A_{2A}$R-immunoreactive elements that co-express mGluR5 immunoreactivity in tissue dually stained for $A_{2A}$R with peroxidase and mGluR5 with gold, while gray bars represent the same quantitative assessment of co-localization in tissue double immunostained for $A_{2A}$R with gold and mGluR5 with peroxidase. There was no statistical difference in the extent of co-localization between these two staining methods. Scale bar: 0.5 µm (valid for A-E).

## 3.5 Discussion

Our results provide the first detailed quantitative assessment of the ultrastructural localization of $A_{2A}R$ in the primate basal ganglia and its degree of subcellular co-localization with mGluR5 in the striatum. In addition to its well-recognized association with indirect striatofugal GABAergic neurons, our data reveal that $A_{2A}Rs$ are also located to subserve presynaptic modulation of glutamatergic afferents to the striatum and GPe in nonhuman primates. In contrast to rodents, a significant level of presynaptic $A_{2A}R$ immunoreactivity was found in putative GABAergic terminals in the monkey SNr, thereby raising the possibility that adenosine may influence basal ganglia outflow, not only through the indirect modulation of GPe or striatal activity, but also via $A_{2A}R$-mediated regulation of GABAergic transmission in the primate SNr. Furthermore, the extensive degree of $A_{2A}R$ and mGluR5 co-localization at the level of striatal spines and dendrites described in our study suggests that functional interactions between these two receptors most likely occur postsynaptically in the primate striatum, a situation different from the presynaptic interactions recently proposed in rodents on the basis of in vitro data (Rodrigues et al., 2005). In addition to a strong neuronal expression, $A_{2A}Rs$ were also found to be significantly enriched in glial cells throughout the monkey basal ganglia, most particularly in the SNr, providing another substrate through which adenosine can mediate its effects upon basal ganglia activity in the normal and diseased state.

### 3.5.1 $A_{2A}R$: A marker of indirect striatopallidal neurons in primates and non-primates

Previous studies have shown that $A_{2A}R$ mRNA and protein in the rodent and primate striatum co-localizes with markers of indirect, but not direct pathway MSNs

(Schiffmann et al., 1991a; Fink et al., 1992; Augood and Emson, 1994; Svenningsson et al., 1997; Svenningsson et al., 1998; Quiroz et al., 2009). This selective expression makes $A_{2A}R$ a highly specific marker of indirect striatopallidal neurons in primates and non-primates.

In line with these data, we found high levels of $A_{2A}R$ immunoreactivity in the monkey striatum and GPe, with very little labeling in the GPi. In agreement with previous rodent data (Hettinger et al., 2001), the majority of striatal $A_{2A}R$ immunoreactivity was located in postsynaptic structures in the monkey striatum, most likely belonging to indirect striatofugal neurons. When considered in conjunction with our findings that almost all neuronal $A_{2A}R$ immunoreactivity in the GPe was located in presynaptic elements and that 47 of 53 classifiable $A_{2A}R$-labeled terminals in the GPe were putatively GABAergic and morphologically resembled striatal-like boutons, our data provide further evidence for strong $A_{2A}R$ expression in striatopallidal medium spiny projection neurons (MSNs) in nonhuman primates.

In the striatum, the preferential expression of $A_{2A}R$ in dendrites and spines suggest the possibility of postsynaptic $A_{2A}R$-mediated effects upon striatal projection neurons. However, many of the known effects of $A_{2A}R$ in striatal MSNs occur through modulation of other receptors with which $A_{2A}R$ interacts, such as dopamine D2 receptors, mGluR5, or CB1 receptors (Stromberg et al., 2000; Domenici et al., 2004; Ferre et al., 2007a; Tozzi et al., 2011). For example, while $A_{2A}R$ activation alone has no effect on the membrane potential of MSNs in rat striatal brain slices, it can block the ability of a D2 receptor agonist to suppress NMDA-induced downstate to upstate transitions (Azdad et al., 2009). Additionally, postsynaptic $A_{2A}R$ activation negatively modulates NMDA

receptor postsynaptic currents in rat striatal slices (Norenberg et al., 1997; Norenberg et al., 1998; Wirkner et al., 2000; Gerevich et al., 2002; Wirkner et al., 2004). While direct electrophysiological effects of postsynaptic $A_{2A}$Rs on MSNs have been rarely reported, the ability of these receptors to regulate biochemical indicators of MSN function, such as cAMP formation, phosphorylation of DARPP-32, as well as 2-amino-3-(5-methyl-3-oxo-1,2- oxazol-4-yl) propanoic acid receptor and L-type calcium channel function is well documented from in vitro or rodent studies (Schiffmann et al., 2007). However, little is known about $A_{2A}$R function in the primate striatum.

The significant level of pre-synaptic $A_{2A}$Rs in striatal-like terminals in the monkey GPe is suggestive of modulatory sites of action that could regulate striatopallidal GABAergic transmission. Patch clamp recording data from rat brain slices have, indeed, shown that $A_{2A}$R agonist presynaptically enhances the amplitude of striatal-evoked IPSCs in GP neurons (Shindou et al., 2001). In line with these in vitro data, local infusions of $A_{2A}$R agonist into the striatum or GP of unlesioned rats led to increased GABA concentrations in the GP, and systemic administration of $A_{2A}$R antagonist reduced extracellular GABA levels in the GP of 6-hydroxydopamine (6-OHDA)-lesioned rats (Ochi et al., 2000). In vivo intrapallidal delivery of $A_{2A}$R antagonist can also block the decrease in GP neuron firing rate induced by striatal stimulation in rats (Querejeta et al., 2010). Together, these findings demonstrate that $A_{2A}$R subserves key regulatory functions of GABAergic transmission along the striatopallidal indirect pathway in rodents. Our electron microscopic data, combined with previous light microscopic studies in monkeys (Svenningsson et al., 1998) and humans (Schiffmann et al., 1991b; Svenningsson et al., 1997; Kaelin-Lang et al., 2000; Calon et al., 2004) demonstrate that

these receptors are located to subserve similar functions at striatopallidal synapses in primates.

However, the expression of $A_{2A}R$ immunoreactivity in putative glutamatergic terminals in the monkey GPe suggests that the influence of adenosine-mediated effects through these receptors may go beyond the striatopallidal GABAergic system. Because there is no further evidence that $A_{2A}R$ activation modulates glutamatergic transmission in the GP, functional studies directly addressing this issue are warranted to better understand the complex and multifarious mechanisms by which $A_{2A}Rs$ modulate basal ganglia activity in normal and diseased states.

### 3.5.2 $A_{2A}R$ expression in striatal terminals

In addition to a significant post-synaptic expression, $A_{2A}R$ immunoreactivity was also found to be frequently associated with both putative glutamatergic and GABAergic terminals, as well as a large number of unmyelinated axons in the monkey putamen. Labeled myelinated axons were much less common, but were present in the striatum (Fig. 3.5E). This pattern is reminiscent of what has been described in the rat striatum, except for the axonal labeling, which was not as prominent in rodents (Hettinger et al., 2001). $A_{2A}$ receptors have, indeed, been found to presynaptically modulate both excitatory and inhibitory transmission in the rodent striatum. For instance, local infusion of $A_{2A}R$ agonist into the rat striatum greatly increases extracellular glutamate levels (Popoli et al., 1995), while infusion of an $A_{2A}R$ antagonist attenuates the increase in striatal glutamate levels induced by cortical stimulation in mice (Quiroz et al., 2009). In line with these data, $A_{2A}R$ agonist increased, while $A_{2A}R$ antagonist decreased the amplitude of EPSCs in mouse striatal slices through presynaptic regulation of cortical glutamatergic inputs

(Quiroz et al., 2009). It is noteworthy that $A_{2A}$R-mediated regulation of glutamatergic transmission may not only affect cortical afferents, but also modulate thalamic inputs (Smith et al., 2004; Raju et al., 2006; Smith et al., 2009). The fact that some of the $A_{2A}$R-labeled terminals formed asymmetric axo-dendritic synapses is, indeed, suggestive that a subset of thalamostriatal afferents from the caudal intralaminar thalamic nuclei expresses pre-synaptic $A_{2A}$Rs (Smith et al., 2009). Furthermore, we found that the monkey thalamus contains low to moderate levels of perikaryal $A_{2A}$R labeling, in agreement with previous evidence for $A_{2A}$R expression in the rodent and primate thalamus (Dixon et al., 1996; Svenningsson et al., 1997; Rosin et al., 1998; Mishina et al., 2007).

In line with previous rodent studies (Hettinger et al., 2001), a subset of $A_{2A}$R-positive terminals in the monkey striatum displayed the ultrastructural features of intrinsic GABAergic terminals, which most likely originate from axon collaterals of indirect pathway GABAergic striatal projection neurons. However, the $A_{2A}$R-mediated regulation of GABAergic transmission in the striatum appears to be more complex than mere pre-synaptic effects, and may involve coupling of the receptor to G-proteins other than $G_s$ (Kirk and Richardson, 1995; Gubitz et al., 1996; Ravyn and Bostwick, 2006).

### 3.5.3 $A_{2A}$R expression in the SNr

One of the interesting findings of our study was the evidence for significant expression of $A_{2A}$R immunoreactivity in the monkey SNr, which in rodents is not a major site of $A_{2A}$R mRNA or protein expression (Schiffmann et al., 1991b; Fink et al., 1992; Dixon et al., 1996; Rosin et al., 1998; Kaelin-Lang et al., 2000; Hettinger et al., 2001). On the other hand, previous studies have reported significant levels of $A_{2A}$R ligand

binding in the human SN using PET or autoradiography detection methods (Svenningsson et al., 1997; Mishina et al., 2007).

At the ultrastructural level, the $A_{2A}$R labeling in the monkey SNr was split almost equally between presynaptic (unmyelinated axons/terminals) and glial elements, with very little postsynaptic expression, indicating predominant presynaptic or glial regulatory functions of basal ganglia output neurons. Since it is known that some striatopallidal axons send collaterals to the SNr (Parent et al., 1995), and most of the identifiable synapses formed by the $A_{2A}$R-positive SNr boutons in our analyses were of the symmetric type, these data strongly suggest that much of the presynaptic labeling in the monkey SNr is accounted for by GABAergic axon collaterals of indirect pathway neurons. Taking into consideration that the GPi is almost completely devoid of $A_{2A}$R immunoreactivity in monkeys, these findings suggest that GABAergic axon collaterals of indirect striatopallidal neurons in the SNr may phenotypically differ from those in the GPi, thereby providing a substrate for specific $A_{2A}$R-mediated regulation of striatal GABAergic inputs to the SNr. However, because a small number of labeled terminals in the SNr displayed features of glutamatergic boutons, $A_{2A}$R-mediated regulation of excitatory transmission in the SNr cannot be ruled out.

### 3.5.4 $A_{2A}$R in glia

Our findings provide further evidence that $A_{2A}$Rs mediate some of their physiological effects in the central nervous system through glial cells, a hypothesis that has been put forward in previous studies largely based on in vitro and in vivo data showing that adenosine and $A_{2A}$R antagonists modulate astrocyte reactivity (Hindley et al., 1994; Brambilla et al., 2003; Dare et al., 2007), as well as glial glutamate release and

uptake (Nishizaki et al., 2002). In monkeys, the most enriched basal ganglia nucleus in glial $A_{2A}R$ expression was the SNr, although the striatum and GP also contained a significant number of $A_{2A}R$-positive glial processes. Glial $A_{2A}Rs$ were also strongly expressed in the external capsule and subcortical white matter of rhesus monkeys. It is noteworthy that the relative prevalence of $A_{2A}R$ in glia appears to be higher in monkey than rodent basal ganglia (Hettinger et al., 2001). Whether this represents a genuine species difference in $A_{2A}R$ expression indicating a more active role of glial $A_{2A}R$ in primates than non-primates remains to be determined.

At the EM level, essentially all labeled large-diameter glial processes belonged to fibrous astrocytes, as can be determined by their content of densely packed intermediate filaments (Fig. 3.4D). However, many finer labeled glial processes were identified, which could belong to other glial cell types. $A_{2A}Rs$ are considered important regulators of microglial reactivity and proliferation towards sites of brain injury or degeneration, thereby suggesting an additional role in neuroinflammation, brain repair, and cell death (Gebicke-Haerter et al., 1996). Because, we did not use specific markers of astrocytes or microglia in this study, our findings cannot confirm or reject evidence for microglial $A_{2A}R$ immunoreactivity in the basal ganglia of normal monkeys. However, the outcome may be different in animal models of basal ganglia disorders and in humans affected with chronic neurodegenerative diseases like PD, as microglia have been shown to upregulate $A_{2A}R$ expression when activated in an animal model of neuroinflammation (Orr et al., 2009).

### 3.5.5 Intracellular and extrasynaptic localization of $A_{2A}R$ in the striatum

Our immunogold data indicate that the majority (75-85%) of $A_{2A}R$ labeling in the striatum and GPe is located in the intracellular compartment of pre- or post-synaptic immunoreactive elements. This could be indicative of a high level of turnover of $A_{2A}$ receptors at the cell membrane. Alternatively, in vitro reports from neuronal and non-neuronal cultures suggest that intracellular $A_{2A}Rs$ could be in latent storage awaiting certain conditions under which they could be mobilized to the plasma membrane, thereby increasing the neuron's sensitivity to extracellular adenosine (Milojevic et al., 2006). It has also been found that $A_{2A}Rs$, like many G-protein-coupled receptors, internalize in response to agonist administration (Brand et al., 2008), suggesting that some of this intracellular labeling may be the result of an abnormal increase in the extracellular concentration of adenosine under hypoxic conditions at the time of perfusion (Hagberg et al., 1987), followed by activation and internalization of receptors. However, in vitro data argue against this hypothesis by showing that $A_{2A}Rs$ mobilize to the plasma membrane under anoxic conditions (Arslan et al., 2002). It is unclear which of these processes would prevail in vivo.

Yet another possibility is that intracellular $A_{2A}Rs$ have a function inside the cell. While this is still a topic of great controversy, a growing body of evidence suggests that intracellular G-protein-coupled receptors may have functional signaling roles at multiple intracellular sites, including the Golgi apparatus, endoplasmic reticulum, and cell nucleus (Boivin et al., 2008). While intracellular functions of $A_{2A}Rs$ have not been reported, it is worth noting that mGluR5, with which $A_{2A}R$ interacts (Ferre et al., 1999; Ferre et al.,

2002), is often localized on the nuclear membrane, through which it regulates nuclear calcium levels (O'Malley et al., 2003).

Of the plasma membrane-bound $A_{2A}R$-associated gold particles, the majority (97-98%) was found at extrasynaptic sites, which is a common feature for many G-protein coupled receptors (Galvan et al., 2006). These extrasynaptic $A_{2A}$ receptors are most likely activated only during high levels of neuronal metabolic activity when large-scale adenosine triphosphate (ATP) hydrolysis leads to grossly increased extracellular adenosine levels across entire nuclei (Nordstrom et al., 1977), via bidirectional non-concentrative nucleoside transporters (Geiger and Fyda, 1991). Astrocytes represent another likely source of adenosine for these extrasynaptic receptors, as they can release both adenosine and ATP (which is rapidly converted to adenosine (Dunwiddie et al., 1997)) via facilitated transport or a calcium-dependent vesicular mechanism, in response to hypoxia or chemical signals (Cunha, 2001; Martin et al., 2007; Parpura and Zorec, 2010). Extracellular adenosine levels in the striatum are in the low to mid nanomolar range under basal conditions (Ballarin et al., 1991), which is enough to produce a low tone of $A_{2A}R$ activation ($EC_{50}$ of adenosine at $A_{2A}R$ is ~700 nm (Dunwiddie and Diao, 1994; Fredholm et al., 2001)). Under hypoxic conditions, striatal adenosine levels can increase into the micromolar range (Hagberg et al., 1987), probably activating most $A_{2A}Rs$.

Although they were rare (2-3%), we did find some pre- and post-synaptic $A_{2A}$ receptors at synaptic and perisynaptic sites in the monkey striatum, which is in agreement with previous rodent data (Ciruela et al., 2006). These $A_{2A}$ receptors most likely respond to synaptically-released adenosine or ATP, which are co-released with other

neurotransmitters (Cunha and Ribeiro, 2000; Latini and Pedata, 2001), even during lower levels of synaptic activity.

### 3.5.6 Postsynaptic co-localization of $A_{2A}R$ and mGluR5 in striatal neurons: Potential sites of functional interactions

As mentioned above, $A_{2A}R$ and mGluR5 physically interact and display a functional synergy whereby simultaneous activation or inhibition of both receptors produces greater effects than the sum of the modulation of each receptor alone (Ferre et al., 1999; Ferre et al., 2002). This functional synergy is relevant to several biological phenomena and possibly therapeutic benefits of $A_{2A}R$ antagonists in movement disorders and other brain disorders (Coccurello et al., 2004; Kachroo et al., 2005; Adams et al., 2008). For instance, in the hippocampus, where $A_{2A}R$ and mGluR5 co-localize at individual glutamatergic synapses, the synergistic effects of both receptor agonists upon their respective targets potentiate NMDA receptor activity more strongly than individual receptor activation, suggesting a possible role for $A_{2A}R$/mGluR5 functional interactions in learning and memory (Tebano et al., 2005).

There is also evidence from in vitro data supporting functional $A_{2A}R$/mGluR5 interactions in the rat striatum (Ferre et al., 1999; Ferre et al., 2002; Nishi et al., 2003). However, in contrast to our findings that support a high level of $A_{2A}R$/mGluR5 co-expression only in postsynaptic elements in the monkey striatum, other in vitro data described as much as 50% of striatal terminals that co-express mGluR5 and $A_{2A}R$ immunoreactivity in isolated striatal nerve terminal preparations (Rodrigues et al., 2005). These findings were corroborated with functional studies showing that agonists for $A_{2A}R$ and mGluR5 synergistically interact to enhance $K^+$-induced glutamate release from rat

synaptosomal preparations. However, these data are at odds with ultrastructural data indicating that striatal mGluR5 immunoreactivity is largely localized post-synaptically in rats (Shigemoto et al., 1993). Similarly, the ultrastructural localization of $A_{2A}R$ and mGluR5 described in the present study, and our previous reports in the monkey striatum showing little evidence for presynaptic mGluR5 (Paquet and Smith, 2003; Mitrano and Smith, 2007), strongly suggest that the main target sites for functional interactions between these receptor subtypes are the spines and dendrites of striatal projection neurons. It is possible that the presynaptic synaptosomal membrane fractions prepared by Rodrigues et al. (2005) also included postsynaptic material containing mGluR5, leading to an overestimation of the prevalence of presynaptic mGluR5 immunoreactivity. Alternatively, the disparity could be due to a shift from a significant pre-synaptic mGluR5 expression in young animals (2-3 weeks old) to an almost exclusive post-synaptic localization in adults (Hubert and Smith, 2004). Whether the discrepancies rely on technical differences remains unknown, but we cannot rule out the possibility that the small amount of presynaptic mGluR5 in the adult striatum is functionally relevant, thereby suggesting that striatal and pallidal axon terminals may be another potential site for $A_{2A}R$/mGluR5 interactions. Although we did find presynaptic co-localization of the two receptors in the monkey putamen, it was rare, accounting for only 2-6% of striatal double-labeled elements.

It is worth noting that the pattern of striatal $A_{2A}R$ immunogold labeling (mainly postsynaptic, largely intracellular with a smaller membrane-bound component composed mostly of extrasynaptic receptors) is very similar to the pattern of striatal mGluR5 immunogold labeling previously described in the monkey striatum (Paquet and Smith,

2003). The neuronal signaling via these large pools of extrasynaptic receptors could become very important during periods of high neuronal activity, like in the parkinsonian state when corticostriatal glutamatergic transmission is abnormally overactive (Calabresi et al., 1993). With large-scale breakdown of ATP and overflow of synaptic glutamate, these two groups of extrasynaptic receptors might be simultaneously activated and synergistically interact to greatly increase the excitability of indirect pathway MSNs. This scenario suggests a potential role for $A_{2A}$R/mGluR5 interactions in PD pathophysiology.

### 3.5.7 Therapeutic relevance of $A_{2A}$R/mGluR5 antagonists in Parkinson's disease

Antagonists at $A_{2A}$R and mGluR5 both decrease motor deficits in experimental rodent models of parkinsonism (Breysse et al., 2002; Ossowska et al., 2002; Breysse et al., 2003; Tanganelli et al., 2004; Ossowska et al., 2005; Ossowska et al., 2007; Pinna et al., 2007). When given together, $A_{2A}$R and mGluR5 antagonists produce a synergistic improvement in locomotion of reserpinized mice (Kachroo et al., 2005) and in the performance of a reaction time task in 6-OHDA-treated rats (Coccurello et al., 2004). Despite some success in preclinical studies (Grondin et al., 1999; Kanda et al., 2000; Bibbiani et al., 2003), the administration of the $A_{2A}$R antagonist istradefylline (also known as KW-6002), alone or in combination with levodopa, has had limited success in alleviating parkinsonian symptoms in PD patients (Bara-Jimenez et al., 2003; Hauser et al., 2003; Fernandez et al., 2010), although the antagonist appeared to be safe and well-tolerated in humans. Based on the rodent behavioral data and our findings suggesting potential sites for $A_{2A}$R/mGluR5 interactions in the primate striatum, it appears reasonable to suggest that the combination of $A_{2A}$R and mGluR5 antagonists might be a

relevant non-dopaminergic approach to PD pharmacotherapeutics with improved efficacy.

Another strong interest for mGluR5 therapeutics in Parkinson's disease relates to the significant effect these drugs have on the development and progression of L-DOPA-induced dyskinesias (Johnston et al., 2010; Morin et al., 2010). $A_{2A}R$ antagonists also have anti-dyskinetic properties, at least in animal models (Morelli et al., 2007), though these pre-clinical data have not led to conclusive evidence for anti-dyskinetic effects in PD patients (Bara-Jimenez et al., 2003; Hauser et al., 2003; LeWitt et al., 2008; Stacy et al., 2008). In addition to their potential to treat the motor symptoms of PD, $A_{2A}R$ and mGluR5 antagonists have neuroprotective effects against degeneration of midbrain dopaminergic neurons in toxin-based models of PD (Chen et al., 2001; Battaglia et al., 2004; Aguirre et al., 2005; Bove et al., 2005; Pierri et al., 2005; Masilamoni et al., 2009; Nobre et al., 2010; Masilamoni et al., 2011).

Together, these findings highlight the exciting possibility that $A_{2A}R$/mGluR5 combination therapy might be used at various stages of the disease to treat multiple aspects of PD symptoms and pathology. The anti-parkinsonian, anti-dyskinetic, and neuroprotective benefits of $A_{2A}R$/mGluR5 combination therapy have never been tested in primates. With future research in these areas, it might be possible to take advantage of the synergy between these two receptors to greatly improve PD pharmacotherapeutics.

**3.6 Acknowledgements**

Thanks are due to Jean-Francois Pare and Susan Jenkins for technical assistance. Funding sources: Supported by a grant from the National Parkinson Foundation, the NIH

base grant to the Yerkes Primate Center (RR00165) and a National Research Service Award (F31 NS061520-01A2) to JB.

# Chapter 4

## *Specific Aim 3*

To characterize the subcellular localization of metabotropic glutamate receptor 4 and examine the electrophysiological effects of local infusion of group III or mGluR4 agonists on firing rates and patterns of neurons in the MPTP-treated monkey GPe and putamen.

Bogenpohl J, Galvan A, Hu X, Wichmann T, Smith Y. Metabotropic glutamate receptor 4 in the basal ganglia of parkinsonian monkeys: Ultrastructural localization and electrophysiological effects of activation in the striatopallidal complex. Neuropharmacology, 2012; In press.

## 4.1 Abstract

Group III metabotropic glutamate receptors (mGluR4,7,8) are widely distributed in the basal ganglia. Injection of group III mGluR agonists into the striatopallidal complex alleviates parkinsonian symptoms in 6-hydroxydopamine-treated rats. *In vitro* rodent studies have suggested that this may be partly due to modulation of synaptic transmission at striatopallidal and corticostriatal synapses through mGluR4 activation. However, the *in vivo* electrophysiological effects of group III mGluRs activation upon basal ganglia neurons activity in nonhuman primates remain unknown. Thus, in order to examine the anatomical substrates and physiological effects of group III mGluRs activation upon striatal and pallidal neurons in monkeys, we used electron microscopy immunohistochemistry to localize mGluR4, combined with local administration of the group III mGluR agonist L-AP4, or the mGluR4 positive allosteric modulator VU0155041, to assess the effects of group III mGluR activation on the firing rate and pattern of striatal and pallidal neurons in 1-methyl 4-phenyl 1,2,3,6-tetrahydropyridine (MPTP)-treated parkinsonian monkeys.

At the ultrastructural level, striatal mGluR4 immunoreactivity was localized in pre- (60%) and post-synaptic (30%) elements, while in the GPe, mGluR4 was mainly expressed presynaptically (90%). In the putamen, terminals expressing mGluR4 were evenly split between putative excitatory and inhibitory terminals, while in the GPe, most labeled terminals displayed the ultrastructural features of striatal-like inhibitory terminals, though putative excitatory boutons were also labeled. No significant difference was found between normal and parkinsonian monkeys. Extracellular recordings in awake MPTP-treated monkeys revealed that local microinjections of small volumes of L-AP4

resulted in increased firing rates in one half of striatal cells and one third of pallidal cells, while a significant number of neurons in both structures showed either opposite effects, or did not display any significant rate changes following L-AP4 application. VU0155041 administration had little effect on firing rates. Both compounds also had subtle effects on bursting and oscillatory properties, acting to increase the irregularity of firing. The occurrence of pauses in firing was reduced in the majority (80%) of GPe neurons after L-AP4 injection. Our findings indicate that glutamate affects striatal and pallidal neurons through activation of pre-synaptic group III mGluRs at inhibitory and excitatory synapses in parkinsonian monkeys.

## 4.2 Introduction

Drugs that antagonize glutamate transmission have been of interest for years as treatments for Parkinson's disease, as they may reverse some of the major pathophysiologic hallmarks of the disease, i.e. the increased glutamatergic corticostriatal and subthalamofugal transmission (Blandini et al., 1996; Greenamyre, 2001; Chase et al., 2003). However, early studies that focused on antagonizing ionotropic glutamate receptors as treatments for Parkinson's disease and other conditions were generally disappointing, largely due to the occurrence of debilitating side effects, which may have resulted from unwanted drug actions outside of the intended targets (Hughes, 1997; Blandini and Greenamyre, 1998; Smith et al., 2012). In contrast, because of their modulatory effects and more restricted regional distributions, the G-protein coupled metabotropic glutamate receptors (mGluRs) have become attractive targets for glutamate-based pharmacotherapies in Parkinson's disease (Breysse et al., 2003; Marino and Conn,

2006; Lopez et al., 2007; Ossowska et al., 2007; Johnson et al., 2009; Smith et al., 2012). These receptors are divided into three major groups based on their structure, pharmacology, and coupling to second messenger systems. Group I mGluRs (mGluR1 and mGluR5) are mainly expressed postsynaptically and increase neuronal excitability when activated, while group II (mGluR2 and mGluR3) and group III (mGluR4, mGluR6, mGluR7, and mGluR8) receptors are commonly found in presynaptic neuronal elements, where they decrease neurotransmitter release by inhibition of adenylyl cyclase.

In light of anatomical, electrophysiological and behavioral studies in rodents, it has become clear that activation of mGluR4 may represent a useful approach to normalize basal ganglia circuit activity, and relieve PD motor symptoms (Marino et al., 2003; Valenti et al., 2003; Lopez et al., 2007; Lopez et al., 2008; Beurrier et al., 2009; Johnson et al., 2009; Smith et al., 2012). In rats, mGluR4 is strongly expressed in the globus pallidus (GP), where it is localized predominantly in putative striatopallidal GABAergic terminals (Bradley et al., 1999; Corti et al., 2002). Activation of mGluR4 attenuates inhibitory postsynaptic currents induced by striatal stimulation in rat GP slices (Matsui and Kita, 2003; Valenti et al., 2003; Beurrier et al., 2009). Through this decrease of the striatopallidal GABAergic transmission, mGluR4 activation can disinhibit GP neurons, thereby increasing the pallidal inhibitory drive to the abnormally overactive subthalamic nucleus (STN) and potentially correcting aberrant basal ganglia circuit activity in the parkinsonian state (Marino and Conn, 2006; Johnson et al., 2009; Niswender and Conn, 2010). Parkinsonian motor signs are, indeed, improved in rodent models of PD following intracerebral administration of group III mGluR agonists or mGluR4 positive allosteric modulators (Marino et al., 2003; Valenti et al., 2003;

MacInnes et al., 2004; Marino et al., 2005; Konieczny et al., 2007; Lopez et al., 2007; Beurrier et al., 2009; Cuomo et al., 2009). The recent development of mGluR4 potentiators with reliable pharmacokinetic properties and efficient brain penetration has set the stage for trials of mGluR4-related PD pharmacotherapeutics (Niswender and Conn, 2010; Engers et al., 2011; Smith et al., 2012).

In light of the promising rodent data, we aimed to characterize the target sites and physiological effects of mGluR4-related drugs in the primate basal ganglia, using a combination of light and electron microscopic immunohistochemistry, local application of group III mGluR-related drugs in the striatopallidal complex, and *in vivo* single unit recordings of striatal and pallidal neurons in awake parkinsonian rhesus monkeys. Some of the findings of this study have been presented in abstract forms (Bogenpohl et al., 2010; Bogenpohl et al., 2011).

## 4.3 Material and Methods

### 4.3.1 Animals

Eleven adult rhesus macaques (7 males, 4 females; 2-9 years old) were used in this study. All experiments were performed in accordance with the National Institutes of Health's Guide for the Care and Use of Laboratory Animals and the United States Public Health Service Policy on Humane Care and Use of Laboratory Animals. Five of these monkeys were treated with weekly systemic injections of 1-methyl-4-phenyl-1,2,3,6-tetrahydropyridine (MPTP; 0.2-0.8 mg/kg/week; Sigma, St. Louis, MO; total cumulative doses ranged from 14 to 33 mg/kg, total treatment time ranged from 8 to 16 months) until moderate parkinsonian motor signs were observed.

The severity of parkinsonism was assessed as previously described (Wichmann et al., 2001; Kliem et al., 2010). Briefly, animals were transferred to an observation cage, in which locomotor behavior was measured by counting infrared beam breaks, and by direct visual quantification of the number of movements made by different body parts. A parkinsonism rating scale was also used to quantify parkinsonism. Following the development of moderate parkinsonian motor signs that remained stable for a period of at least 6-8 weeks after MPTP administration, two of the parkinsonian monkeys and three normal, untreated monkeys were trained to sit calmly in a restraint chair before being chronically implanted with transcranial recording chambers for electrophysiological experiments.

The remaining three MPTP-treated parkinsonian monkeys and three untreated animals were deeply anesthetized with pentobarbital (100 mg/kg i.v.) and transcardially perfused with cold oxygenated Ringer's solution, followed by a fixative containing 4% paraformaldehyde and 0.1% glutaraldehyde in a phosphate buffer (PB) solution, for immunohistochemistry. After perfusion, brains were removed from the skull, sliced coronally into thick (~1 cm) blocks, and post-fixed overnight in 4% paraformaldehyde. These blocks were cut into 60 μm-thick coronal sections using a vibrating microtome and stored at -20° C in an anti-freeze solution, containing 30% ethylene glycol and 30% glycerol in PB, until ready for immunohistochemistry.

### 4.3.2 Immunohistochemistry

#### *4.3.2.1 Pre-embedding immunoperoxidase for light microscopy*

The localization of mGluR4 was achieved using a highly specific polyclonal antibody (Invitrogen, Carlsbad, CA; Catalog # 51-3100; 1:200 dilution) raised in rabbit

against a 200 amino acid C-terminal fragment of the rat mGluR4 protein. This antibody is specific for the mGluR4a splice variant. Reactivity with other related proteins has not been detected on immunoblots of transfected cells expressing other mGluR subtypes (Invitrogen). This antibody does not stain brain tissue from mGluR4 knockout mice (unpublished data). Depletion of the dopaminergic nigrostriatal system in MPTP-treated animals was confirmed in 3 of the 5 animals in this study (the 2 remaining animals are still alive at the time of this report) by staining sections at the level of the striatum and the substantia nigra with mouse anti-tyrosine hydroxylase (TH) antibodies (1:1000, Millipore; not shown).

Brain sections taken from various antero-posterior levels of the basal ganglia in 2 normal and 2 MPTP-treated monkeys were processed for light microscopy (LM) immunohistochemical localization of mGluR4. Prior to immunohistochemical (IHC) processing, brain sections were washed with phosphate buffered saline (PBS; 0.01M, pH 7.4), treated with a 1% sodium borohydride solution for 20 minutes, and washed in PBS once more.

Sections were incubated for 1 hour in PBS containing 10% normal goat serum (NGS), 1% bovine serum albumin (BSA), and 0.3% Triton X-100, followed by incubation in the primary antibody solution containing 1% NGS, 1% BSA, and 0.3% Triton X-100 in PBS for 48 hours at 4°C. Sections were then rinsed three times in PBS and incubated in the secondary antibody solution containing 1% NGS, 1% BSA, 0.3% Triton X-100, and biotinylated goat anti-rabbit IgGs (Vector Laboratories, Burlingame, CA) at a dilution of 1:200 for 90 minutes at room temperature. After three rinses in PBS, sections were incubated for 90 minutes in avidin-biotin peroxidase complex (ABC)

solution at a dilution of 1:100 (Vectastain standard ABC kit, Vector Laboratories) including 1% BSA.

To reveal the antigenic sites, sections were first rinsed with PBS and Tris buffer (50 mM; pH 7.6), then incubated in a solution containing 0.025% 3,3'-diaminobenzidine tetrahydrochloride (DAB; Sigma), 10 mM imidazole, and 0.005% hydrogen peroxide in Tris buffer for 10 minutes. Sections were then washed several times in PBS, mounted on gelatin-coated glass slides, dehydrated, and coverslipped with Permount™.

The slides were scanned at 20X using a ScanScope CS scanning light microscope system (Aperio Technologies, Vista, CA). Digital representations of the slides were saved and analyzed using ImageScope software (Aperio Technologies).

*4.3.2.2 Pre-embedding immunoperoxidase for electron microscopy*

Sections containing the striatopallidal complex from 3 normal and 3 MPTP-treated monkeys were transferred to a cryoprotectant solution containing 25% sucrose and 10% glycerol in PB (0.05M, pH 7.4) for 20 minutes and then placed in a -80°C freezer for 20 min to permeabilize cell membranes. They were then thawed through washes in decreasing concentrations of cryoprotectant solution until being washed in PBS. The subsequent tissue processing was identical to that used for light microscopy, up to the point of DAB revelation, with two important differences: Triton X-100 was omitted from all solutions, and sections were incubated in the primary antibody solution for 48 hours at 4°C.

After DAB revelation, the tissue was rinsed in PB (0.1M, pH 7.4) and treated with 1% osmium tetroxide for 20 minutes. It was then rinsed with PB and dehydrated with increasing concentrations of ethanol, up to 100%. Uranyl acetate (1%) was added to the

70% EtOH dehydration solution and incubated for 35 minutes in order to increase the contrast of membranes in the electron microscope. After alcohol dehydration, sections were treated with propylene oxide, embedded in epoxy resin (Durcupan ACM; Fluka, Buchs, Switzerland) for at least 12 hours, mounted onto slides, and placed in a 60°C oven for 48 hours to cure the resin.

*4.3.2.3 EM observations and analysis*

Small blocks of tissue from the dorsolateral putamen or GPe were cut out from the embedded sections and glued onto resin blocks for ultrathin sectioning with an ultramicrotome (Leica Ultracut T2). Sixty-nanometer-thick sections were collected from the surface of the tissue block to ensure that antibody penetration was optimal in the tissue analyzed in the EM. Sections were mounted on single-slot pioloform-coated copper grids, stained for 5 minutes with lead citrate, and examined with a Zeiss EM-10C transmission electron microscope. Electron micrographs were captured and saved with a CCD camera (DualView 300W; Gatan, Inc., Pleasanton, CA) controlled by DigitalMicrograph software (version 3.11.1; Gatan, Inc.). Fifty micrographs of randomly-encountered mGluR4-labeled neuronal elements were captured at 25,000X in the GPe and putamen of each monkey, giving a total of 581 $\mu m^2$ of tissue analyzed per structure per animal. Immunoperoxidase labeling for mGluR4 could be identified as a dark, amorphous deposit in the cytoplasm of labeled neuronal elements. Immunoreactive elements were classified based on ultrastructural features (Peters et al., 1991), quantified, and plotted as distribution histograms.

**4.3.3 Electrophysiology**

*4.3.3.1 Surgical procedure*

Two of the MPTP-treated parkinsonian monkeys and three normal monkeys were implanted with bilateral chronic recording chambers. Under aseptic conditions and isofluorane anesthesia (1-3%), recording chambers were stereotaxically positioned over trephine holes in the skull to provide chronic access to striatum and GP, using a lateral coronal approach (36º angle from the vertical). The chambers and a head post receptacle were attached to the animal's skull with dental acrylic and stainless steel bone screws. After surgery, monkeys were allowed to recover for at least one week.

*4.3.3.2 Electrophysiological mapping of brain structures*

All recordings were performed in fully awake monkeys (determined by video surveillance showing open eyes and occasional movements). The animals were sitting in a restraint chair with the head immobilized and the body and limbs free to move. In each session, the dura was pierced with a guide tube, and a tungsten microelectrode (Z = 0.5-1.0 MΩ at 1 kHz; FHC, Bowdoinham, ME) was lowered into the brain using a microdrive (MO-95B; Narishige, Tokyo, Japan), using pre-determined anteroposterior and mediolateral positions. Extracellular neuronal electrical signals were recorded, amplified (DAM-80 amplifier; WPI, Sarasota, FL), filtered (400-6,000 Hz; Krohn-Hite, Brockton, MA), displayed on a digital oscilloscope (DL1540; Yokogawa, Tokyo, Japan), and made audible via an audio amplifier. Neuronal signals were digitized (sampling rate 25 kHz) and stored on a hard drive using a data acquisition interface (Power1401; CED, Cambridge, UK) and commercial software (Spike2, CED) for off-line analysis.

The actual locations of brain structures below the chambers were delineated by electrophysiological mapping. The putamen region was characterized by a mixture of

neurons, some showing slow background firing rate, while others presented sustained spontaneous activity and regular discharge (see below for further details on these two neuronal types). GPe cells were identified by their location in relation to the overlying putamen and their characteristic high frequency discharge, interspersed with pauses (DeLong, 1971; Elias et al., 2007).

| | | Normal | MPTP |
|---|---|---|---|
| Number of neurons | | 24 | 51 |
| ISI CV | | 1.6±1.6 | 1.3±0.6 |
| Firing rate (spikes/s) | | 65.1±34.1 | 55.2±22.0 |
| Power spectral components (% within stated spectral bins) | 1-3 Hz | 2.8±2.4 | 2.18±1.56 |
| | 3-8 Hz | 1.4±0.9 | 1.4±0.9 |
| | 8-13 Hz | 0.7±0.4 | 0.9±0.5* |
| | 13-30 Hz | 0.6±0.2 | 0.7±0.2* |
| | 30-100 Hz | 1.1±0.2 | 1.0±0.2 |
| Burst index (spikes, %) | | 26.0±22.1 | 29.4±17.6 |
| Burst index (time, %) | | 8.1±6.2 | 8.7±4.5 |
| Deceleration index (spikes, %) | | 3.6±2.8 | 4.3±2.6 |
| Deceleration index (time, %) | | 14.1±14.7 | 14.3±10.7 |
| Pause index (spikes, %) | | 0.4±0.5 | 0.1±0.2* |
| Pause index (time, %) | | 9.5±8.7 | 3.2±3.5* |

**Table 4.1** – Descriptors of neuronal firing in the GPe; comparison of MPTP-treated monkeys with data from normal monkeys previously acquired (Galvan et al., 2011). Values are means ± standard deviation. *statistically different from normal; t-test, $p<0.05$

*4.3.3.3 Intracerebral injections*

Intracerebral microinjections were performed in two MPTP-treated monkeys with a custom-built device ("injectrode"), consisting of a tungsten microelectrode which was fused to a thin silica tube, as described previously (Kliem and Wichmann, 2004; Galvan et al., 2005; Galvan et al., 2010). The injection tubing was connected to a 1 ml gas-tight syringe (CMA Microdialysis, Solna, Sweden), driven by a computer-controlled infusion pump (Model 102, CMA).

The injectrode was lowered into the putamen or GPe using the microdrive, and positioned to isolate single neurons for recording. If two or more neurons were present near the tip of the injectrode (as determined by visual inspection of the recorded waveforms on the oscilloscope), the injectrode was moved slightly up or down to isolate a single neuron. If adjustments could be made to obtain a difference in spike amplitude of approximately two-fold, recording and injection commenced with focus on the larger-amplitude cell. In these cases, spikes from the two recorded cells were separated in the spike sorting step (see below).

Spontaneous baseline activity of each cell was recorded for at least 60 seconds before drug infusion. Recording continued through the drug injection (0.4 µL at 0.2 µL/min) and for at least 5 min after the end of the infusion. In some cases, more than one injection was performed along the same tract. In these cases, the recording/injection sites were separated by at least 1 mm, and a time lapse of at least 30 min was allowed to pass before the next recording could begin, to minimize residual effects of the previous injection.

*4.3.3.4 Drugs*

The group III mGluR agonist L-AP4 (20 or 50 mM; Tocris Bioscience, Bristol, UK), and the mGluR4 allosteric potentiator VU0155041 (4 mM, generous gift of Niswender, Conn et al., Vanderbilt University) were used (Engers et al., 2009; Engers et al., 2010; Engers et al., 2011). The choice of optimal concentrations was based on previous rodent data showing antiparkinsonian efficacy (Lopez et al., 2007; Cuomo et al., 2009). Due to the limited solubility of VU0155041 in aqueous solutions, 4mM was the highest concentration achieved for the intracerebral injections. The drugs were dissolved in artificial cerebrospinal fluid (aCSF, comprised of (in mM) 143 NaCl, 2.8 KCl, 1.2 $CaCl_2$, 1.2 $MgCl_2$, 1 $Na_2HPO_4$), and the pH adjusted to 7.2-7.4. Before being loaded into the injection syringe, all solutions were filtered with a 0.2 µm pore size nylon membrane (Fisher Scientific). Artificial CSF was used for control injections.

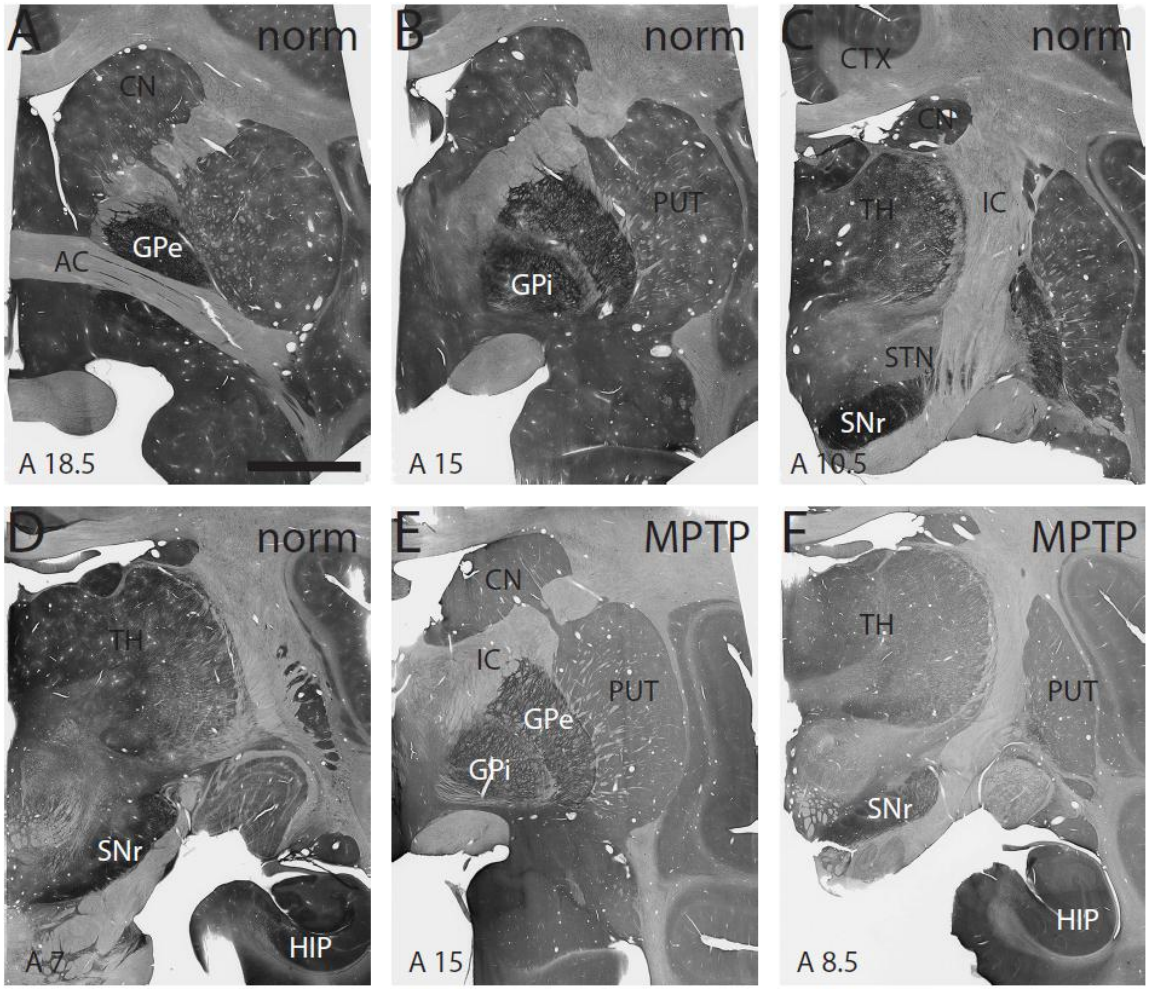


**Figure 4.1** – Light micrographs of coronal monkey brain sections showing immunostaining for mGluR4 at various levels of a normal (A-D) and an MPTP-treated monkey (E,F). The approximate interaural coordinate for each section is designated in the lower left of each panel. Scale bar in A equals 5 mm and applies to all panels. AC – anterior commissure, CN – caudate nucleus, CTX – cortex, GPe – external globus pallidus, GPi – internal globus pallidus, HIP – hippocampus, IC – internal capsule, PUT – putamen, SNc – substantia nigra pars compacta, SNr – substantia nigra pars reticulata, TH - thalamus.

*4.3.3.5 Analysis of electrophysiological data*

Spike sorting was performed off-line with a waveform matching algorithm, followed by principal component analysis (Spike2). Inter-spike interval (ISI) distribution histograms were generated and examined for each cell to verify the quality of the

recording and spike sorting. All subsequent steps of the analysis were done in Matlab (Mathworks, Natick, MA).

ISI data were used to generate second-by-second readouts of firing rates (FRs) and coefficients of variance (CV; ISI standard deviation/mean ISI; an index of the irregularity of neuronal firing) in 20 sec bins, which were subsequently smoothed using a sliding 20-point moving average. These readouts were plotted and used to select a 'baseline segment' (at least 60 sec immediately preceding drug or aCSF infusion) and a drug 'effect segment'. Drug effect segments were selected by determining if the firing rate or CV passed beyond the $90^{th}$ or below the $10^{th}$ percentile of the baseline segment data, continuously for at least 90 sec. Drug effects had to begin within an 'effect window' beginning 30 sec after the beginning of drug infusion, and ending 120 sec after the end of the drug infusion. A 60 sec 'effect segment' containing the peak of the drug effect was selected for further analysis. For cells which did not fulfill the above requirements to define a drug effect, a 60 sec segment of firing rate and CV data was randomly selected from the effect window for further analysis.

The magnitude of each drug effect was calculated as the mean firing rate or CV during the effect segment, expressed as a ratio (mean of effect segment/mean of baseline segment, termed FR ratios, or CV ratios, respectively). For the group of cells infused with aCSF, the $90^{th}$ and $10^{th}$ percentiles of FR ratios and CV ratios were calculated (Figs. 4.6, 4.7; dashed horizontal lines). Cells infused with L-AP4 or VU0155041 whose FR ratios or CV ratios were above the $90^{th}$ percentile or below the $10^{th}$ percentile of the aCSF group were classified as having significantly increased or decreased their firing rate or

CV values in response to the drug infusion, respectively. Otherwise, cells were classified as having no effect in response to drug infusion.

The Legendy and Salcman burst detection method was used to calculate burst indices (Legendy and Salcman, 1985; Wichmann and Soares, 2006). The method described by Elias et al. (2007), a variant of the Legendy-Salcman algoritm, was used to define deceleration of neuronal firing. A 'surprise' value of 3 was used for bursting or deceleration events. Burst and deceleration indices were defined as the proportion of spikes in the bursts or decelerations compared to the total number of spikes, or they were based on the proportion of time the cell spent in bursts or decelerations. Bursts were further classified as 'rebound bursts' if the ISI immediately preceding each burst was at least three times longer than the mean ISI for that neuron. Finally, pauses in firing were defined as cessations of neuronal activity of 500 ms or longer.

To examine oscillatory properties of neuronal discharge, a power spectral analysis was performed using the Neurospec 2.0 Matlab functions for frequency domain analyses, written by David Halliday (Halliday et al., 1995; Nielsen et al., 2005). For each neuron, the raw spectra were integrated in the 1-3 Hz, 3-8 Hz, 8-13 Hz, 13-30 Hz, and 30-100 Hz ranges, and the resulting values were expressed as fractions of the power in the entire 1-100 Hz band (for a similar approach see Soares et al., 2004).

*4.3.3.6 Characterization of striatal neurons*

Based on previous publications, striatal cells were classified as phasically active neurons (PANs, likely medium spiny neurons) if they had a FR $\leq$ 2.5 spikes/s and an ISI-CV $\geq$ 1; and as tonically active neurons (TANs, likely cholinergic interneurons) if they had a FR > 2 and < 12, and a CV <1. Cells that did not fulfill these criteria remained

"unclassified" and may represent other types of striatal interneurons, or PANs and TANs with uncharacteristic firing properties. It has been described that striatal cells might show increased firing rates after dopaminergic denervation induced by MPTP treatment (Liang et al., 2008). The only difference in the mean FR or CV of striatal cells that we recorded in normal and MPTP-treated monkeys was a small decrease in the FR of PANs of MPTP-treated monkeys (see Table 4.3).

*4.3.3. Data from normal monkeys*

For comparisons of basic neuronal firing characteristics of normal and MPTP-treated monkeys, we used data previously collected from normal monkeys, in the GPe (Galvan et al., 2005) and striatum (n=3 monkeys). The recording methods and analysis of data from normal monkeys was identical to that described above for MPTP-treated monkeys.

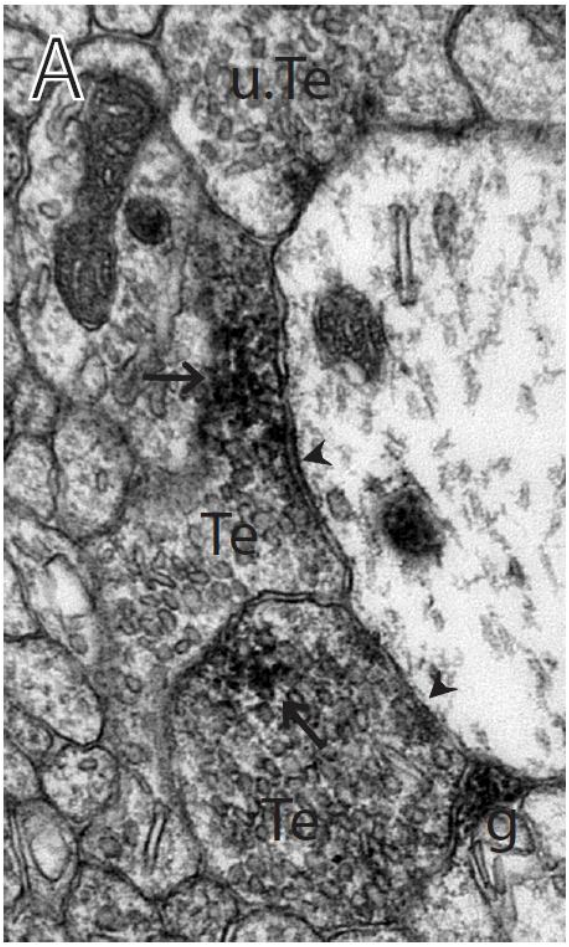
A
u.Te
Te
Te
g

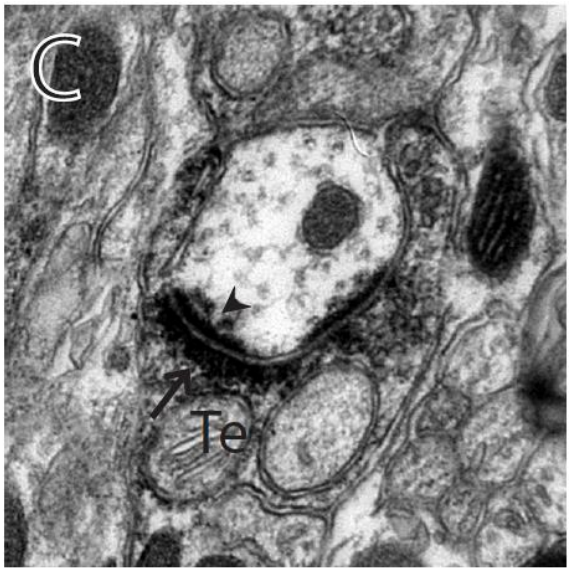
C
Te

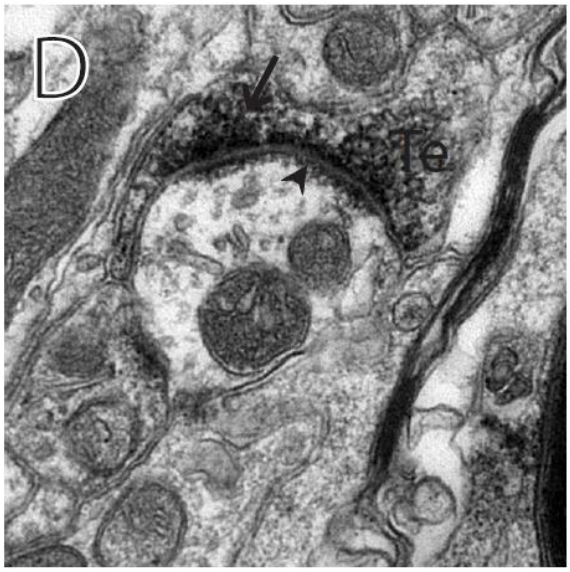
D
Te

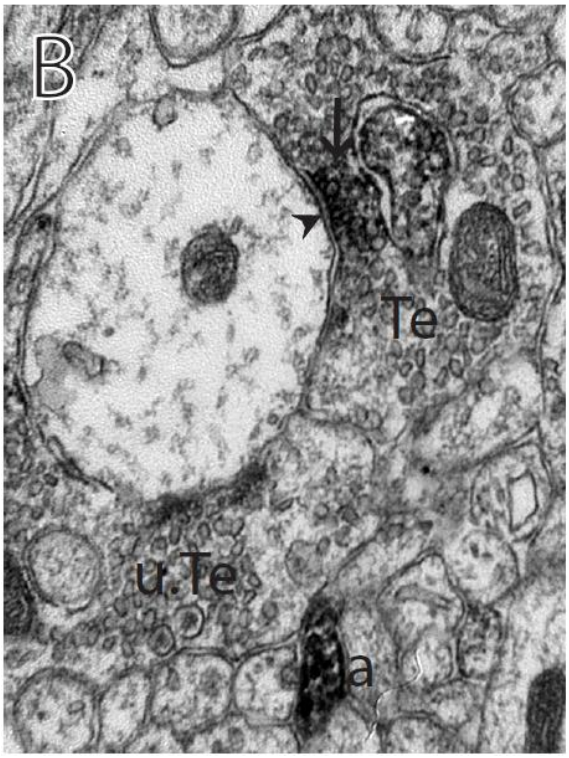
B
Te
u.Te
a

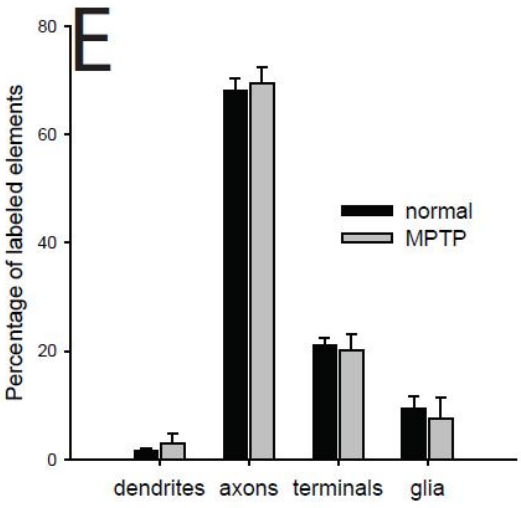
E
Percentage of labeled elements
80
60
40
20
0
normal
MPTP
dendrites
axons
terminals
glia

**Figure 4.2** – Immunolabeling for mGluR4 at the electron microscopic level in the monkey external globus pallidus. A, B) Labeled terminals form symmetric synapses on dendrites in the GPe. C, D) Labeled terminals form asymmetric synapses on dendrites in the GPe. E) Histogram showing the breakdown of the proportions of each type of labeled element found in the GPe of normal and MPTP-treated monkeys. n=3 normal, 3 MPTP-treated monkeys. Error bars represent SEM. No significant difference was found between normal and MPTP-treated monkeys. Synapses are identified with arrowheads. Immunoperoxidase labeling is identified with arrows. a – labeled axon, g – labeled glial process, Te – labeled terminal, u.Te – unlabeled terminal.

## 4.4 Results

### 4.4.1 mGluR4 localization in the primate basal ganglia

In order to characterize the potential sites through which mGluR4-related drugs could mediate their symptomatic antiparkinsonian effects in the primate brain, we examined the overall distribution of mGluR4 immunoreactivity in the basal ganglia nuclei of normal and parkinsonian monkeys. At the light microscopic level, mGluR4 immunoreactivity was expressed to varying degrees in the neuropil of cortical and subcortical forebrain regions, but the GPe and GPi were, by far, the two most strongly labeled forebrain regions (Fig. 4.1). The entire extent of GPe and GPi was invaded by a rich plexus of mGluR4-immunoreactive fibers. In contrast, significantly lighter labeling was found in the caudate nucleus, putamen, thalamus, hippocampus, and cerebral cortex which, in addition to modest neuropil immunoreactivity, also contained some immunoreactive perikarya. The SNr harbored dense mGluR4 neuropil immunoreactivity, while the SNc contained light to moderate perikaryal labeling with minimal neuropil immunoreactivity often associated with dendrite-like processes. STN neuronal cell bodies and proximal dendrites displayed light to moderate immunoreactivity. Overall, there was no clear difference in the pattern of mGluR4 labeling between normal and MPTP-treated monkeys (Fig. 4.1).

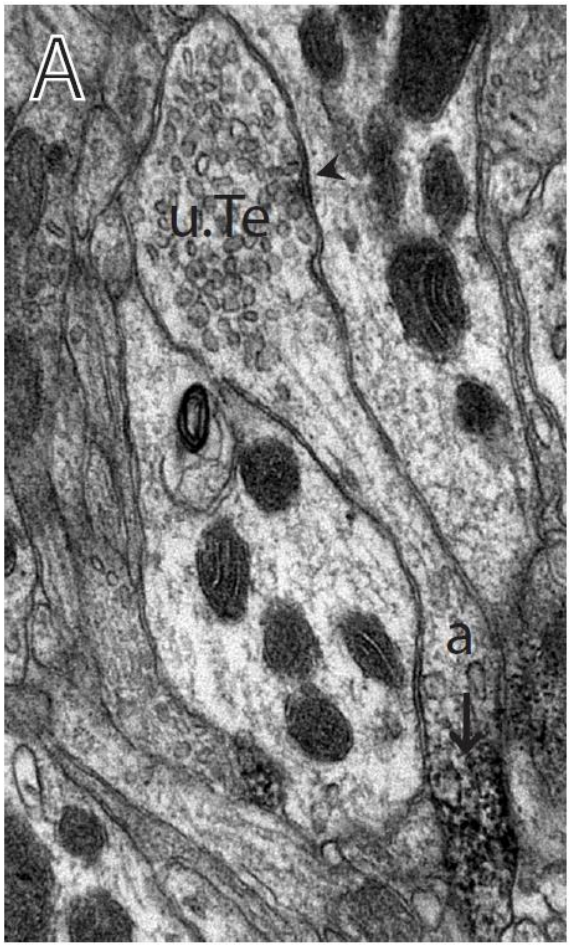
A
u.Te
a

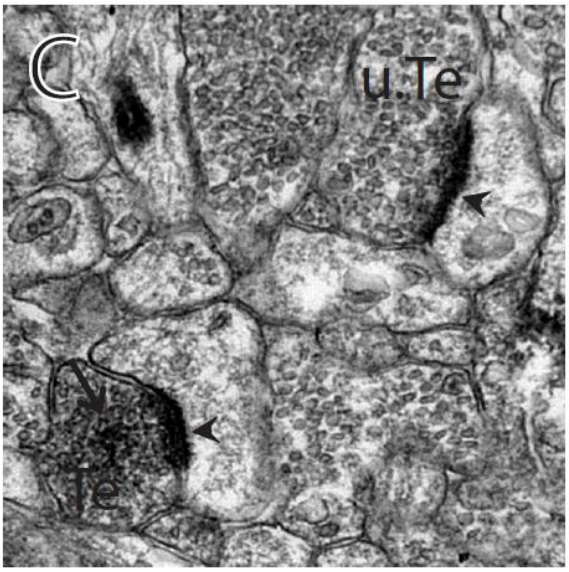
C
u.Te
Te

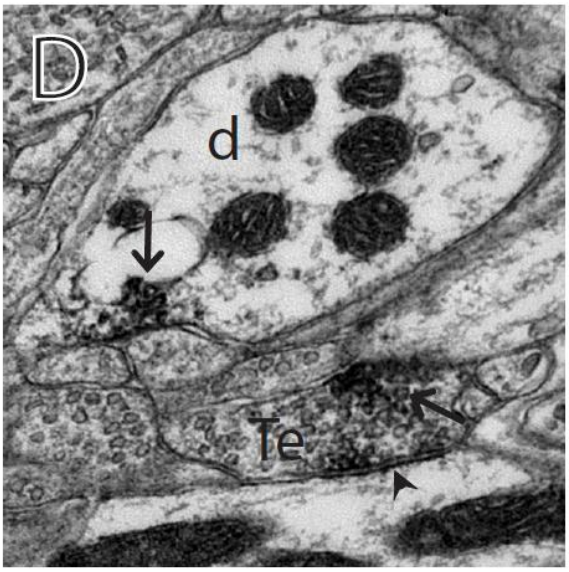
D
d
Te

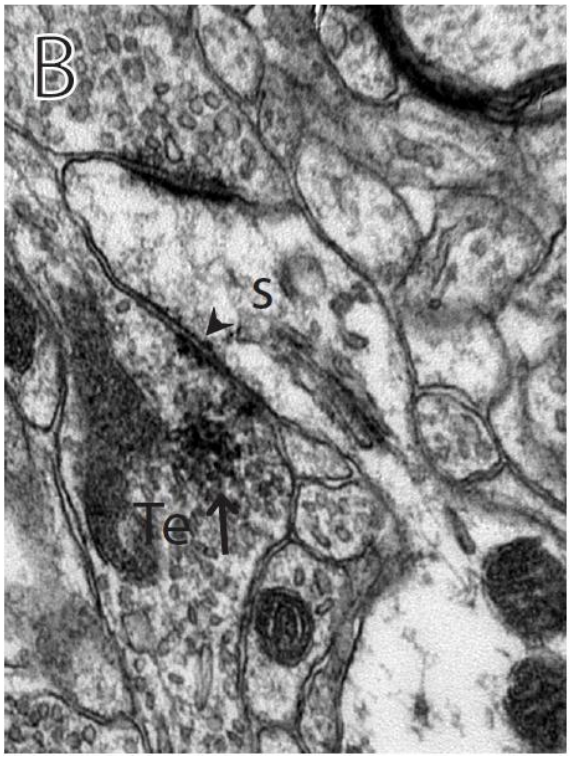
B
s
Te

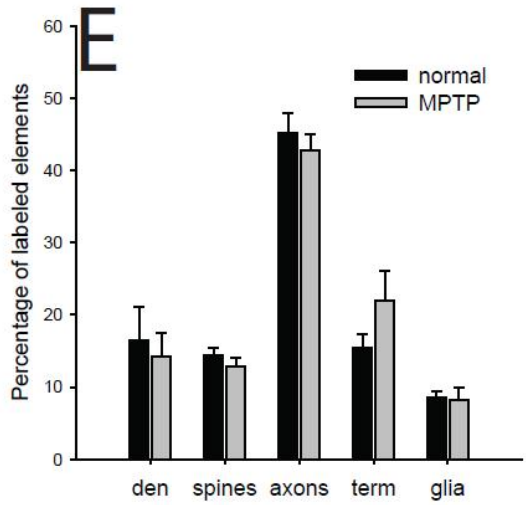
E
Percentage of labeled elements
60
50
40
30
20
10
0
normal
MPTP
den
spines
axons
term
glia

**Figure 4.3** – Immunolabeling for mGluR4 at the electron microscopic level in the monkey putamen. A) An unlabeled terminal arising from a labeled axon and forming a symmetric synapse on a dendrite. B) A labeled terminal forming a symmetric synapse on a spine. C) A labeled and an unlabeled terminal forming asymmetric synapses on spines. D) A labeled dendrite and a labeled terminal forming a symmetric synapse on a dendrite. E) Histogram showing the breakdown of the proportions of each type of labeled element found in the putamen of normal and MPTP-treated monkeys. n=3 normal, 3 MPTP-treated monkeys. Error bars represent SEM. No significant difference was found between normal and MPTP-treated monkeys. Synapses are identified with arrowheads. Immunoperoxidase labeling is identified with arrows. a – labeled axon, d – labeled dendrite, s - spine, Te – labeled terminal, u.Te – unlabeled terminal.

### 4.4.2 Ultrastructural analysis of mGluR4 in the striatopallidal complex

In the GPe of normal monkeys, mGluR4 immunoreactivity was primarily found in axons (68±2% of labeled elements, mean±SEM) and terminals (21±1%), with little postsynaptic (2±0.4%) or glial immunoreactivity (9±2%) (Fig. 4.2). Although the mGluR4 labeling in the putamen was also found predominantly in presynaptic elements (axons and terminals; 45±3% and 15±2% of labeled elements, respectively), a small but significant proportion of labeling was expressed postsynaptically (dendrites and spines; 16±5% and 14±1%, respectively), while glial immunostaining was rare (9±1%) (Fig. 4.3). No significant difference was found in the relative prevalence of labeled elements in the GPe (Pearson chi-square = 2.508, p=0.474) or the putamen (Pearson chi-square = 4.248, p=0.373) between normal and MPTP-treated monkeys (Figs. 4.2E and 4.3E).

Of the 52 mGluR4-immunoreactive axon terminals with clear synaptic specializations seen in the putamen of normal monkeys, 28 formed symmetric synapses, preferentially onto dendritic shafts and rarely onto spines (Fig. 4.3B), and 24 formed asymmetric synapses, usually onto spines and rarely onto dendritic shafts (Fig 4.4A), thereby suggesting that mGluR4 is localized to subserve presynaptic regulatory functions towards both glutamatergic and GABAergic transmission in the primate striatum. We

obtained similar findings in the putamen of MPTP-treated monkeys, where 21 of 56 mGluR4-positive terminals formed symmetric synapses, and the remaining 35 formed asymmetric synapses. Unlike the putamen, most mGluR4-immunoreactive terminals (122 of 128 in normal monkeys; 106 of 120 in MPTP-treated monkeys) in the GPe of normal animals formed symmetric axo-dendritic synapses and had ultrastructural features of striatal GABAergic boutons (Shink and Smith, 1995; Smith et al., 1998), while the remainder formed asymmetric axo-dendritic synapses (Fig. 4.4A).

Because GABAergic terminals account for almost 90% of the total population of axon terminals in the monkey GPe (Shink and Smith, 1995), the relative prevalence of the different categories of mGluR4-labeled terminals based on their type of synaptic specializations, must be interpreted cautiously. In order to provide a more accurate assessment of the preponderance of mGluR4-containing boutons relative to the size of the populations of putative GABAergic or glutamatergic terminals in the GPe, we quantified the percentages of the total populations of terminals forming symmetric or asymmetric synapses that displayed mGluR4 immunoreactivity (Fig 4.4B). We found that 30±4% of all GPe boutons involved in symmetric synapses contained mGluR4 labeling, while 23±6% of putative glutamatergic boutons forming asymmetric synapses did so in normal monkeys. No significant difference was found in the proportions of labeled terminals forming symmetric (t-test, $p=0.96$) or asymmetric synapses between normal and MPTP-treated monkeys, although there was a trend for a higher proportion of labeled asymmetric terminals in the GPe of MPTP-treated monkeys (40±4%; t-test, $p=0.063$).

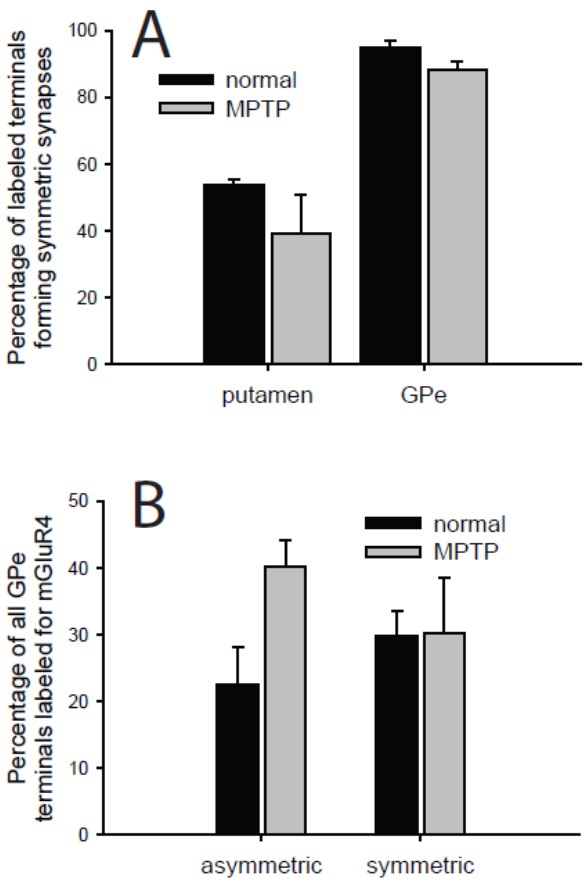


**Figure 4.4** – Prevalence of mGluR4-labeled terminal subtypes in the putamen and GPe. A) The percentage of mGluR4-positive terminals that formed symmetric synapses in normal and MPTP-treated monkeys. (N total labeled terminals=Normal: 52 in putamen, 128 in GPe; MPTP: 56 in putamen, 120 in GPe) B) The percentage of the total population of GPe terminals, forming asymmetric or symmetric synapses, that contained mGluR4 immunoreactivity. (N total GPe terminals labeled and unlabeled=Normal: 26 asymmetric, 412 asymmetric; MPTP: 33 asymmetric, 351 symmetric) Error bars represent SEM. No significant difference was found between normal and MPTP-treated monkeys. (N monkeys=3 normal, 3 MPTP-treated)

### 4.4.3 Electrophysiological effects of group III mGluR activation

*4.4.3.1 Basic firing characteristics of GPe neurons in normal vs. MPTP-treated monkeys*

To assess the electrophysiological effects of group III mGluRs activation on GPe neurons, single unit recordings were obtained from 51 GPe neurons in 2 MPTP-treated monkeys, in which the stability and isolation of single units was maintained before, during and after microinjections of aCSF or drugs in the vicinity of the recorded cells. Table 4.1 compares descriptors of neuronal firing recorded during the pre-injection (control) period in parkinsonian animals with values obtained under similar conditions in normal monkeys (data from normal monkeys obtained from (Galvan et al., 2011)).

The pause indices (based on the proportion of spikes or the proportion of time within pauses) were significantly lower in MPTP-treated monkeys than in controls. In

addition, we found higher oscillatory power in the 8-13 Hz and 13-30 Hz bands in the GPe of MPTP-treated monkeys than in controls (all differences assessed with t-test, $p<0.05$). The firing rate of GPe cells was lower in the MPTP-treated state, but this did not reach significance.

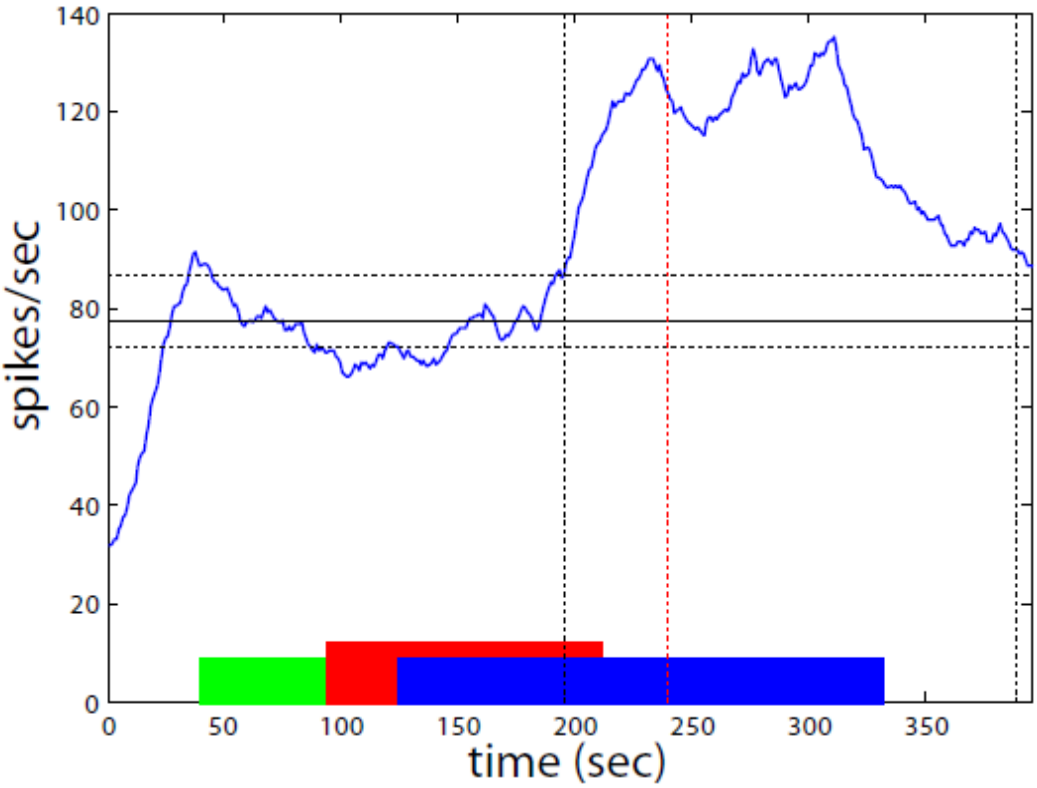


**Figure 4.5** – An example trace of a GPe neuron that increased its firing rate in response to L-AP4. The green bar represents the control period. The red bar represents the drug injection. The blue bar represents the window of time during which a drug effect may begin, in order to be considered as such. The solid horizontal line indicates the median firing rate at baseline, and the dashed lines show the 90$^{th}$ and 10$^{th}$ percentiles. The red vertical dotted line represents the center of the 60 sec period analyzed for drug effect.

*4.4.3.2 Group III mGluRs activation in the GPe*

The effects of local injections of L-AP4 (20 and 50 mM) and VU0155041 (4 mM) on the firing rate and CV values of GPe cells are summarized in Table 4.2 and Fig. 4.6. Increases and decreases in firing rate or CV are considered as such if they were above the

90th or below the 10th percentile of the aCSF cases' distribution (see Methods). No significant differences were found between cells treated with 20 and 50 mM L-AP4, so these data were pooled.

Eight of 27 GPe cells increased their firing rates after L-AP4 infusion (an example is shown in Fig. 4.5), while the remaining 19 cells showed no significant change in firing rate. The proportions of cells showing increased, decreased, or no change in firing rate were statistically different between the L-AP4 and aCSF groups (Chi-square test, p=0.02). VU0155041 (4 mM) had no significant effect on the firing rate of GPe neurons.

| GPe cells | Number of neurons | FR below 10th percentile | No FR effect | FR above 90th percentile | CV below 10th percentile | No CV effect | CV above 90th percentile |
|---|---|---|---|---|---|---|---|
| aCSF | 14 | 1 | 12 | 1 | 1 | 12 | 1 |
| L-AP4 | 27 | 0 | 19 | 8 | 2 | 22 | 3 |
| VU0155041 | 10 | 0 | 10 | 0 | 0 | 10 | 0 |

| Striatal cells | Number of neurons | FR below 10th percentile | No FR effect | FR above 90th percentile | CV below 10th percentile | No CV effect | CV above 90th percentile |
|---|---|---|---|---|---|---|---|
| aCSF | 9 | 0 | 8 | 1 | 0 | 9 | 0 |
| L-AP4 | 24 | 3 | 9 | 12 | 1 | 14 | 9 |
| VU0155041 | 13 | 1 | 10 | 2 | 1 | 7 | 5 |

**Table 4.2** – Summary of changes in firing rate (FR) and pattern (CV) of neurons in the GPe and striatum, in response to drug infusion.

As can be seen in Fig. 4.6B, most GPe neurons did not display significant changes in their firing patterns (as determined by CV values) after infusion of the group III mGluR agonists, as compared with aCSF. Only 3/27 GPe cells showed an increased CV in response to L-AP4, while 2/27 GPe cells showed a decreased CV. It is worth noting, however, that the characteristic pauses in firing that are commonly seen in GPe neurons under baseline conditions were completely abolished after infusion of L-AP4 in 11 out of

27 recorded cells. VU0155041 did not affect this parameter in the 10 recorded GPe neurons. Neither L-AP4 nor VU0155041 affected other parameters of firing, such as bursting or oscillatory activity.

None of the pallidal (or striatal) drug injections produced obvious behavioral changes. However, this study was not designed to assess behavioral drug effects, which would likely necessitate larger drug injection volumes.

*4.4.3.3 Effect of MPTP on basic firing characteristics of striatal neurons*

We recorded from 46 striatal neurons in 2 MPTP-treated monkeys, in which the stability and isolation of single units were maintained before, during and after microinjections of aCSF or drugs in the vicinity of the recorded cells. In Table 4.3, we show a comparison of different descriptors of the discharge of striatal neurons which were either recorded during the pre-injection (control) period in parkinsonian animals or under similar conditions in three normal monkeys. Striatal cells were divided into PANs, TANs, or not classified (NC), based on firing rates and CV values (see Methods). We found no statistical differences in these parameters between the groups of neurons recorded in the normal and MPTP-treated states, except in the firing rate of PANs, which was lower after MPTP treatment.

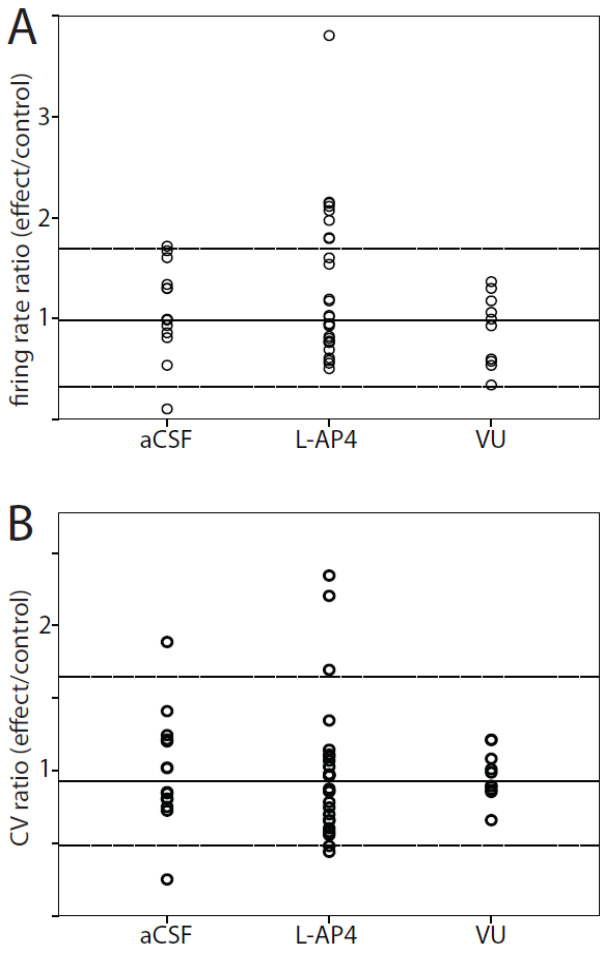


**Figure 4.6** – Responses of GPe neurons in MPTP-treated monkeys to infusion of aCSF, L-AP4, or VU0155041 (VU). A) Changes in firing rate (expressed as firing rate ratios, effect/baseline) of GPe neurons in response to drug infusion. The proportions of cells showing increased, decreased, or no change in firing rate were statistically different between the L-AP4 and aCSF groups (chi-squared, p=0.02). B) Changes in firing pattern (expressed as coefficient of variance ratios) of GPe neurons in response to drug infusion. Solid horizontal line represents the mean of aCSF data. Upper and lower dashed lines represent 90$^{th}$ and 10$^{th}$ percentiles of aCSF data, respectively. aCSF n=14, L-AP4 n=27, VU n=10.

*4.4.3.4 Group III mGluR activation in the striatum*

The effects of local injections of L-AP4 and VU0155041 on the firing rates and coefficients of variation of striatal cells are summarized in Table 4.2 and Fig. 4.7. Half of our sample of striatal cells (12/24) showed increased firing rates in response to L-AP4 infusion, while a few (3/24) significantly decreased their firing rates. The remaining 9 cells showed no significant change in firing rate. The proportions of cells showing increased, decreased, or no change in firing rate were statistically different between the L-AP4 and aCSF groups (chi-squared, p=0.02). Cells infused with VU0155041 responded similarly to cells infused with aCSF, except for a single outlier that significantly increased its firing rate (Fig. 4.7A).

In contrast to GPe injection results, many striatal cells showed increases in CV after L-AP4 (9/24) and VU0155041 (5/13), indicating less regular firing patterns following the drug infusion. The distribution of responses (increases, decreases, or no effect, based on the aCSF $10^{th}$/$90^{th}$ percentiles) showed a tendency towards a significant difference from the aCSF group (chi-squared; aCSF vs. L-AP4, p=0.058; aCSF vs. VU0155041, p=0.068). Other changes recorded in striatal neurons included an increase in the power of the 13 to 30 Hz band after L-AP4 injections, as well as an increase in the time spent in bursts after the VU0155041 injections.

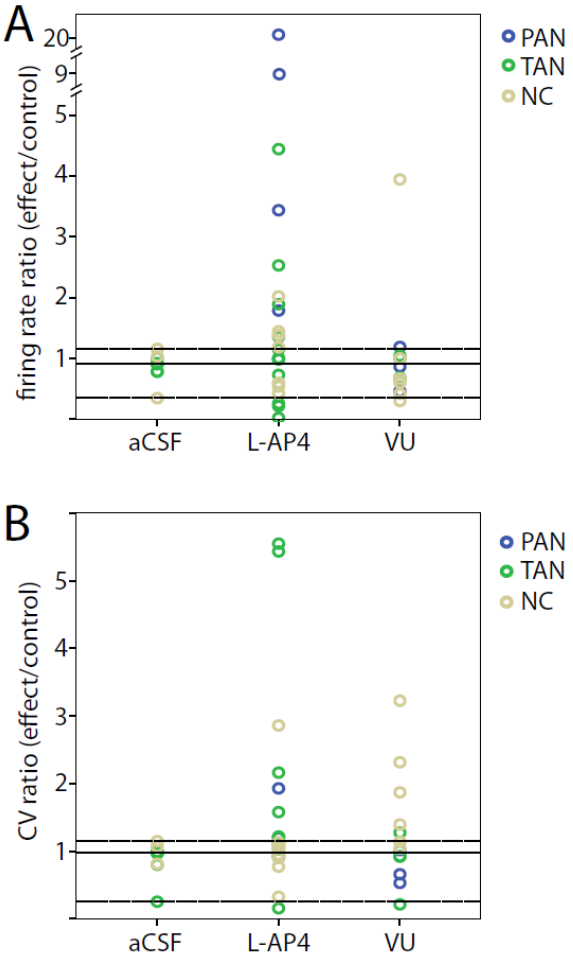


**Figure 4.7** - Responses of striatal neurons in MPTP-treated monkeys to infusion of aCSF, L-AP4, or VU0155041 (VU). A) Changes in firing rate (expressed as firing rate ratios, effect/baseline) of striatal neurons in response to drug infusion. B) Changes in firing pattern (expressed as coefficient of variance ratios) of striatal neurons in response to drug infusion. Blue circles represent PANs, green circles represent TANs, and tan circles represent striatal cells that were not classified (NC). Solid horizontal line represents the mean of aCSF data. Upper and lower dashed lines represent $90^{th}$ and $10^{th}$ percentiles of aCSF data, respectively. aCSF n=9, L-AP4 n=24, VU n=13.

## 4.5 Discussion

Our results demonstrate that mGluR4 is heavily expressed throughout the primate basal ganglia circuitry, and that its overall distribution is not significantly affected in the parkinsonian condition. In the striatopallidal complex, mGluR4 is located to subserve presynaptic regulation of glutamatergic and GABAergic transmission. Among responding cells, local intrastriatal or intrapallidal applications of the group III mGluRs agonist, L-AP4, induced predominantly increases in firing rates. L-AP4 application also altered striatopallidal firing patterns through the attenuation of the characteristic pauses in firing of GPe cells and increased CVs in the putamen. The striatal effects of L-AP4 were partly mimicked by local application of the GluR4 allosteric potentiator, VU0155041.

| | | PANs | | | | TANs | | | | Not Classified | | | |
|---|---|---|---|---|---|---|---|---|---|---|---|---|---|
| | | Normal | | MPTP | | Normal | | MPTP | | Normal | | MPTP | |
| Number of neurons | | 22 | | 8 | | 27 | | 21 | | 18 | | 17 | |
| | | Mean | SD | Mean | SD | Mean | SD | Mean | SD | Mean | SD | Mean | SD |
| ISI CV | | 1.77 | 0.60 | 1.75 | 0.60 | 0.66 | 0.17 | 0.68 | 0.18 | 1.62 | 0.72 | 1.53 | 0.32 |
| Firing rate (spikes/s) | | 1.14 | 0.76 | .5958* | 0.52 | 6.21 | 3.96 | 7.56 | 3.26 | 8.14 | 4.65 | 9.72 | 8.17 |
| Power spectral components (% within stated spectral bins) | 1-3 Hz | 0.96 | 0.39 | 1.40 | N/A | 0.70 | 0.43 | 0.53 | 0.23 | 1.06 | 0.53 | 1.69 | 1.66 |
| | 3-8 Hz | 1.15 | 0.13 | 1.44 | N/A | 1.12 | 0.23 | 1.05 | 0.23 | 1.40 | 0.67 | 1.57 | 0.90 |
| | 8-13 Hz | 1.13 | 0.13 | 1.32 | N/A | 0.91 | 0.24 | 0.97 | 0.12 | 1.20 | 0.44 | 1.10 | 0.56 |
| | 13-30 Hz | 1.06 | 0.11 | 1.03 | N/A | 0.98 | 0.11 | 0.99 | 0.05 | 1.08 | 0.25 | 0.94 | 0.27 |
| | 30-100 Hz | 0.98 | 0.03 | 0.94 | N/A | 1.03 | 0.04 | 1.03 | 0.02 | 0.95 | 0.13 | 0.96 | 0.14 |
| Burst index (spikes %) | | 51.35 | 15.59 | 51.96 | N/A | 8.93 | 7.50 | 8.53 | 6.30 | 35.52 | 21.46 | 45.27 | 12.06 |
| Burst index (time, %) | | 8.14 | 2.10 | 7.12 | N/A | 1.99 | 1.83 | 2.15 | 1.67 | 8.11 | 4.40 | 9.67 | 3.17 |

**Table 4.3** – Descriptors of neuronal firing in the striatum; comparison of MPTP-treated monkeys with normal monkeys. Data reported as mean ± standard deviation. *statistically different from normal; t-test, $p<0.05$. Cases with <100 ISIs were not included in the power spectral and burst analysis (for those cells classified as PANs in the MPTP-treated monkeys, only one cell had >100 ISIs, and therefore the power spectral and burst analysis values are based on a single case).

Together, these anatomical and electrophysiological effects suggest that the neural mechanisms underlying the possible antiparkinsonian effects of mGluR4-related drugs in primates may involve modulation of both GABAergic and glutamatergic synapses in GPe and striatum. Although not studied in great detail here, other structures such as the

cerebral cortex, thalamus, or SNr may be involved as well, as mGluR4 expression is fairly widespread (see Fig. 4.1).

### 4.5.1 mGluR4 expression in the primate basal ganglia: Potential significance towards mGluR4-mediated antiparkinsonian effects

Our light and electron microscopic data from normal and MPTP-treated monkeys are consistent with those previously described in rodents, showing that striatal-like GABAergic terminals account for most of the mGluR4-immunoreactive elements in the GPe (Bradley et al., 1999; Corti et al., 2002). These findings are also in line with slice electrophysiology data showing that group III mGluRs activation reduces striatopallidal GABAergic transmission in normal rats (Marino et al., 2003; Matsui and Kita, 2003; Valenti et al., 2003; Beurrier et al., 2009). However, our results also demonstrate that mGluR4 is present in putative glutamatergic terminals in the monkey GPe. These observations, combined with our light microscopic evidence for perikaryal mGluR4 immunoreactivity in the STN, suggest that mGluR4 is expressed at the subthalamopallidal synapse. These receptors may thus regulate both GABAergic and glutamatergic transmission in the GPe of normal and parkinsonian monkeys. This possible dual regulatory role may be one of the reasons why group III mGluRs activation had relatively heterogeneous effects on the electrical activities of GPe neurons. Recent microdialysis data from 6-OHDA-treated parkinsonian rats showing that the local application of an orthosteric group III mGluRs agonist decreases extracellular GABA and glutamate levels in the GP are also in line with these observations (Deltheil et al., 2011). Expression of mGluR4 in STN neurons also suggests that modulation of glutamatergic

transmission in the GPi/SNr may play an important role in the effects of mGluR4 activation as well.

Indeed, in addition to its strong expression in the striatum and GPe, mGluR4 was also found to be enriched in the neuropil of both GPi and SNr of normal and MPTP-treated monkeys, a pattern reminiscent to that described in a previous study in which striatal GABAergic and putative glutamatergic terminals immunoreactive for mGluR4 were identified in the SNr and entopeduncular nucleus of normal rats (Corti et al., 2002). Together with earlier data showing that both direct and indirect pathway GABAergic neurons in the striatum express mGluR4 mRNA (Kerner et al., 1997), these findings provide evidence for mGluR4-mediated presynaptic modulation of GABAergic and glutamatergic synapses in both the GPe and basal ganglia output nuclei.

Several previous studies have linked the antiparkinsonian effects of group III mGluR agonists specifically to the mGluR4-mediated modulation of GABA release, over other group III mGluR subtypes, in GPe (See Niswender and Conn, 2010 for review). By inhibiting GABA release from terminals of the overactive striato-GPe pathway, mGluR4 activation may indeed have antiparkinsonian effects, allowing GPe neurons to regain their inhibitory control over STN activity (Hopkins et al., 2009). However, the concomitant expression of mGluR4 in putative glutamatergic synapses in the GPe, and in striatal GABAergic projections to the SNr and GPi would have the opposite effect. Amalric and colleagues have, indeed, shown that infusion of group III agonists into the GP improves, while infusion into the SNr, worsens motor deficits in parkinsonian rats (Lopez et al., 2007). Furthermore, as discussed in more detail below, group III mGluR activation is also likely to affect glutamatergic and GABAergic transmission in the

striatum. In light of these findings, it appears that the antiparkinsonian effects of group III mGluR agonists (or mGluR4 allosteric potentiators) are probably not simply mediated by modulation of GABA release from the overactive striatopallidal pathway, but may involve more complex regulation of GABAergic and glutamatergic synaptic mechanisms at various levels of the basal ganglia circuitry. It is possible that some of these mechanisms are adaptive in character, and would only be seen with chronic application of the group III mGluR agonists, an issue that was not addressed in the present study.

### 4.5.2 mGluR4 in the striatum: A target for the regulation of extrinsic glutamatergic and intrinsic GABAergic circuitry

The striatum is another target through which mGluR4 activation could influence the activity of basal ganglia neurons, and elicit antiparkinsonian effects. We found that about half of mGluR4-immunoreactive terminals in the monkey striatum formed asymmetric synapses, the large majority of which contacted spines, suggesting that the main source of mGluR4-containing glutamatergic terminals in the primate striatum is the cerebral cortex (although some may also originate from the thalamus) (Smith et al., 2004). Taking into consideration evidence for increased corticostriatal glutamatergic transmission in parkinsonism (Galarraga et al., 1987; Calabresi et al., 1993; Calabresi et al., 1996; Gubellini et al., 2002), increased activation of mGluR4 in striatal glutamatergic afferents by agonist application may help tone down this abnormal corticostriatal overactivity. Cuomo and colleagues have, in fact, shown that cortically-evoked striatal excitatory postsynaptic potentials are attenuated by activation of group III mGluRs, and that intrastriatal injection of group III agonist improves akinesia in parkinsonian rats (Cuomo et al., 2009). Although drugs used in these studies could not discriminate

between the different subtypes of group III mGluRs, there is strong evidence that mGluR4 is the most likely receptor involved in these effects (see below).

In addition to the modulation of striatal glutamatergic transmission, activation of group III mGluRs also attenuates inhibitory postsynaptic potentials induced by intrastriatal stimulation in rat brain slices (Cuomo et al., 2009). In light of our anatomical data showing that about half of mGluR4-containing terminals in the monkey striatum form symmetric synapses with the ultrastructural features of GABAergic terminals, combined with the fact that the most common response of striatal neurons to group III activation was an increase in firing rate, the inhibition of intrastriatal GABAergic transmission may be an important mechanism by which group III mGluRs mediate their functional effects upon the basal ganglia circuitry in normal and parkinsonian states.

### 4.5.3 mGluR4 regulation of striatal and pallidal firing rates

Local infusion of L-AP4 increased the firing rate of about one third of GPe cells and half of striatal neurons in parkinsonian monkeys. These effects were likely due to mGluR4-mediated inhibition of overactive GABAergic striatopallidal terminals in the GPe, and blockade of intrastriatal GABAergic inhibition in the striatum, respectively. It is important to note that while many striatal and pallidal neurons increased their firing rates in response to L-AP4, half of striatal neurons and two thirds of pallidal neurons showed either an opposite response, or did not display any significant effect in response to L-AP4. Such diverse physiological effects, combined with the fact that presynaptic mGluR4 is also heavily expressed in GPi and SNr (Corti et al., 2002), warrant consideration, and highlight the complex mechanisms through which systemically administered mGluR4-related compounds could mediate their behavioral and therapeutic

effects in normal and diseased states (Niswender et al., 2008; East and Gerlach, 2010; Niswender and Conn, 2010).

### 4.5.4 Effects of group III mGluRs agonist vs. mGluR4 PAM on striatal and pallidal activity

Two drugs were used in our study to activate group III mGluRs in the monkey striatopallidal complex: L-AP4, a classical group III mGluR orthosteric agonist with strong affinity for mGluR4 and mGluR8 but much less for mGluR7, and VU0155041, a highly selective mGluR4 positive allosteric modulator (Niswender et al., 2008). Because of the striking differences in the EC50 of L-AP4 for mGluR4/8 versus mGluR7, the lack of significant mGluR8-mediated physiological and behavioral effects in the striatum and GPe (Valenti et al., 2003; Lopez et al., 2007; Cuomo et al., 2009), the lack of L-AP4 effects in mGluR4 knockout mice (Valenti et al., 2003; Cuomo et al., 2009), and the restricted expression of mGluR6 in the retina (Nakajima et al., 1993), it is reasonable to suggest that the main L-AP4-mediated physiological effects described in the present study were induced by mGluR4 activation, although minor contributions of mGluR7 and mGluR8 cannot be completely ruled out.

In contrast to L-AP4, VU0155041 was much less effective at changing the firing rates of striatal and pallidal neurons in parkinsonian monkeys. One reason for this somewhat surprising result could be that the two drugs have different mechanisms of action. L-AP4 directly activates mGluR4 via the glutamate binding site, while VU0155041 is a mixed allosteric agonist/positive allosteric modulator which binds mGluR4s at a site distinct from the glutamate binding site, necessitating activation of the receptor by endogenous glutamate for optimal effects (Niswender et al., 2008; Niswender

and Conn, 2010). We also cannot rule out the possibility that the concentration of VU0155041 used in our study (4 mM) was too low to produce electrophysiological effects in the majority of recorded GPe neurons. Although this remains to be assessed using compounds that display better solubility properties, it is worth noting that this concentration of VU0155041 induced significant changes in the firing pattern of some striatal neurons, thereby suggesting differential properties between GPe and striatal neurons in their responses to mGluR4 allosteric potentiators (Fig. 4.7B).

Several individual striatal neurons, indeed, showed significant increases in CV when treated with L-AP4 or VU0155041, suggesting that activation of mGluR4 increases firing irregularity in a subpopulation of striatal neurons. Most GPe neurons did not display CV changes in response to drug microinjections, but in many cells the incidence of pauses in discharge was greatly reduced in response to L-AP4 treatment (Table 4.1). Based on the observation that, at baseline, GPe neurons in MPTP-treated monkeys showed a significant reduction in indices of pausing (Table 4.1), this effect of L-AP4 might be considered pro-parkinsonian. To our knowledge there are no previous reports of decreased pausing in GPe neurons in parkinsonism, but an increase in pausing in the GPe has sometimes been associated with hyperkinetic disorders (Matsumura et al., 1995; Bronfeld et al., 2010).

### 4.5.5 Concluding Remarks

In conclusion, our results demonstrate that mGluR4 receptors are widely distributed throughout the primate basal ganglia circuitry in both normal and parkinsonian conditions. Our data suggest that the use of mGluR4-related compounds as antiparkinsonian agents in primates is not simply explained through an inhibition of

GABA release from striatopallidal terminals, but may depend on a more complex and balanced regulation of glutamatergic and GABAergic transmission at various key synapses throughout the entire basal ganglia circuitry. Such effects need to be taken into account in future studies evaluating the efficacy of mGluR4-mediated antiparkinsonian therapy in MPTP-treated monkeys.

## 4.6 Acknowledgements

This work was supported by grants from the RJG Foundation, the Michael J Fox Foundation, the Udall Center for Parkinson's Disease Research (NIH P50 NS071669), and the Yerkes National Primate Research Center base grant (NIH P51 RR-000165). Many thanks are due to Jeff Conn and Colleen Niswender for providing VU0155041, and to Jeff Paré and Susan Jenkins for technical support.

# Chapter 5

# Discussion

## 5.1 Summary of findings and their implications for Parkinson's disease

Through this thesis work, we have examined various anatomical, electrophysiological, and behavioral features of three highly promising non-dopaminergic drug targets currently under research for the treatment of PD. The main findings of our studies can be summarized as follows.

First, we showed that the mGluR5 antagonist MTEP has some modest antiparkinsonian effects and potentiates some of the antiparkinsonian effects of the D2LR agonist pramipexole in MPTP-treated monkeys. This potentiation may be in part due to functional interactions between mGluR5 and $D_2R$ in the striatum (Fig 5.1A; (Ferre et al., 1999; Popoli et al., 2001; Ferre et al., 2003; Cabello et al., 2009)). Antagonists of mGluR5 may help to normalize corticostriatal (Fig. 5.1A) and subthalamofugal (Fig. 5.1A,B) glutamatergic transmission, which are overactive in parkinsonism. Our findings suggest that mGluR5 antagonists might be beneficial as an adjunct treatment to extend the clinical efficacy and decrease the side effects of D2LR agonist therapy in PD patients, by allowing for lower dosing of these agents.

Second, we provided electron microscopic evidence that mGluR5 and $A_{2A}$ receptors are located in key elements of the nonhuman primate basal ganglia circuits where their co-modulation could potentially have significant clinical relevance for PD. Knowing that adenosine $A_{2A}$ receptors synergistically interact with mGluR5 and $D_2R$ in the striatum (Ferre et al., 1999; Popoli et al., 2001), and that the modulation of $A_{2A}$ receptors may be able to further potentiate the antiparkinsonian effects of mGluR5 antagonists and D2LR agonists seen in our first series of studies (see also Coccurello et al., 2004; Kachroo et al., 2005), we used immunoperoxidase/immunogold double labeling

with electron microscopy to show that $A_{2A}R$ and mGluR5 colocalize in dendrites and spines of striatal neurons (Fig. 5.1A). This finding highlights a possible anatomical site where mGluR5/$A_{2A}R$/$D_2R$ interactions might occur. We also used immunoperoxidase labeling with electron microscopy to show that $A_{2A}Rs$ are found in the dendrites and spines of striatal neurons, as well as in excitatory and inhibitory terminals in the striatum, GPe, and SNr (Fig. 5.1A,B,C). These findings implicate the striatopallidal complex as a potential site of action for the antiparkinsonian effects of $A_{2A}R$ antagonists (through inhibition of indirect pathway striatal MSNs), in addition to providing a foundation for better understanding of $A_{2A}R$ function in general. Our immunolabeling and Western blots showed that the monkey, but not the rat, SNr contains $A_{2A}Rs$ (Fig. 5.1C). This may explain in part why $A_{2A}R$ antagonists have been less effective in primates than in rodents, because $A_{2A}R$ antagonist-mediated inhibition of GABA release in the SNr might counteract antiparkinsonian effects induced through regulation of indirect pathway neurons. While it is found at highest levels in the striatum and GPe, $A_{2A}R$ expression extends well beyond the striatopallidal complex, so other structures and circuits may also be involved in the antiparkinsonian mechanism of action of $A_{2A}R$ modulation.

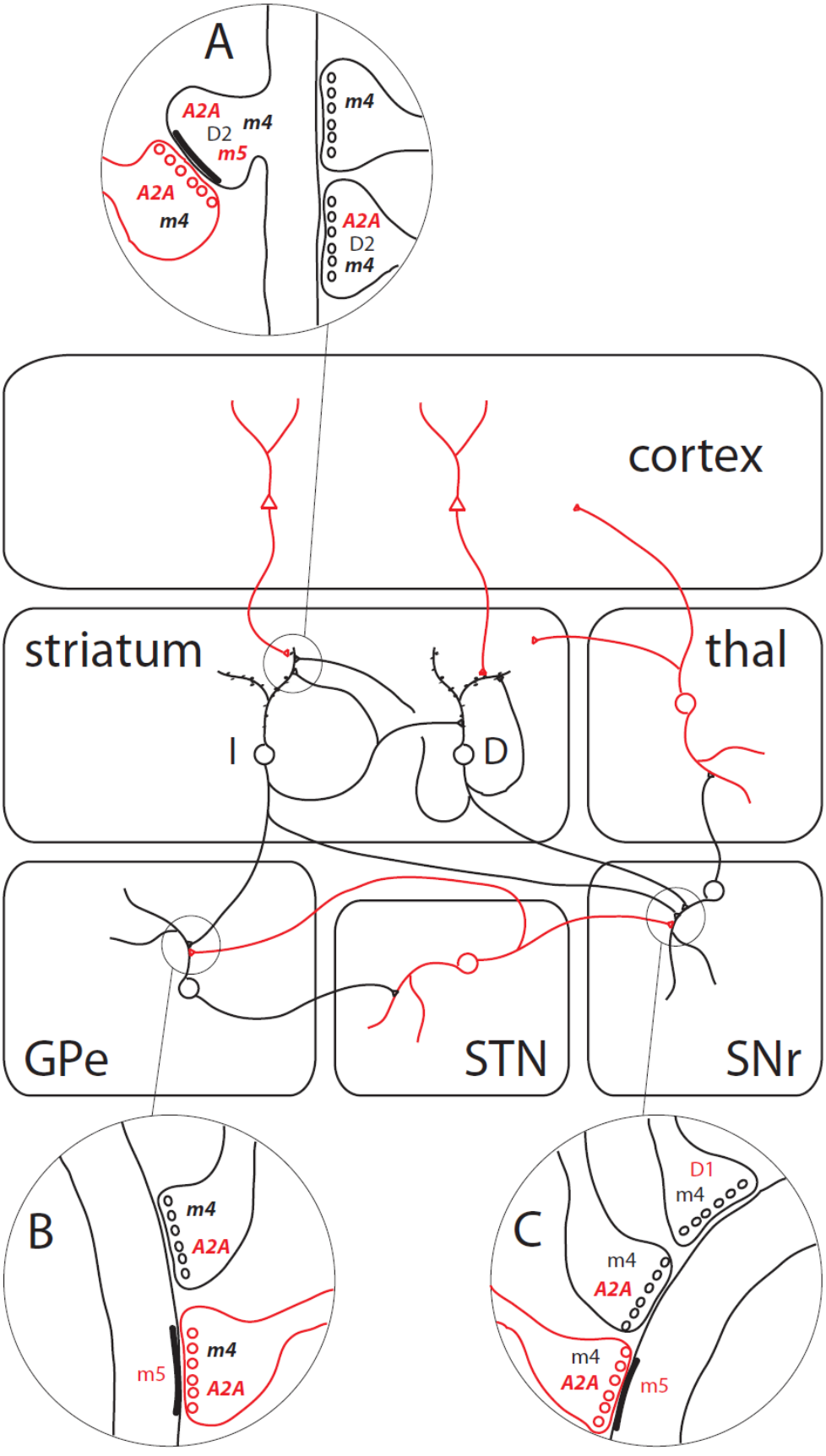
A
A2A
D2
m4
m5
A2A
m4
m4
A2A
D2
m4
cortex
striatum
thal
I
D
GPe
STN
SNr
B
m4
A2A
m5
m4
A2A
C
D1
m4
m4
A2A
m4
A2A
m5

**Figure 5.1 .** (A-C) Schematic summary showing expression of mGluRs (mGluR5, mGluR4) and adenosine ($A_{2A}$) receptors examined in this thesis at key synapses in the monkey basal ganglia circuitry. Putative excitatory cells, terminals, and receptors are shown in red, inhibitory elements are depicted in black. The localization of receptors labeled in bold italic characters has been shown in this dissertation. A) A corticostriatal terminal (left) is shown forming a synapse with the spine of a MSN dendrite. We propose that this is a location for possible mGluR5, $D_2$R, $A_{2A}$R interactions. Local MSN collaterals are shown contacting the dendritic shaft (right). All elements depicted are possible sites of mGluR4 modulation. B) Striatopallidal (top) and subthalamopallidal (bottom) terminals are shown contacting the dendrite of a GPe projection neuron. Both of these terminals are possible sites of $A_{2A}$R- and mGluR4-mediated effects. C) Inputs from the direct (top) and indirect (bottom) pathways, as well as an $A_{2A}$R-containing collateral of a striatopallidal neuron (middle), are shown contacting the dendrite of a nigral projection neuron. $A_{2A}$ – adenosine $A_{2A}$ receptor, I – indirect pathway MSN, D – direct pathway MSN, D1 – dopamine D1 receptor, D2 – dopamine D2 receptor, GPe – external globus pallidus, I – indirect pathway MSN, m4 – metabotropic glutamate receptor 4, m5 – metabotropic glutamate receptor 5, SNr – substantia nigra pars reticulata, STN – subthalamic nucleus, thal – thalamus. D1 localization (Yung et al., 1995), D2 localization (Hersch et al., 1995), nigral mGluR4 localization (Corti et al., 2002), Pallidal and nigral mGluR5 localization (Hanson and Smith, 1999; Hubert et al., 2001).

Third, we showed anatomical and electrophysiological evidence for a complex pattern of localization and function in the monkey striatopallidal complex, that could be critical in the design and interpretation of future studies aimed at assessing the antiparkinsonian effects of mGluR4-related drugs in primates. Through the use of immunoperoxidase labeling with electron microscopy, we showed that mGluR4 is located in excitatory and inhibitory terminals in the striatum and GPe, as well as in postsynaptic structures in the striatum. This widespread localization puts mGluR4 in position to broadly modulate transmission across much of the basal ganglia (note mGluR4 localization in all terminals depicted in figure 5.1). These anatomical data are in agreement with our electrophysiological findings gathered from in vivo extracellular

recording in awake parkinsonian monkeys that received local intrastriatal and intrapallidal infusions of mGluR4 agonists. These experiments demonstrated that striatal and pallidal neurons respond in various ways to mGluR4 activation, showing both increases and decreases in firing rates, as well as changes in firing patterns. Increases in firing rate were more common than decreases which, in the GPe, is consistent with an antiparkinsonian change. However, the widespread localization of mGluR4 in the basal ganglia, and its diverse effects on neuronal activity suggest that the antiparkinsonian mechanism of action of mGluR4 agonists likely involves more than modulation of the striatopallidal complex in primates.

## 5.2 A critical look at methodology

We have used a variety of methods in this dissertation, and each has its own set of strengths and weaknesses. By and large, we have chosen methods that have been well validated through repeated use in scientific endeavors over the years. However, it is important to consider possible limitations of our work. In this section, we take a critical look at the methodology used in this dissertation, pointing out limitations and measures taken to counteract them.

### 5.2.1 Immunohistochemistry

Immunohistochemical labeling is only as good as the specificity of the antibody used. We have used only antibodies that are proven to be highly specific for the desired antigen. We performed control experiments to show that immunolabeling is truly antigen-specific: Western blots and antibody pre-adsorption with synthetic antigen peptide to test specificity of primary antibodies, and omission of primary antibodies from

immunohistochemical reactions to test specificity of secondary antibodies. Background labeling can be a problem, especially when using the immunogold labeling technique. One way we have tried to avoid false-positive classification of unlabeled elements is to look at electron micrographs and compare the density of gold particles in the element of interest with the density in elements known to be devoid of the antigen protein. If the element of interest contains a significantly higher density of gold particles, it can be considered as positively labeled for the antigen protein. On the other hand, whenever knowledge of the exact ultrastructural/subsynaptic location of receptors is not needed, we use the immunoperoxidase technique to determine receptor localization which, due to a large degree of signal amplification, is a more reliable and sensitive immunohistochemical technique.

Fixation of the tissue is another important issue to consider. Weak fixation can lead to degradation of the ultrastructure of the tissue and difficulty in reliably classifying the different types of neuronal elements on the electron microscope. Too much fixation can lead to excessive protein cross-linkage throughout the tissue, which can hamper antibody penetration, leading to false-negative classification of elements. Very strong fixation can also destroy antigen sites. For these reasons, we have used a specific blend of fixatives (4% paraformaldehyde with 0.1% glutaraldehyde) for EM labeling, which has been shown to be quite effective by our lab. We also use other techniques to improve antibody penetration, such as treatment with sodium borohydride to break some of the cross-linkages, as well as temperature-shocking the tissue. For unknown reasons, the $A_{2A}R$ antibody used in our studies did not work in glutaraldehyde-fixed tissue, so we had to switch to the more noxious fixative acrolein. This was a new procedure for our

laboratory, but with some testing and experimentation, we were able to get good ultrastructure and reliable $A_{2A}R$ labeling.

As alluded to above, antibody penetration is another important concern in immunohistochemistry, especially when using double-labeling to determine colocalization of receptors, as was done in Chapter 2. Secondary antibodies for immunoperoxidase labeling penetrate tissue much more efficiently than secondary antibodies for immunogold labeling, which are conjugated to a bulky gold particle. Therefore, we had to undertake certain measures to ensure that we were examining ultrathin sections that had been penetrated by both types of antibody, otherwise colocalization would be underestimated. First, ultrathin sections for EM analysis were only taken from the very surface of the tissue block, where antibody penetration was maximal. Second, we switched the secondary antibody labeling techniques between the two receptors and ran a second immunohistochemical reaction and EM analysis. Because this switch in antibody localization methods did not lead to any significant change in the percentages of double labeled elements, we interpreted these data as evidence that our double labeling approach was not a major source of false negative data.

### 5.2.2 Electrophysiology

Performing intracerebral drug infusions with in vivo extracellular recordings in awake monkeys is a difficult technique, and some parts require careful attention. Perhaps the most obvious difficulty of recording in awake monkeys is that they move. However, anesthesia can cause alterations in firing rates and patterns (Mahon et al., 2006; Gatev and Wichmann, 2009) that could confound the effects of mGluR4 modulation, so it is necessary for the monkeys to be awake. While the head is restrained during awake

recordings, violent movements made by the monkeys can shake the entire rig enough to cause small movements in the electrode and loss of the cell that is being recorded. To counteract this problem, monkeys were trained for several weeks to sit calmly in the recording chair with head restrained, which makes them much calmer and stiller during recordings. However, problems can arise if the animal is too calm and falls asleep. Sleep, much like anesthesia, causes alterations in basal ganglia firing rates and patterns (Mahon et al., 2006; Gatev and Wichmann, 2009). So, monkeys were monitored via video surveillance to assure that they were awake. If monkeys fell asleep, they were awakened with noise.

In addition, it is very important, but not always easy, to know the location of the electrode tip. In the absence of MRI guidance, one must empirically map the locations of brain structures underlying the recording chamber. This is done by making several electrode penetrations and examining the locations and characteristic firing patterns of cells in different areas. Some structures are easy to tell apart, but some are not. For instance, with the vertical or lateral approaches used in our studies, the electrode first reaches the putamen, which contains cells with low firing rates. Then, it passes into the GPe, providing a stark contrast with its high density of cells with high firing rates. However, as the electrode is lowered deeper, it reaches the GPi, which contains a similar density of high-frequency cells that fire with less intermittent pauses. This transition between the two pallidal segments is not always easy to recognize, but one can sometimes find “border cells,” which have different characteristic firing properties and are found at the edge of the structure.

Once a desirable cell in the correct structure is found, it is important to position the sharp electrode so that the cell is well isolated from neighboring cells. If action potentials from a nearby neuron are picked up at similar amplitude to those from the desired cell, it can be difficult to sort the two apart in the data analysis stage. Improper sorting of action potential data can lead to erroneous conclusions about firing properties. To properly achieve this sorting, recordings were individually analyzed using sophisticated waveform matching software (Spike2). To ensure that cells were properly isolated and sorted, our findings were examined and confirmed by colleagues in my laboratory with expertise in these analyzes.

Additionally, the drugs and drug infusions can be a source of limitations for these experiments. The outflow of drug solution near the tip of the electrode can sometimes push the cell away, causing its waveform to shrink and possibly become confused with other cells in the background. To avoid such confound in our data interpretation, such recordings were discarded from the analysis. Another point to consider in the interpretation of such studies is the spread and variable concentration of drugs that affect the recorded cells. For instance, our experiments showed that the mGluR4 allosteric potentiator VU0155041 had little effect on neuronal firing rates in the globus pallidus, but because this drug had poor solubility in the vehicle used for intracerebral infusion, the maximum concentration we could administer was limited. Due to these limitations, we cannot rule out the possibility that cells didn't respond to VU0155041 simply because the drug concentration was too low. However, the drug did seem to induce some changes in firing patterns, suggesting that it had at least some effects on neuronal activity when used at this concentration. Another potential pitfall of the drug infusions pertains to the spread

of drug infusions from one cell to the next. In many cases, more than one drug infusion was made during the same recording session, or even during the same electrode penetration. In order to avoid effects of previous drug infusions on subsequent recordings, drug infusions were spaced physically by 1 mm and temporally by 30 min.

The group III mGluR agonist L-AP4 was more effective than VU0155041, but its non-selective nature is another source of limitations in our electrophysiological studies. Albeit to a much lower degree, L-AP4 has some affinity for mGluR7, another abundant group III mGluRs in the striatopallidal complex (Lopez et al., 2007). Thus, although unlikely, the possibility that some of the L-AP4-mediated effects result from modulation of mGluR7 cannot be completely ruled out. Another group III mGluR that L-AP4 could affect is mGluR8. However, because the striatal and pallidal effects of L-AP4 on synaptic transmission in rat brain slices cannot be reproduced by an mGluR8 selective agonist (Valenti et al., 2003; Lopez et al., 2007; Cuomo et al., 2009), and because L-AP4 has no effect in mGluR4-null mice (Valenti et al., 2003; Cuomo et al., 2009), we believe mGluR4 is responsible for most of the effects of L-AP4 described in our experiments.

Other potential analytical pitfalls exist for this set of experiments. For example, the method of defining a drug effect must be somewhat arbitrarily chosen. We chose fairly stringent parameters to define a drug effect (effect must pass outside of the $90^{th}$ or $10^{th}$ percentile of the baseline data and remain outside for at least 90 sec, beginning within 2 min of the start of drug infusion), in order to avoid confusion of drug effects with normal fluctuations in cell firing. Drug effects that were small in amplitude, had less than 90 sec duration, or that occurred with greater than 2 min latency would not have been caught by our analysis.

There are also limitations surrounding the classification of PANs and TANs. PANs and TANs have sometimes been equated to striatal MSNs and cholinergic interneurons, respectively, but this distinction cannot always be simply made. As was the case in our data, there is not always a clear division between a group of slow-firing PANs and a group of fast-firing TANs. Instead, striatal cells showed a continuum of different firing rates. Most previous studies have used the firing rate, in addition to the width of the action potential waveforms to make the distinction between TANs and PANs (Kimura et al., 1996; Sardo et al., 2000; Blazquez et al., 2002; Lee et al., 2006). However, our data showed a continuum of spike widths, rather than two clusters, which is why we used the CV to help us make the distinction. Differences between rodents and primates (Apicella 2002; Berke et al., 2004), as well as reported large increases in striatal firing rates after MPTP treatment (Liang et al., 2008) further confuse the issue. In any case, extracellular recordings, as were done in our study, cannot be used to definitively classify striatal neuron subtypes. The only way to do this is to perform intracellular recording, followed by juxtacellular labeling and neurochemical identification of neurons through immunocytochemistry, as has been recently done in rodents (Sharott et al., 2012).

### 5.2.3 Behavioral experiments

In the battery of tests we used to quantify the parkinsonian motor symptoms in our studies, it is important to avoid experimenter bias, especially since some of the measurements have subjective components. This is especially true for the parkinsonism rating scale, which is clearly the most subjective measure used. To avoid bias, the two observers scoring each video were blinded to the drug treatment, and the two scores for each video were averaged to minimize subjective differences between the two observers.

However, blinding the observer was not always possible, as was the case for the quantification of movements. While this is a less subjective measure of quantifying parkinsonism than the rating scale, some bias can still be introduced at the level of deciding what constitutes a movement. To ensure that little bias was introduced, the movement data were compared with the infrared beam break data, which is a completely objective measure. The pattern of motor activity seen in the movement quantification was almost always mirrored by similar patterns in the infrared beams data.

The determination of eye blink rate also presented some challenges. Mainly, it was often difficult to find extended periods of time when the eyes were visible to the video camera, as the monkey moved around its cage. To overcome this problem, shorter periods throughout the 15-min observation had to be pieced together to get an entire minute of eye blink observation. However, sampling eye blink rate throughout the entire observation in this manner is probably preferable to only sampling during one contiguous minute at the beginning.

## 5.3 Future directions

This dissertation has provided valuable information about the anatomical, electrophysiological, and behavioral properties of three promising antiparkinsonian drug targets, but much work still remains to be done. Probably the most important future direction of this work involves testing the antiparkinsonian effects of a triple combination of D2LR agonist, mGluR5 antagonist, and $A_{2A}R$ antagonist in parkinsonian monkeys or humans. These three receptors interact synergistically in the striatum (Popoli et al., 2001), and the combination of mGluR5 and $A_{2A}R$ antagonists has antiparkinsonian

effects in rodents, even in the absence of a dopaminergic agent (Coccurello et al., 2004; Kachroo et al., 2005). Research from this work, and from previous studies, has shown that mGluR5 and $A_{2A}R$ individually can potentiate the effects of dopamine replacement drugs in parkinsonian monkeys (Grondin et al., 1999; Kanda et al., 2000). Both of these classes of drugs appear to have anti-dyskinetic and neuroprotective properties in primates and rodents, as well (Ikeda et al., 2002; Bibbiani et al., 2003; Johnston et al., 2010; Masilamoni et al., 2011). Thus, combined mGluR5/D2LR/$A_{2A}R$ pharmacotherapy represents an exciting strategy for future testing of anti-PD medications.

Another future direction of the work presented here involves the development of mGluR4 agonists as an antiparkinsonian treatment. The antiparkinsonian activity of mGluR4 activators has never been shown in primates. However, the recent development of orally bioavailable mGluR4-active compounds has set the stage for testing of their antiparkinsonian properties in primates (Celanire and Campo, 2012). Additionally, an mGluR4 antagonist has recently been shown to enhance the ability of an $A_{2A}R$ antagonist to relieve haloperidol-induced catalepsy in rats (Jones et al., 2012), which provides further avenues for future examination of drug combinations.

Thus, it appears that the upcoming years may open up highly exciting paths for the development of novel pharmacotherapeutic approaches for PD. The combination of basic preclinical work and a solid knowledge of the localization and function of potential new targets for non-dopaminergic antiparkinsonian drugs, like studies performed in this thesis, remain the foundation for significant advances in the development of new symptomatic therapies for brain disorders.

**References**

Adams CL, Cowen MS, Short JL, Lawrence AJ. 2008. Combined antagonism of glutamate mGlu5 and adenosine A2A receptors interact to regulate alcohol-seeking in rats. Int J Neuropsychopharmacol 11(2):229-241.

Addy C, Assaid C, Hreniuk D, Stroh M, Xu Y, Herring WJ, Ellenbogen A, Jinnah HA, Kirby L, Leibowitz MT, Stewart RM, Tarsy D, Tetrud J, Stoch SA, Gottesdiener K, Wagner J. 2009. Single-dose administration of MK-0657, an NR2B-selective NMDA antagonist, does not result in clinically meaningful improvement in motor function in patients with moderate Parkinson's disease. J Clin Pharmacol 49(7):856-864.

Agostino R, Bologna M, Dinapoli L, Gregori B, Fabbrini G, Accornero N, Berardelli A. 2008. Voluntary, spontaneous, and reflex blinking in Parkinson's disease. Mov Disord 23(5):669-675.

Aguirre JA, Kehr J, Yoshitake T, Liu FL, Rivera A, Fernandez-Espinola S, Andbjer B, Leo G, Medhurst AD, Agnati LF, Fuxe K. 2005. Protection but maintained dysfunction of nigral dopaminergic nerve cell bodies and striatal dopaminergic terminals in MPTP-lesioned mice after acute treatment with the mGluR5 antagonist MPEP. Brain Res 1033(2):216-220.

Aizman O, Brismar H, Uhlen P, Zettergren E, Levey AI, Forssberg H, Greengard P, Aperia A. 2000. Anatomical and physiological evidence for D1 and D2 dopamine receptor colocalization in neostriatal neurons. Nat Neurosci 3(3):226-230.

Amalric M, Moukhles H, Nieoullon A, Daszuta A. 1995. Complex deficits on reaction time performance following bilateral intrastriatal 6-OHDA infusion in the rat. The European journal of neuroscience 7(5):972-980.

Annic A, Devos D, Seguy D, Dujardin K, Destee A, Defebvre L. 2009. [Continuous dopaminergic stimulation by Duodopa in advanced Parkinson's disease: Efficacy and safety]. Rev Neurol (Paris) 165(8-9):718-727.

Ansah TA, Ferguson MC, Nayyar T, Deutch AY. 2011. Age- and duration-dependent effects of MPTP on cortical serotonin systems. Neuroscience letters 504(2):160-164.

Antonini A, Odin P. 2009. Pros and cons of apomorphine and L-dopa continuous infusion in advanced Parkinson's disease. Parkinsonism & related disorders 15 Suppl 4:S97-100.

Apicella P. 2002. Tonically active neurons in the primate striatum and their role in the processing of information about motivationally relevant events. Eur J Neurosci. 16(11):2017-26.

Armentero MT, Fancellu R, Nappi G, Bramanti P, Blandini F. 2006. Prolonged blockade of NMDA or mGluR5 glutamate receptors reduces nigrostriatal degeneration while inducing selective metabolic changes in the basal ganglia circuitry in a rodent model of Parkinson's disease. Neurobiol Dis 22(1):1-9.

Arslan G, Kull B, Fredholm BB. 2002. Anoxia redistributes adenosine A(2A) receptors in PC12 cells and increases receptor-mediated formation of cAMP. Naunyn Schmiedebergs Arch Pharmacol 365(2):150-157.

Augood SJ, Emson PC. 1994. Adenosine A2a receptor mRNA is expressed by enkephalin cells but not by somatostatin cells in rat striatum: a co-expression study. Brain research 22(1-4):204-210.

Azdad K, Gall D, Woods AS, Ledent C, Ferre S, Schiffmann SN. 2009. Dopamine D2 and adenosine A2A receptors regulate NMDA-mediated excitation in accumbens neurons through A2A-D2 receptor heteromerization. Neuropsychopharmacology 34(4):972-986.

Ballarin M, Fredholm BB, Ambrosio S, Mahy N. 1991. Extracellular levels of adenosine and its metabolites in the striatum of awake rats: inhibition of uptake and metabolism. Acta Physiol Scand 142(1):97-103.

Bara-Jimenez W, Sherzai A, Dimitrova T, Favit A, Bibbiani F, Gillespie M, Morris MJ, Mouradian MM, Chase TN. 2003. Adenosine A(2A) receptor antagonist treatment of Parkinson's disease. Neurology 61(3):293-296.

Battaglia G, Busceti CL, Molinaro G, Biagioni F, Storto M, Fornai F, Nicoletti F, Bruno V. 2004. Endogenous activation of mGlu5 metabotropic glutamate receptors contributes to the development of nigro-striatal damage induced by 1-methyl-4-phenyl-1,2,3,6-tetrahydropyridine in mice. J Neurosci 24(4):828-835.

Beneyto M, Meador-Woodruff JH. 2004. Expression of transcripts encoding AMPA receptor subunits and associated postsynaptic proteins in the macaque brain. J Comp Neurol. 468(4):530-54.

Berg D, Godau J, Trenkwalder C, Eggert K, Csoti I, Storch A, Huber H, Morelli-Canelo M, Stamelou M, Ries V, Wolz M, Schneider C, Di Paolo T, Gasparini F, Hariry S, Vandemeulebroecke M, Abi-Saab W, Cooke K, Johns D, Gomez-Mancilla B.

2011. AFQ056 treatment of levodopa-induced dyskinesias: results of 2 randomized controlled trials. Mov Disord 26(7):1243-1250.

Bergman H, Wichmann T, Karmon B, DeLong MR. 1994. The primate subthalamic nucleus. II Neuronal activity in the MPTP model of parkinsonism. J Neurophysiol 72:507–520.

Berke JD, Okatan M, Skurski J, Eichenbaum HB. 2004. Oscillatory entrainment of striatal neurons in freely moving rats. Neuron 43(6): 883-896.

Berretta S, Parthasarathy HB, Graybiel AM. 1997. Local release of GABAergic inhibition in the motor cortex induces immediate-early gene expression in indirect pathway neurons of the striatum. J Neurosci 17(12):4752-4763.

Beurrier C, Lopez S, Revy D, Selvam C, Goudet C, Lherondel M, Gubellini P, Kerkerian-LeGoff L, Acher F, Pin JP, Amalric M. 2009. Electrophysiological and behavioral evidence that modulation of metabotropic glutamate receptor 4 with a new agonist reverses experimental parkinsonism. FASEB J 23(10):3619-3628.

Bevan MD, Booth PA, Eaton SA, Bolam JP. 1998. Selective innervation of neostriatal interneurons by a subclass of neuron in the globus pallidus of the rat. J Neurosci. 18(22):9438-52.

Bibbiani F, Oh JD, Kielaite A, Collins MA, Smith C, Chase TN. 2005. Combined blockade of AMPA and NMDA glutamate receptors reduces levodopa-induced motor complications in animal models of PD. Experimental neurology 196(2):422-429.

Bibbiani F, Oh JD, Petzer JP, Castagnoli N, Jr., Chen JF, Schwarzschild MA, Chase TN. 2003. A2A antagonist prevents dopamine agonist-induced motor complications in animal models of Parkinson's disease. Experimental neurology 184(1):285-294.

Blandini F, Greenamyre JT. 1998. Prospects of glutamate antagonists in the therapy of Parkinson's disease. Fundam Clin Pharmacol 12(1):4-12.

Blandini F, Greenamyre JT, Nappi G. 1996. The role of glutamate in the pathophysiology of Parkinson's disease. Funct Neurol 11(1):3-15.

Blazquez PM, Fujii N, Kojima J, Graybiel AM. 2002. A network representation of response probability in the striatum. Neuron. 33(6):973-82.

Bogenpohl JW, Galvan A, Hu X, Pare JF, Wichmann T, Smith Y. Electrophysiological and behavioral effects of activation of group III metabotropic glutamate receptors in the striatopallidal complex of parkinsonian monkeys; 2010; Amsterdam, Netherlands.

Bogenpohl JW, Galvan A, Hu X, Pare JF, Wichmann T, Smith Y. Subcellular localization and electrophysiological effects of metabotropic glutamate receptor 4 activation in the striatopallidal complex of parkinsonian monkeys; 2011; Washington D.C.

Boivin B, Vaniotis G, Allen BG, Hebert TE. 2008. G protein-coupled receptors in and on the cell nucleus: a new signaling paradigm? J Recept Signal Transduct Res 28(1-2):15-28.

Bologna M, Fasano A, Modugno N, Fabbrini G, Berardelli A. 2012. Effects of subthalamic nucleus deep brain stimulation and L-DOPA on blinking in Parkinson's disease. Experimental neurology 235(1):265-272.

Bové J, Serrats J, Mengod G, Cortes R, Tolosa E, Marin C. 2005. Neuroprotection induced by the adenosine A2A antagonist CSC in the 6-OHDA rat model of parkinsonism: effect on the activity of striatal output pathways. Exp Brain Res 165(3):362-374.

Bové J, Perier C. 2012. Neurotoxin-based models of Parkinson's disease. Neuroscience. 211:51-76.

Bracco F, Battaglia A, Chouza C, Dupont E, Gershanik O, Marti Masso JF, Montastruc JL. 2004. The long-acting dopamine receptor agonist cabergoline in early Parkinson's disease: final results of a 5-year, double-blind, levodopa-controlled study. CNS Drugs 18(11):733-746.

Bradley SR, Standaert DG, Rhodes KJ, Rees HD, Testa CM, Levey AI, Conn PJ. 1999. Immunohistochemical localization of subtype 4a metabotropic glutamate receptors in the rat and mouse basal ganglia. The Journal of comparative neurology 407(1):33-46.

Brambilla R, Cottini L, Fumagalli M, Ceruti S, Abbracchio MP. 2003. Blockade of A2A adenosine receptors prevents basic fibroblast growth factor-induced reactive astrogliosis in rat striatal primary astrocytes. Glia 43(2):190-194.

Brand F, Klutz AM, Jacobson KA, Fredholm BB, Schulte G. 2008. Adenosine A(2A) receptor dynamics studied with the novel fluorescent agonist Alexa488-APEC. European journal of pharmacology 590(1-3):36-42.

Breysse N, Amalric M, Salin P. 2003. Metabotropic glutamate 5 receptor blockade alleviates akinesia by normalizing activity of selective basal-ganglia structures in parkinsonian rats. J Neurosci 23(23):8302-8309.

Breysse N, Baunez C, Spooren W, Gasparini F, Amalric M. 2002. Chronic but not acute treatment with a metabotropic glutamate 5 receptor antagonist reverses the akinetic deficits in a rat model of parkinsonism. J Neurosci 22(13):5669-5678.

Bronfeld M, Belelovsky K, Erez Y, Bugaysen J, Korngreen A, Bar-Gad I. 2010. Bicuculline-induced chorea manifests in focal rather than globalized abnormalities in the activation of the external and internal globus pallidus. Journal of neurophysiology 104(6):3261-3275.

Brown P. 2007. Abnormal oscillatory synchronisation in the motor system leads to impaired movement. Current opinion in neurobiology 17(6):656-664.

Brown RM, Short JL. 2008. Adenosine A(2A) receptors and their role in drug addiction. J Pharm Pharmacol 60(11):1409-1430.

Brundin P, Barker RA, Parmar M. 2010. Neural grafting in Parkinson's disease Problems and possibilities. Prog Brain Res 184:265-294.

Cabello N, Gandia J, Bertarelli DC, Watanabe M, Lluis C, Franco R, Ferre S, Lujan R, Ciruela F. 2009. Metabotropic glutamate type 5, dopamine D2 and adenosine A2a receptors form higher-order oligomers in living cells. Journal of neurochemistry 109(5):1497-1507.

Calabresi P, Mercuri NB, Sancesario G, Bernardi G. 1993. Electrophysiology of dopamine-denervated striatal neurons. Implications for Parkinson's disease. Brain 116 ( Pt 2):433-452.

Calabresi P, Pisani A, Mercuri NB, Bernardi G. 1996. The corticostriatal projection: from synaptic plasticity to dysfunctions of the basal ganglia. Trends in neurosciences 19(1):19-24.

Calon F, Dridi M, Hornykiewicz O, Bedard PJ, Rajput AH, Di Paolo T. 2004. Increased adenosine A2A receptors in the brain of Parkinson's disease patients with dyskinesias. Brain 127(Pt 5):1075-1084.

Calon F, Rajput AH, Hornykiewicz O, Bedard PJ, Di Paolo T. 2003. Levodopa-induced motor complications are associated with alterations of glutamate receptors in Parkinson's disease. Neurobiol Dis 14(3):404-416.

Canals M, Marcellino D, Fanelli F, Ciruela F, de Benedetti P, Goldberg SR, Neve K, Fuxe K, Agnati LF, Woods AS, Ferre S, Lluis C, Bouvier M, Franco R. 2003. Adenosine A2A-dopamine D2 receptor-receptor heteromerization: qualitative and quantitative assessment by fluorescence and bioluminescence energy transfer. The Journal of biological chemistry 278(47):46741-46749.

Canavan AG, Nixon PD, Passingham RE. 1989. Motor learning in monkeys (Macaca fascicularis) with lesions in motor thalamus. Exp Brain Res 77:113–126.

Carlsson A, Lindqvist M, Magnusson T. 1957. 3,4-Dihydroxyphenylalanine and 5-hydroxytryptophan as reserpine antagonists. Nature 180(4596):1200.

Carpenter MB, Carleton SC, Keller JT, Conte P. 1981. Connections of the subthalamic nucleus in the monkey. Brain Res. 224(1):1-29.

Celanire S, Campo B. 2012. Recent advances in the drug discovery of metabotropic glutamate receptor 4 (mGluR4) activators for the treatment of CNS and non-CNS disorders. Expert Opin Drug Discov 7(3):261-280.

Chase TN, Bibbiani F, Oh JD. 2003. Striatal glutamatergic mechanisms and extrapyramidal movement disorders. Neurotox Res 5(1-2):139-146.

Chen JF, Xu K, Petzer JP, Staal R, Xu YH, Beilstein M, Sonsalla PK, Castagnoli K, Castagnoli N, Jr., Schwarzschild MA. 2001. Neuroprotection by caffeine and A(2A) adenosine receptor inactivation in a model of Parkinson's disease. J Neurosci 21(10):RC143.

Chen L, Ding Y, Cagniard B, Van Laar AD, Mortimer A, Chi W, Hastings TG, Kang UJ, Zhuang X. 2008. Unregulated cytosolic dopamine causes neurodegeneration associated with oxidative stress in mice. J Neurosci 28(2):425-433.

Christine CW, Starr PA, Larson PS, Eberling JL, Jagust WJ, Hawkins RA, VanBrocklin HF, Wright JF, Bankiewicz KS, Aminoff MJ. 2009. Safety and tolerability of putaminal AADC gene therapy for Parkinson disease. Neurology 73(20):1662-1669.

Ciruela F, Burgueno J, Casado V, Canals M, Marcellino D, Goldberg SR, Bader M, Fuxe K, Agnati LF, Lluis C, Franco R, Ferre S, Woods AS. 2004. Combining mass spectrometry and pull-down techniques for the study of receptor heteromerization. Direct epitope-epitope electrostatic interactions between adenosine A2A and dopamine D2 receptors. Anal Chem 76(18):5354-5363.

Ciruela F, Casado V, Rodrigues RJ, Lujan R, Burgueno J, Canals M, Borycz J, Rebola N, Goldberg SR, Mallol J, Cortes A, Canela EI, Lopez-Gimenez JF, Milligan G, Lluis C, Cunha RA, Ferre S, Franco R. 2006. Presynaptic control of striatal glutamatergic neurotransmission by adenosine A1-A2A receptor heteromers. J Neurosci 26(7):2080-2087.

Coccurello R, Breysse N, Amalric M. 2004. Simultaneous blockade of adenosine A2A and metabotropic glutamate mGlu5 receptors increase their efficacy in reversing Parkinsonian deficits in rats. Neuropsychopharmacology 29(8):1451-1461.

Conn PJ, Jones CK, Lindsley CW. 2009. Subtype-selective allosteric modulators of muscarinic receptors for the treatment of CNS disorders. Trends in pharmacological sciences 30(3):148-155.

Constantinescu R, Romer M, McDermott MP, Kamp C, Kieburtz K. 2007. Impact of pramipexole on the onset of levodopa-related dyskinesias. Mov Disord 22(9):1317-1319.

Corti C, Aldegheri L, Somogyi P, Ferraguti F. 2002. Distribution and synaptic localisation of the metabotropic glutamate receptor 4 (mGluR4) in the rodent CNS. Neuroscience 110(3):403-420.

Cunha RA. 2001. Adenosine as a neuromodulator and as a homeostatic regulator in the nervous system: different roles, different sources and different receptors. Neurochemistry international 38(2):107-125.

Cunha RA, Ferre S, Vaugeois JM, Chen JF. 2008. Potential therapeutic interest of adenosine A2A receptors in psychiatric disorders. Curr Pharm Des 14(15):1512-1524.

Cunha RA, Ribeiro JA. 2000. ATP as a presynaptic modulator. Life sciences 68(2):119-137.

Cuomo D, Martella G, Barabino E, Platania P, Vita D, Madeo G, Selvam C, Goudet C, Oueslati N, Pin JP, Acher F, Pisani A, Beurrier C, Melon C, Kerkerian-Le Goff L, Gubellini P. 2009. Metabotropic glutamate receptor subtype 4 selectively

modulates both glutamate and GABA transmission in the striatum: implications for Parkinson's disease treatment. Journal of neurochemistry 109(4):1096-1105.

Dare E, Schulte G, Karovic O, Hammarberg C, Fredholm BB. 2007. Modulation of glial cell functions by adenosine receptors. Physiol Behav 92(1-2):15-20.

Davie CA. 2008. A review of Parkinson's disease. Br Med Bull. 86:109-27.

Davis GC, Williams AC, Markey SP, Ebert MH, Caine ED, Reichert CM, Kopin IJ. 1979. Chronic Parkinsonism secondary to intravenous injection of meperidine analogues. Psychiatry Res 1(3):249-254.

Day M, Wang Z, Ding J, An X, Ingham CA, Shering AF, Wokosin D, Ilijic E, Sun Z, Sampson AR, Mugnaini E, Deutch AY, Sesack SR, Arbuthnott GW, Surmeier DJ. 2006. Selective elimination of glutamatergic synapses on striatopallidal neurons in Parkinson disease models. Nat Neurosci 9(2):251-259.

Dekundy A, Pietraszek M, Schaefer D, Cenci MA, Danysz W. 2006. Effects of group I metabotropic glutamate receptors blockade in experimental models of Parkinson's disease. Brain research bulletin 69(3):318-326.

DeLong MR. 1971. Activity of pallidal neurons during movement. Journal of neurophysiology 34(3):414-427.

Deltheil T, Turle-Lorenzo N, Amalric M. Orthosteric group III mGlu receptor agonists for Parkinson’s disease treatment: symptomatic and neurochemical action on pallidal synaptic transmission; 2011; Taormina, Italy.

Deuschl G, Goddemeier C. 1998. Spontaneous and reflex activity of facial muscles in dystonia, Parkinson's disease, and in normal subjects. Journal of neurology, neurosurgery, and psychiatry 64(3):320-324.

Digby GJ, Shirey JK, Conn PJ. 2010. Allosteric activators of muscarinic receptors as novel approaches for treatment of CNS disorders. Mol Biosyst 6(8):1345-1354.

Dixon AK, Gubitz AK, Sirinathsinghji DJ, Richardson PJ, Freeman TC. 1996. Tissue distribution of adenosine receptor mRNAs in the rat. British journal of pharmacology 118(6):1461-1468.

Domenici MR, Pepponi R, Martire A, Tebano MT, Potenza RL, Popoli P. 2004. Permissive role of adenosine A2A receptors on metabotropic glutamate receptor 5 (mGluR5)-mediated effects in the striatum. Journal of neurochemistry 90(5):1276-1279.

Dunwiddie TV, Diao L. 1994. Extracellular adenosine concentrations in hippocampal brain slices and the tonic inhibitory modulation of evoked excitatory responses. The Journal of pharmacology and experimental therapeutics 268(2):537-545.

Dunwiddie TV, Diao L, Proctor WR. 1997. Adenine nucleotides undergo rapid, quantitative conversion to adenosine in the extracellular space in rat hippocampus. J Neurosci 17(20):7673-7682.

East SP, Gerlach K. 2010. mGluR4 positive allosteric modulators with potential for the treatment of Parkinson's disease: WO09010455. Expert Opin Ther Pat 20(3):441-445.

Eggert K, Squillacote D, Barone P, Dodel R, Katzenschlager R, Emre M, Lees AJ, Rascol O, Poewe W, Tolosa E, Trenkwalder C, Onofrj M, Stocchi F, Nappi G, Kostic V, Potic J, Ruzicka E, Oertel W. 2010. Safety and efficacy of perampanel in advanced Parkinson's disease: a randomized, placebo-controlled study. Mov Disord 25(7):896-905.

Elias S, Joshua M, Goldberg JA, Heimer G, Arkadir D, Morris G, Bergman H. 2007. Statistical properties of pauses of the high-frequency discharge neurons in the external segment of the globus pallidus. J Neurosci 27(10):2525-2538.

Engers DW, Field JR, Le U, Zhou Y, Bolinger JD, Zamorano R, Blobaum AL, Jones CK, Jadhav S, Weaver CD, Conn PJ, Lindsley CW, Niswender CM, Hopkins CR. 2011. Discovery, synthesis, and structure-activity relationship development of a series of N-(4-acetamido)phenylpicolinamides as positive allosteric modulators of metabotropic glutamate receptor 4 (mGlu(4)) with CNS exposure in rats. Journal of medicinal chemistry 54(4):1106-1110.

Engers DW, Gentry PR, Williams R, Bolinger JD, Weaver CD, Menon UN, Conn PJ, Lindsley CW, Niswender CM, Hopkins CR. 2010. Synthesis and SAR of novel, 4-(phenylsulfamoyl)phenylacetamide mGlu4 positive allosteric modulators (PAMs) identified by functional high-throughput screening (HTS). Bioorganic & medicinal chemistry letters 20(17):5175-5178.

Engers DW, Niswender CM, Weaver CD, Jadhav S, Menon UN, Zamorano R, Conn PJ, Lindsley CW, Hopkins CR. 2009. Synthesis and evaluation of a series of heterobiarylamides that are centrally penetrant metabotropic glutamate receptor 4 (mGluR4) positive allosteric modulators (PAMs). Journal of medicinal chemistry 52(14):4115-4118.

Factor S, Mark MH, Watts R, Struck L, Mori A, Ballerini R, Sussman NM. 2010. A long-term study of istradefylline in subjects with fluctuating Parkinson's disease. Parkinsonism & related disorders 16(6):423-426.

Feinberg M. 1993. The problems of anticholinergic adverse effects in older patients. Drugs & Aging. 3(4):335-48.

Fernandez HH, Greeley DR, Zweig RM, Wojcieszek J, Mori A, Sussman NM. 2010. Istradefylline as monotherapy for Parkinson disease: results of the 6002-US-051 trial. Parkinsonism & related disorders 16(1):16-20.

Ferre S, Ciruela F, Quiroz C, Lujan R, Popoli P, Cunha RA, Agnati LF, Fuxe K, Woods AS, Lluis C, Franco R. 2007a. Adenosine receptor heteromers and their integrative role in striatal function. ScientificWorldJournal 7:74-85.

Ferre S, Ciruela F, Woods AS, Canals M, Burgueno J, Marcellino D, Karcz-Kubicha M, Hope BT, Morales M, Popoli P, Goldberg SR, Fuxe K, Lluis C, Franco R, Agnati L. 2003. Glutamate mGlu5-adenosine A2A–dopamine D2 receptor interactions in the striatum. Implications for drug therapy in neuro-psychiatric disorders and drug abuse. Current Medicinal Chemistry-Central Nervous System Agents(3):1-26.

Ferre S, Diamond I, Goldberg SR, Yao L, Hourani SM, Huang ZL, Urade Y, Kitchen I. 2007b. Adenosine A2A receptors in ventral striatum, hypothalamus and nociceptive circuitry implications for drug addiction, sleep and pain. Progress in neurobiology 83(5):332-347.

Ferre S, Fredholm BB, Morelli M, Popoli P, Fuxe K. 1997. Adenosine-dopamine receptor-receptor interactions as an integrative mechanism in the basal ganglia. Trends in neurosciences 20(10):482-487.

Ferre S, Karcz-Kubicha M, Hope BT, Popoli P, Burgueno J, Gutierrez MA, Casado V, Fuxe K, Goldberg SR, Lluis C, Franco R, Ciruela F. 2002. Synergistic interaction between adenosine A2A and glutamate mGlu5 receptors: implications for striatal

neuronal function. Proceedings of the National Academy of Sciences of the United States of America 99(18):11940-11945.

Ferre S, Popoli P, Gimenez-Llort L, Rimondini R, Muller CE, Stromberg I, Ogren SO, Fuxe K. 2001. Adenosine/dopamine interaction: implications for the treatment of Parkinson's disease. Parkinsonism & related disorders 7(3):235-241.

Ferre S, Popoli P, Rimondini R, Reggio R, Kehr J, Fuxe K. 1999. Adenosine A2A and group I metabotropic glutamate receptors synergistically modulate the binding characteristics of dopamine D2 receptors in the rat striatum. Neuropharmacology 38(1):129-140.

Fink JS, Weaver DR, Rivkees SA, Peterfreund RA, Pollack AE, Adler EM, Reppert SM. 1992. Molecular cloning of the rat A2 adenosine receptor: selective co-expression with D2 dopamine receptors in rat striatum. Brain research 14(3):186-195.

Franco R, Ferre S, Agnati L, Torvinen M, Gines S, Hillion J, Casado V, Lledo P, Zoli M, Lluis C, Fuxe K. 2000. Evidence for adenosine/dopamine receptor interactions: indications for heteromerization. Neuropsychopharmacology 23(4 Suppl):S50-59.

Fredholm BB, Irenius E, Kull B, Schulte G. 2001. Comparison of the potency of adenosine as an agonist at human adenosine receptors expressed in Chinese hamster ovary cells. Biochem Pharmacol 61(4):443-448.

Freed CR, Greene PE, Breeze RE, Tsai WY, DuMouchel W, Kao R, Dillon S, Winfield H, Culver S, Trojanowski JQ, Eidelberg D, Fahn S. 2001. Transplantation of embryonic dopamine neurons for severe Parkinson's disease. N Engl J Med 344(10):710-719.

Galarraga E, Bargas J, Martinez-Fong D, Aceves J. 1987. Spontaneous synaptic potentials in dopamine-denervated neostriatal neurons. Neuroscience letters 81(3):351-355.

Galvan A, Hu X, Smith Y, Wichmann T. 2010. Localization and function of GABA transporters in the globus pallidus of parkinsonian monkeys. Experimental neurology 223(2):505-515.

Galvan A, Hu X, Smith Y, Wichmann T. 2011. Localization and pharmacological modulation of GABA-B receptors in the globus pallidus of parkinsonian monkeys. Experimental neurology 229(2):429-439.

Galvan A, Kuwajima M, Smith Y. 2006. Glutamate and GABA receptors and transporters in the basal ganglia: what does their subsynaptic localization reveal about their function? Neuroscience 143(2):351-375.

Galvan A, Villalba RM, West SM, Maidment NT, Ackerson LC, Smith Y, Wichmann T. 2005. GABAergic modulation of the activity of globus pallidus neurons in primates: in vivo analysis of the functions of GABA receptors and GABA transporters. Journal of neurophysiology 94(2):990-1000.

Garber JC, Barbee RW, Bielitzki JT, Clayton LA, Donovan JC, Hendriksen CFM, Kohn DF, Lipman NS, Locke PA, Melcher J, Quimby FW, Turner PV, Wood GA, Würbel H. 2010. Guide for the Care and Use of Laboratory Animals (8th Edition). Washington D.C.: The National Academies Press.

Gatev P, Wichmann T. 2009. Interactions between cortical rhythms and spiking activity of single basal ganglia neurons in the normal and parkinsonian state. Cereb Cortex. 19(6):1330-44.

Gebicke-Haerter PJ, Christoffel F, Timmer J, Northoff H, Berger M, Van Calker D. 1996. Both adenosine A1- and A2-receptors are required to stimulate microglial proliferation. Neurochemistry international 29(1):37-42.

Geiger JD, Fyda DM. 1991. Adenosine transport in nervous tissues. In: Stone TW, editor. Adenosine in the Central Nervous System. London: Academic Press. p 1-23.

Gerevich Z, Wirkner K, Illes P. 2002. Adenosine A2A receptors inhibit the N-methyl-D-aspartate component of excitatory synaptic currents in rat striatal neurons. European journal of pharmacology 451(2):161-164.

Gertler TS, Chan CS, Surmeier DJ. 2008. Dichotomous anatomical properties of adult striatal medium spiny neurons. J Neurosci 28(43):10814-10824.

Gonzales KK, Pare J-F, Wichmann T, Smith Y. GABAergic microcircuitry of cholinergic interneurons in the monkey putamen. Program No. 245.02. 2011 Neuroscience Meeting Planner. Washington, DC: Society for Neuroscience, 2011. Online.

Gravius A, Dekundy A, Nagel J, More L, Pietraszek M, Danysz W. 2008. Investigation on tolerance development to subchronic blockade of mGluR5 in models of learning, anxiety, and levodopa-induced dyskinesia in rats. J Neural Transm 115(12):1609-1619.

Granger B, Albu S. 2005. The haloperidol story. Ann Clin Psychiatry. 17(3):137-40.

Greenamyre JT. 2001. Glutamatergic influences on the basal ganglia. Clinical neuropharmacology 24(2):65-70.

Gregoire L, Morin N, Ouattara B, Gasparini F, Bilbe G, Johns D, Vranesic I, Sahasranaman S, Gomez-Mancilla B, Di Paolo T. 2011. The acute antiparkinsonian and antidyskinetic effect of AFQ056, a novel metabotropic

glutamate receptor type 5 antagonist, in L-Dopa-treated parkinsonian monkeys. Parkinsonism & related disorders 17(4):270-276.

Grondin R, Bedard PJ, Hadj Tahar A, Gregoire L, Mori A, Kase H. 1999. Antiparkinsonian effect of a new selective adenosine A2A receptor antagonist in MPTP-treated monkeys. Neurology 52(8):1673-1677.

Group PS. 2000a. Pramipexole vs levodopa as initial treatment for Parkinson disease: A randomized controlled trial. Parkinson Study Group. JAMA 284(15):1931-1938.

Group PS. 2000b. A randomized controlled trial comparing pramipexole with levodopa in early Parkinson's disease: design and methods of the CALM-PD Study. Parkinson Study Group. Clinical neuropharmacology 23(1):34-44.

Group PS. 2009. Long-term effect of initiating pramipexole vs levodopa in early Parkinson disease. Archives of neurology 66(5):563-570.

Gubellini P, Picconi B, Bari M, Battista N, Calabresi P, Centonze D, Bernardi G, Finazzi-Agro A, Maccarrone M. 2002. Experimental parkinsonism alters endocannabinoid degradation: implications for striatal glutamatergic transmission. J Neurosci 22(16):6900-6907.

Gubitz AK, Widdowson L, Kurokawa M, Kirkpatrick KA, Richardson PJ. 1996. Dual signalling by the adenosine A2a receptor involves activation of both N- and P-type calcium channels by different G proteins and protein kinases in the same striatal nerve terminals. Journal of neurochemistry 67(1):374-381.

Hagberg H, Andersson P, Lacarewicz J, Jacobson I, Butcher S, Sandberg M. 1987. Extracellular adenosine, inosine, hypoxanthine, and xanthine in relation to tissue

nucleotides and purines in rat striatum during transient ischemia. Journal of neurochemistry 49(1):227-231.

Halliday DM, Rosenberg JR, Amjad AM, Breeze P, Conway BA, Farmer SF. 1995. A framework for the analysis of mixed time series/point process data--theory and application to the study of physiological tremor, single motor unit discharges and electromyograms. Prog Biophys Mol Biol 64(2-3):237-278.

Hammond C, Bergman H, Brown P. 2007. Pathological synchronization in Parkinson's disease: networks, models and treatments. Trends Neurosci. 30(7):357-64.

Hanson JE, Smith Y. 1999. Group I metabotropic glutamate receptors at GABAergic synapses in monkeys. J Neurosci 19(15):6488-6496.

Hargus G, Cooper O, Deleidi M, Levy A, Lee K, Marlow E, Yow A, Soldner F, Hockemeyer D, Hallett PJ, Osborn T, Jaenisch R, Isacson O. 2010. Differentiated Parkinson patient-derived induced pluripotent stem cells grow in the adult rodent brain and reduce motor asymmetry in Parkinsonian rats. Proceedings of the National Academy of Sciences of the United States of America 107(36):15921-15926.

Hauser RA, Hubble JP, Truong DD. 2003. Randomized trial of the adenosine A(2A) receptor antagonist istradefylline in advanced PD. Neurology 61(3):297-303.

Hauser RA, Cantillon M, Pourcher E, Micheli F, Mok V, Onofrj M, Huyck S, Wolski K. 2011. Preladenant in patients with Parkinson's disease and motor fluctuations: a phase 2, double-blind, randomised trial. Lancet Neurol. 10(3):221-9.

Henry JP, Scherman D. 1989. Radioligands of the vesicular monoamine transporter and their use as markers of monoamine storage vesicles. Biochem Pharmacol. 38(15):2395-404.

Hersch SM, Ciliax BJ, Gutekunst CA, Rees HD, Heilman CJ, Yung KK, Bolam JP, Ince E, Yi H, Levey AI. 1995. Electron microscopic analysis of D1 and D2 dopamine receptor proteins in the dorsal striatum and their synaptic relationships with motor corticostriatal afferents. J Neurosci 15(7 Pt 2):5222-5237.

Hettinger BD, Lee A, Linden J, Rosin DL. 2001. Ultrastructural localization of adenosine A2A receptors suggests multiple cellular sites for modulation of GABAergic neurons in rat striatum. The Journal of comparative neurology 431(3):331-346.

Hillion J, Canals M, Torvinen M, Casado V, Scott R, Terasmaa A, Hansson A, Watson S, Olah ME, Mallol J, Canela EI, Zoli M, Agnati LF, Ibanez CF, Lluis C, Franco R, Ferre S, Fuxe K. 2002. Coaggregation, cointernalization, and codesensitization of adenosine A2A receptors and dopamine D2 receptors. The Journal of biological chemistry 277(20):18091-18097.

Hindley S, Herman MA, Rathbone MP. 1994. Stimulation of reactive astrogliosis in vivo by extracellular adenosine diphosphate or an adenosine A2 receptor agonist. Journal of neuroscience research 38(4):399-406.

Hodgson RA, Bedard PJ, Varty GB, Kazdoba TM, Di Paolo T, Grzelak ME, Pond AJ, Hadjtahar A, Belanger N, Gregoire L, Dare A, Neustadt BR, Stamford AW, Hunter JC. 2010. Preladenant, a selective A(2A) receptor antagonist, is active in primate models of movement disorders. Experimental neurology 225(2):384-390.

Hodgson RA, Bertorelli R, Varty GB, Lachowicz JE, Forlani A, Fredduzzi S, Cohen-Williams ME, Higgins GA, Impagnatiello F, Nicolussi E, Parra LE, Foster C, Zhai Y, Neustadt BR, Stamford AW, Parker EM, Reggiani A, Hunter JC. 2009. Characterization of the potent and highly selective A2A receptor antagonists preladenant and SCH 412348 [7-[2-[4-2,4-difluorophenyl]-1-piperazinyl]ethyl]-2-(2-furanyl)-7H-pyrazol o[4,3-e][1,2,4]triazolo[1,5-c]pyrimidin-5-amine] in rodent models of movement disorders and depression. The Journal of pharmacology and experimental therapeutics 330(1):294-303.

Holloway RG, Shoulson I, Fahn S, Kieburtz K, Lang A, Marek K, McDermott M, Seibyl J, Weiner W, Musch B, Kamp C, Welsh M, Shinaman A, Pahwa R, Barclay L, Hubble J, LeWitt P, Miyasaki J, Suchowersky O, Stacy M, Russell DS, Ford B, Hammerstad J, Riley D, Standaert D, Wooten F, Factor S, Jankovic J, Atassi F, Kurlan R, Panisset M, Rajput A, Rodnitzky R, Shults C, Petsinger G, Waters C, Pfeiffer R, Biglan K, Borchert L, Montgomery A, Sutherland L, Weeks C, DeAngelis M, Sime E, Wood S, Pantella C, Harrigan M, Fussell B, Dillon S, Alexander-Brown B, Rainey P, Tennis M, Rost-Ruffner E, Brown D, Evans S, Berry D, Hall J, Shirley T, Dobson J, Fontaine D, Pfeiffer B, Brocht A, Bennett S, Daigneault S, Hodgeman K, O'Connell C, Ross T, Richard K, Watts A. 2004. Pramipexole vs levodopa as initial treatment for Parkinson disease: a 4-year randomized controlled trial. Archives of neurology 61(7):1044-1053.

Hoover, B.R., and Marshall, J.F. 1999. Population characteristics of preproenkephalin mRNA-containing neurons in the globus pallidus of the rat. Neurosci. Lett. 265, 199–202.

Hopkins CR, Lindsley CW, Niswender CM. 2009. mGluR4-positive allosteric modulation as potential treatment for Parkinson's disease. Future Med Chem 1(3):501-513.

Hsieh MH, Ho SC, Yeh KY, Pawlak CR, Chang HM, Ho YJ, Lai TJ, Wu FY. 2012. Blockade of metabotropic glutamate receptors inhibits cognition and neurodegeneration in an MPTP-induced Parkinson's disease rat model. Pharmacol Biochem Behav 102(1):64-71.

Hubert GW, Paquet M, Smith Y. 2001. Differential subcellular localization of mGluR1a and mGluR5 in the rat and monkey Substantia nigra. J Neurosci 21(6):1838-1847.

Hubert GW, Smith Y. 2004. Age-related changes in the expression of axonal and glial group I metabotropic glutamate receptor in the rat substantia nigra pars reticulata. The Journal of comparative neurology 475(1):95-106.

Hughes AJ. 1997. Drug treatment of Parkinson's disease in the 1990s. Achievements and future possibilities. Drugs 53(2):195-205.

Hughes AJ, Bishop S, Kleedorfer B, Turjanski N, Fernandez W, Lees AJ, Stern GM. 1993. Subcutaneous apomorphine in Parkinson's disease: response to chronic administration for up to five years. Mov Disord 8(2):165-170.

Hyson HC, Johnson AM, Jog MS. 2002. Sublingual atropine for sialorrhea secondary to parkinsonism: a pilot study. Mov Disord. 17(6):1318-20.

Ikeda K, Kurokawa M, Aoyama S, Kuwana Y. 2002. Neuroprotection by adenosine A2A receptor blockade in experimental models of Parkinson's disease. Journal of neurochemistry 80(2):262-270.

Inzelberg R, Bonuccelli U, Schechtman E, Miniowich A, Strugatsky R, Ceravolo R, Logi C, Rossi C, Klein C, Rabey JM. 2006. Association between amantadine and the onset of dementia in Parkinson's disease. Mov Disord 21(9):1375-1379.

Jarraya B, Boulet S, Ralph GS, Jan C, Bonvento G, Azzouz M, Miskin JE, Shin M, Delzescaux T, Drouot X, Herard AS, Day DM, Brouillet E, Kingsman SM, Hantraye P, Mitrophanous KA, Mazarakis ND, Palfi S. 2009. Dopamine gene therapy for Parkinson's disease in a nonhuman primate without associated dyskinesia. Sci Transl Med 1(2):2ra4.

Jellinger KA. 1991. Pathology of Parkinson's disease. Changes other than the nigrostriatal pathway. Mol Chem Neuropathol 14(3):153-197.

Johnson KA, Conn PJ, Niswender CM. 2009. Glutamate receptors as therapeutic targets for Parkinson's disease. CNS Neurol Disord Drug Targets 8(6):475-491.

Johnston TH, Fox SH, McIldowie MJ, Piggott MJ, Brotchie JM. 2010. Reduction of L-DOPA-induced dyskinesia by the selective metabotropic glutamate receptor 5 antagonist 3-[(2-methyl-1,3-thiazol-4-yl)ethynyl]pyridine in the 1-methyl-4-phenyl-1,2,3,6-tetrahydropyridine-lesioned macaque model of Parkinson's disease. The Journal of pharmacology and experimental therapeutics 333(3):865-873.

Jones CK, Bubser M, Thompson AD, Dickerson JW, Turle-Lorenzo N, Amalric M, Blobaum AL, Bridges TM, Morrison RD, Jadhav S, Engers DW, Italiano K, Bode J, Daniels JS, Lindsley CW, Hopkins CR, Conn PJ, Niswender CM. 2012. The metabotropic glutamate receptor 4-positive allosteric modulator VU0364770 produces efficacy alone and in combination with L-DOPA or an adenosine 2A

antagonist in preclinical rodent models of Parkinson's disease. The Journal of pharmacology and experimental therapeutics 340(2):404-421.

Kachroo A, Orlando LR, Grandy DK, Chen JF, Young AB, Schwarzschild MA. 2005. Interactions between metabotropic glutamate 5 and adenosine A2A receptors in normal and parkinsonian mice. J Neurosci 25(45):10414-10419.

Kaelin-Lang A, Liniger P, Probst A, Lauterburg T, Burgunder JM. 2000. Adenosine A2A receptor gene expression in the normal striatum and after 6-OH-dopamine lesion. J Neural Transm 107(8-9):851-859.

Kanda T, Jackson MJ, Smith LA, Pearce RK, Nakamura J, Kase H, Kuwana Y, Jenner P. 2000. Combined use of the adenosine A(2A) antagonist KW-6002 with L-DOPA or with selective D1 or D2 dopamine agonists increases antiparkinsonian activity but not dyskinesia in MPTP-treated monkeys. Experimental neurology 162(2):321-327.

Kanda T, Shiozaki S, Shimada J, Suzuki F, Nakamura J. 1994. KF17837: a novel selective adenosine A2A receptor antagonist with anticataleptic activity. European journal of pharmacology 256(3):263-268.

Kaneko K, Sakamoto K. 2001. Spontaneous blinks of Parkinson's disease patients evaluated by EMG and EOG. Electromyogr Clin Neurophysiol 41(2):87-95.

Karson CN, Burns RS, LeWitt PA, Foster NL, Newman RP. 1984. Blink rates and disorders of movement. Neurology 34(5):677-678.

Kerner JA, Standaert DG, Penney JB, Jr., Young AB, Landwehrmeyer GB. Expression of Group II and III mGluR mRNAs in identified striatal and cortical neurons.; 1997; New Orleans, LA.

Kimura M, Kato M, Shimazaki H, Watanabe K, Matsumoto N. 1996. Neural information transferred from the putamen to the globus pallidus during learned movement in the monkey. J Neurophysiol. 76(6):3771-86.

Kirk IP, Richardson PJ. 1995. Inhibition of striatal GABA release by the adenosine A2a receptor is not mediated by increases in cyclic AMP. Journal of neurochemistry 64(6):2801-2809.

Kita H, Kitai ST. 1994. The morphology of globus pallidus projection neurons in the rat: an intracellular staining study. Brain Res. 636(2):308-19.

Kliem MA, Pare JF, Khan ZU, Wichmann T, Smith Y. 2010. Ultrastructural localization and function of dopamine D1-like receptors in the substantia nigra pars reticulata and the internal segment of the globus pallidus of parkinsonian monkeys. The European journal of neuroscience 31(5):836-851.

Kliem MA, Wichmann T. 2004. A method to record changes in local neuronal discharge in response to infusion of small drug quantities in awake monkeys. Journal of neuroscience methods 138(1-2):45-49.

Klockgether T, Turski L, Honore T, Zhang ZM, Gash DM, Kurlan R, Greenamyre JT. 1991. The AMPA receptor antagonist NBQX has antiparkinsonian effects in monoamine-depleted rats and MPTP-treated monkeys. Annals of neurology 30(5):717-723.

Kobylecki C, Hill MP, Crossman AR, Ravenscroft P. 2011. Synergistic antidyskinetic effects of topiramate and amantadine in animal models of Parkinson's disease. Mov Disord 26(13):2354-2363.

Koller WC (1986). Pharmacologic treatment of parkinsonian tremor. Arch Neurol 43: 126–127.

Konieczny J, Wardas J, Kuter K, Pilc A, Ossowska K. 2007. The influence of group III metabotropic glutamate receptor stimulation by (1S,3R,4S)-1-aminocyclo-pentane-1,3,4-tricarboxylic acid on the parkinsonian-like akinesia and striatal proenkephalin and prodynorphin mRNA expression in rats. Neuroscience 145(2):611-620.

Kühn AA, Kupsch A, Schneider GH, Brown P. 2006 Reduction in subthalamic 8-35 Hz oscillatory activity correlates with clinical improvement in Parkinson's disease. Eur J Neurosci. 23(7):1956-60.

Kuwajima M, Hall RA, Aiba A, Smith Y. 2004. Subcellular and subsynaptic localization of group I metabotropic glutamate receptors in the monkey subthalamic nucleus. The Journal of comparative neurology 474(4):589-602.

Kvernmo T, Hartter S, Burger E. 2006. A review of the receptor-binding and pharmacokinetic properties of dopamine agonists. Clin Ther 28(8):1065-1078.

Landwehrmeyer GB, Standaert DG, Testa CM, Penney JB, Jr., Young AB. 1995. NMDA receptor subunit mRNA expression by projection neurons and interneurons in rat striatum. J Neurosci 15(7 Pt 2):5297-5307.

Langston JW, Forno LS, Rebert CS, Irwin I. 1984. Selective nigral toxicity after systemic administration of 1-methyl-4-phenyl-1,2,5,6-tetrahydropyrine (MPTP) in the squirrel monkey. Brain Res 292(2):390-394.

Langston J, Palfremann J. 1995. The Case of the Frozen Addicts. New York: Random House.

Latini S, Pedata F. 2001. Adenosine in the central nervous system: release mechanisms and extracellular concentrations. Journal of neurochemistry 79(3):463-484.

Leblois A, Meissner W, Bioulac B, Gross CE, Hansel D, Boraud T. 2007. Late emergence of synchronized oscillatory activity in the pallidum during progressive Parkinsonism. Eur J Neurosci. 26(6):1701-13.

Lee IH, Seitz AR, Assad JA. 2006. Activity of tonically active neurons in the monkey putamen during initiation and withholding of movement. J Neurophysiol. 95(4):2391-403.

Lee J, Ziering A, et al. 1947. Piperidine derivatives; 2-phenyl- and 2-phenylalkyl-piperidines. J Org Chem 12(6):885-893.

Lees A, Fahn S, Eggert KM, Jankovic J, Lang A, Micheli F, Mouradian MM, Oertel WH, Olanow CW, Poewe W, Rascol O, Tolosa E, Squillacote D, Kumar D. 2012. Perampanel, an AMPA antagonist, found to have no benefit in reducing "off" time in Parkinson's disease. Mov Disord 27(2):284-288.

Legendy CR, Salcman M. 1985. Bursts and recurrences of bursts in the spike trains of spontaneously active striate cortex neurons. Journal of neurophysiology 53(4):926-939.

Lester J, Fink S, Aronin N, DiFiglia M. 1993. Colocalization of D1 and D2 dopamine receptor mRNAs in striatal neurons. Brain Res 621(1):106-110.

Levandis G, Bazzini E, Armentero MT, Nappi G, Blandini F. 2008. Systemic administration of an mGluR5 antagonist, but not unilateral subthalamic lesion, counteracts l-DOPA-induced dyskinesias in a rodent model of Parkinson's disease. Neurobiol Dis 29(1):161-168.

LeWitt PA, Guttman M, Tetrud JW, Tuite PJ, Mori A, Chaikin P, Sussman NM. 2008. Adenosine A2A receptor antagonist istradefylline (KW-6002) reduces "off" time in Parkinson's disease: a double-blind, randomized, multicenter clinical trial (6002-US-005). Annals of neurology 63(3):295-302.

Liang L, DeLong MR, Papa SM. 2008. Inversion of dopamine responses in striatal medium spiny neurons and involuntary movements. J Neurosci 28(30):7537-7547.

Lopez S, Turle-Lorenzo N, Acher F, De Leonibus E, Mele A, Amalric M. 2007. Targeting group III metabotropic glutamate receptors produces complex behavioral effects in rodent models of Parkinson's disease. J Neurosci 27(25):6701-6711.

Lopez S, Turle-Lorenzo N, Johnston TH, Brotchie JM, Schann S, Neuville P, Amalric M. 2008. Functional interaction between adenosine A2A and group III metabotropic glutamate receptors to reduce parkinsonian symptoms in rats. Neuropharmacology 55(4):483-490.

Loschmann PA, Kunow M, Wachtel H. 1992. Synergism of NBQX with dopamine agonists in the 6-OHDA rat model of Parkinson's disease. Journal of neural transmission 38:55-64.

MacInnes N, Messenger MJ, Duty S. 2004. Activation of group III metabotropic glutamate receptors in selected regions of the basal ganglia alleviates akinesia in the reserpine-treated rat. British journal of pharmacology 141(1):15-22.

Mahon S, Vautrelle N, Pezard L, Slaght SJ, Deniau JM, Chouvet G, Charpier S. 2006. Distinct patterns of striatal medium spiny neuron activity during the natural sleep-wake cycle. J Neurosci. 26(48):12587-95.

Mallet N, Micklem BR, Henny P, Brown MT, Williams C, Bolam JP, Nakamura KC, Magill PJ. 2012. Dichotomous organization of the external globus pallidus. Neuron 74(6):1075-1086.

Marino MJ, Conn PJ. 2006. Glutamate-based therapeutic approaches: allosteric modulators of metabotropic glutamate receptors. Current opinion in pharmacology 6(1):98-102.

Marino MJ, Hess JF, Liverton N. 2005. Targeting the metabotropic glutamate receptor mGluR4 for the treatment of diseases of the central nervous system. Current topics in medicinal chemistry 5(9):885-895.

Marino MJ, Williams DL, Jr., O'Brien JA, Valenti O, McDonald TP, Clements MK, Wang R, DiLella AG, Hess JF, Kinney GG, Conn PJ. 2003. Allosteric modulation of group III metabotropic glutamate receptor 4: a potential approach to Parkinson's disease treatment. Proceedings of the National Academy of Sciences of the United States of America 100(23):13668-13673.

Marino MJ, Wittmann M, Bradley SR, Hubert GW, Smith Y, Conn PJ. 2001. Activation of group I metabotropic glutamate receptors produces a direct excitation and disinhibition of GABAergic projection neurons in the substantia nigra pars reticulata. J Neurosci 21(18):7001-7012.

Martin ED, Fernandez M, Perea G, Pascual O, Haydon PG, Araque A, Cena V. 2007. Adenosine released by astrocytes contributes to hypoxia-induced modulation of synaptic transmission. Glia 55(1):36-45.

Martinez-Mir MI, Probst A, Palacios JM. 1991. Adenosine A2 receptors: selective localization in the human basal ganglia and alterations with disease. Neuroscience 42(3):697-706.

Masilamoni GJ, Bogenpohl JW, Alagille D, Delevich K, Tamagnan G, Votaw JR, Wichmann T, Smith Y. 2011. Metabotropic glutamate receptor 5 antagonist protects dopaminergic and noradrenergic neurons from degeneration in MPTP-treated monkeys. Brain 134(Pt 7):2057-2073.

Masilamoni JG, Alagille D, Bogenpohl JW, Delevich K, Reddy V, Votaw JR, Tamagnan G, Wichmann T, Smith Y. 2009. Potential neuroprotective effects of metabotropic glutamate receptor type 5 (mGluR5) antagonist in MPTP-treated monkeys. Movement Disorders Society 13th International Congress. Paris, France.

Matsubayashi H, Swanson KL, Albuquerque EX. 1997. Amantadine inhibits nicotinic acetylcholine receptor function in hippocampal neurons. J Pharmacol Exp Ther. 281(2):834-44.

Matsui T, Kita H. 2003. Activation of group III metabotropic glutamate receptors presynaptically reduces both GABAergic and glutamatergic transmission in the rat globus pallidus. Neuroscience 122(3):727-737.

Matsumura M, Tremblay L, Richard H, Filion M. 1995. Activity of pallidal neurons in the monkey during dyskinesia induced by injection of bicuculline in the external pallidum. Neuroscience 65(1):59-70.

McDowell K, Chesselet MF. 2012. Animal models of the non-motor features of Parkinson's disease. Neurobiol Dis. 46(3):597-606.

Meissner, W., Leblois, A., Hansel, D., Bioulac, B., Gross, C., Benazzouz, A. & Boraud, T. 2005. Subthalamic high frequency stimulation resets subthalamic firing and reduces abnormal oscillations. Brain, 128, 2372–2382.

Mela F, Marti M, Dekundy A, Danysz W, Morari M, Cenci MA. 2007. Antagonism of metabotropic glutamate receptor type 5 attenuates l-DOPA-induced dyskinesia and its molecular and neurochemical correlates in a rat model of Parkinson's disease. Journal of neurochemistry 101(2):483-497.

Milojevic T, Reiterer V, Stefan E, Korkhov VM, Dorostkar MM, Ducza E, Ogris E, Boehm S, Freissmuth M, Nanoff C. 2006. The ubiquitin-specific protease Usp4 regulates the cell surface level of the A2A receptor. Molecular pharmacology 69(4):1083-1094.

Mishina M, Ishiwata K, Kimura Y, Naganawa M, Oda K, Kobayashi S, Katayama Y, Ishii K. 2007. Evaluation of distribution of adenosine A2A receptors in normal human brain measured with [11C]TMSX PET. Synapse (New York, NY 61(9):778-784.

Mitrano DA, Smith Y. 2007. Comparative analysis of the subcellular and subsynaptic localization of mGluR1a and mGluR5 metabotropic glutamate receptors in the shell and core of the nucleus accumbens in rat and monkey. The Journal of comparative neurology 500(4):788-806.

Montastruc JL, Rascol O, Senard JM, Rascol A. 1992. A pilot study of N-methyl-D-aspartate (NMDA) antagonist in Parkinson's disease. Journal of neurology, neurosurgery, and psychiatry 55(7):630-631.

Morelli M, Di Paolo T, Wardas J, Calon F, Xiao D, Schwarzschild MA. 2007. Role of adenosine A2A receptors in parkinsonian motor impairment and l-DOPA-induced motor complications. Progress in neurobiology 83(5):293-309.

Morelli M, Pinna A. 2001. Interaction between dopamine and adenosine A2A receptors as a basis for the treatment of Parkinson's disease. Neurol Sci 22(1):71-72.

Morin N, Gregoire L, Gomez-Mancilla B, Gasparini F, Di Paolo T. 2010. Effect of the metabotropic glutamate receptor type 5 antagonists MPEP and MTEP in parkinsonian monkeys. Neuropharmacology 58(7):981-986.

Nakajima Y, Iwakabe H, Akazawa C, Nawa H, Shigemoto R, Mizuno N, Nakanishi S. 1993. Molecular characterization of a novel retinal metabotropic glutamate receptor mGluR6 with a high agonist selectivity for L-2-amino-4-phosphonobutyrate. The Journal of biological chemistry 268(16):11868-11873.

Nayyar T, Bubser M, Ferguson MC, Neely MD, Shawn Goodwin J, Montine TJ, Deutch AY, Ansah TA. 2009. Cortical serotonin and norepinephrine denervation in parkinsonism: preferential loss of the beaded serotonin innervation. The European journal of neuroscience 30(2):207-216.

Newman-Tancredi A, Cussac D, Audinot V, Nicolas JP, De Ceuninck F, Boutin JA, Millan MJ. 2002. Differential actions of antiparkinson agents at multiple classes of monoaminergic receptor. II. Agonist and antagonist properties at subtypes of

dopamine D(2)-like receptor and alpha(1)/alpha(2)-adrenoceptor. The Journal of pharmacology and experimental therapeutics 303(2):805-814.

Nicoletti F, Bockaert J, Collingridge GL, Conn PJ, Ferraguti F, Schoepp DD, Wroblewski JT, Pin JP. 2011. Metabotropic glutamate receptors: from the workbench to the bedside. Neuropharmacology 60(7-8):1017-1041.

Nielsen JB, Conway BA, Halliday DM, Perreault MC, Hultborn H. 2005. Organization of common synaptic drive to motoneurones during fictive locomotion in the spinal cat. The Journal of physiology 569(Pt 1):291-304.

Nini, A., Feingold, A., Slovin, H. & Bergman, H. 1995. Neurons in the globus pallidus do not show correlated activity in the normal monkey, but phase-locked oscillations appear in the MPTP model of parkinsonism. J. Neurophysiol., 74, 1800–1805.

Nishi A, Liu F, Matsuyama S, Hamada M, Higashi H, Nairn AC, Greengard P. 2003. Metabotropic mGlu5 receptors regulate adenosine A2A receptor signaling. Proceedings of the National Academy of Sciences of the United States of America 100(3):1322-1327.

Nishizaki T, Nagai K, Nomura T, Tada H, Kanno T, Tozaki H, Li XX, Kondoh T, Kodama N, Takahashi E, Sakai N, Tanaka K, Saito N. 2002. A new neuromodulatory pathway with a glial contribution mediated via A(2a) adenosine receptors. Glia 39(2):133-147.

Niswender CM, Conn PJ. 2010. Metabotropic glutamate receptors: physiology, pharmacology, and disease. Annu Rev Pharmacol Toxicol 50:295-322.

Niswender CM, Johnson KA, Weaver CD, Jones CK, Xiang Z, Luo Q, Rodriguez AL, Marlo JE, de Paulis T, Thompson AD, Days EL, Nalywajko T, Austin CA,

Williams MB, Ayala JE, Williams R, Lindsley CW, Conn PJ. 2008. Discovery, characterization, and antiparkinsonian effect of novel positive allosteric modulators of metabotropic glutamate receptor 4. Molecular pharmacology 74(5):1345-1358.

Nobre HV, Jr., Cunha GM, de Vasconcelos LM, Magalhaes HI, Oliveira Neto RN, Maia FD, de Moraes MO, Leal LK, Viana GS. 2010. Caffeine and CSC, adenosine A2A antagonists, offer neuroprotection against 6-OHDA-induced neurotoxicity in rat mesencephalic cells. Neurochemistry international 56(1):51-58.

Nordstrom CH, Rehncrona S, Siesjo BK, Westerberg E. 1977. Adenosine in rat cerebral cortex: its determination, normal values, and correlation to AMP and cyclic AMP during shortlasting ischemia. Acta Physiol Scand 101(1):63-71.

Norenberg W, Wirkner K, Assmann H, Richter M, Illes P. 1998. Adenosine A2A receptors inhibit the conductance of NMDA receptor channels in rat neostriatal neurons. Amino acids 14(1-3):33-39.

Norenberg W, Wirkner K, Illes P. 1997. Effect of adenosine and some of its structural analogues on the conductance of NMDA receptor channels in a subset of rat neostriatal neurones. British journal of pharmacology 122(1):71-80.

Nutt JG, Gunzler SA, Kirchhoff T, Hogarth P, Weaver JL, Krams M, Jamerson B, Menniti FS, Landen JW. 2008. Effects of a NR2B selective NMDA glutamate antagonist, CP-101,606, on dyskinesia and Parkinsonism. Mov Disord 23(13):1860-1866.

O'Malley KL, Jong YJ, Gonchar Y, Burkhalter A, Romano C. 2003. Activation of metabotropic glutamate receptor mGlu5 on nuclear membranes mediates

intranuclear Ca2+ changes in heterologous cell types and neurons. The Journal of biological chemistry 278(30):28210-28219.

Ochi M, Koga K, Kurokawa M, Kase H, Nakamura J, Kuwana Y. 2000. Systemic administration of adenosine A(2A) receptor antagonist reverses increased GABA release in the globus pallidus of unilateral 6-hydroxydopamine-lesioned rats: a microdialysis study. Neuroscience 100(1):53-62.

Olanow CW, Goetz CG, Kordower JH, Stoessl AJ, Sossi V, Brin MF, Shannon KM, Nauert GM, Perl DP, Godbold J, Freeman TB. 2003. A double-blind controlled trial of bilateral fetal nigral transplantation in Parkinson's disease. Annals of neurology 54(3):403-414.

Olanow CW, Obeso JA, Stocchi F. 2006. Continuous dopamine-receptor treatment of Parkinson's disease: scientific rationale and clinical implications. Lancet Neurol 5(8):677-687.

Orr AG, Orr AL, Li XJ, Gross RE, Traynelis SF. 2009. Adenosine A(2A) receptor mediates microglial process retraction. Nat Neurosci 12(7):872-878.

Ossowska K, Konieczny J, Wardas J, Golembiowska K, Wolfarth S, Pilc A. 2002. The role of striatal metabotropic glutamate receptors in Parkinson's disease. Amino acids 23(1-3):193-198.

Ossowska K, Konieczny J, Wardas J, Pietraszek M, Kuter K, Wolfarth S, Pilc A. 2007. An influence of ligands of metabotropic glutamate receptor subtypes on parkinsonian-like symptoms and the striatopallidal pathway in rats. Amino acids 32(2):179-188.

Ossowska K, Konieczny J, Wolfarth S, Pilc A. 2005. MTEP, a new selective antagonist of the metabotropic glutamate receptor subtype 5 (mGluR5), produces antiparkinsonian-like effects in rats. Neuropharmacology 49(4):447-455.

Ouattara B, Gasparini F, Morissette M, Gregoire L, Samadi P, Gomez-Mancilla B, Di Paolo T. 2010. Effect of L-Dopa on metabotropic glutamate receptor 5 in the brain of parkinsonian monkeys. Journal of neurochemistry 113(3):715-724.

Ouattara B, Gregoire L, Morissette M, Gasparini F, Vranesic I, Bilbe G, Johns DR, Rajput A, Hornykiewicz O, Rajput AH, Gomez-Mancilla B, Di Paolo T. 2011. Metabotropic glutamate receptor type 5 in levodopa-induced motor complications. Neurobiol Aging 32(7):1286-1295.

Paquet M, Smith Y. 2003. Group I metabotropic glutamate receptors in the monkey striatum: subsynaptic association with glutamatergic and dopaminergic afferents. J Neurosci 23(20):7659-7669.

Parent A, Charara A, Pinault D. 1995. Single striatofugal axons arborizing in both pallidal segments and in the substantia nigra in primates. Brain Res 698(1-2):280-284.

Parent A, Sato F, Wu Y, Gauthier J, Levesque M, Parent M. 2000. Organization of the basal ganglia: the importance of axonal collateralization. Trends in neurosciences 23(10 Suppl):S20-27.

Parkinson J. 1817. An essay on the shaking palsy. London: Whittingham and Rowland for Sherwood, Neely, and Jones. 66 p. p.

Parpura V, Zorec R. 2010. Gliotransmission: Exocytotic release from astrocytes. Brain Res Rev 63(1-2):83-92.

Paxinos G, Huang XF, Toga AW. 2000. The rhesus monkey brain in stereotaxic coordinates. San Diego, CA: Academic Press. 163 p. p.

Peterfreund RA, MacCollin M, Gusella J, Fink JS. 1996. Characterization and expression of the human A2a adenosine receptor gene. Journal of neurochemistry 66(1):362-368.

Peters A, Palay SL, Webster Hd. 1991. The fine structure of the nervous system : neurons and their supporting cells. New York: Oxford University Press. xviii, 494 p. p.

Picconi B, Centonze D, Hakansson K, Bernardi G, Greengard P, Fisone G, Cenci MA, Calabresi P. 2003. Loss of bidirectional striatal synaptic plasticity in L-DOPA-induced dyskinesia. Nat Neurosci 6(5):501-506.

Picconi B, Centonze D, Rossi S, Bernardi G, Calabresi P. 2004. Therapeutic doses of L-dopa reverse hypersensitivity of corticostriatal D2-dopamine receptors and glutamatergic overactivity in experimental parkinsonism. Brain 127(Pt 7):1661-1669.

Picconi B, Pisani A, Centonze D, Battaglia G, Storto M, Nicoletti F, Bernardi G, Calabresi P. 2002. Striatal metabotropic glutamate receptor function following experimental parkinsonism and chronic levodopa treatment. Brain 125(Pt 12):2635-2645.

Pierri M, Vaudano E, Sager T, Englund U. 2005. KW-6002 protects from MPTP induced dopaminergic toxicity in the mouse. Neuropharmacology 48(4):517-524.

Pinna A. 2009. Novel investigational adenosine A2A receptor antagonists for Parkinson's disease. Expert Opin Investig Drugs 18(11):1619-1631.

Pinna A, Pontis S, Borsini F, Morelli M. 2007. Adenosine A2A receptor antagonists improve deficits in initiation of movement and sensory motor integration in the unilateral 6-hydroxydopamine rat model of Parkinson's disease. Synapse (New York, NY 61(8):606-614.

Popoli P, Betto P, Reggio R, Ricciarello G. 1995. Adenosine A2A receptor stimulation enhances striatal extracellular glutamate levels in rats. European journal of pharmacology 287(2):215-217.

Popoli P, Pezzola A, Torvinen M, Reggio R, Pintor A, Scarchilli L, Fuxe K, Ferre S. 2001. The selective mGlu(5) receptor agonist CHPG inhibits quinpirole-induced turning in 6-hydroxydopamine-lesioned rats and modulates the binding characteristics of dopamine D(2) receptors in the rat striatum: interactions with adenosine A(2a) receptors. Neuropsychopharmacology 25(4):505-513.

Przedborski S, Jackson-Lewis V, Naini AB, Jakowec M, Petzinger G, Miller R, Akram M. 2001. The parkinsonian toxin 1-methyl-4-phenyl-1,2,3,6-tetrahydropyridine (MPTP): a technical review of its utility and safety. Journal of neurochemistry 76(5):1265-1274.

Querejeta E, Martinez-Romero B, Miranda JE, Delgado A. 2010. Modulation of the striato-pallidal pathway by adenosine A2a receptors depends on dopaminergic striatal input. Brain Res 1349:137-142.

Quiroz C, Lujan R, Uchigashima M, Simoes AP, Lerner TN, Borycz J, Kachroo A, Canas PM, Orru M, Schwarzschild MA, Rosin DL, Kreitzer AC, Cunha RA, Watanabe M, Ferre S. 2009. Key modulatory role of presynaptic adenosine A2A receptors in

cortical neurotransmission to the striatal direct pathway. ScientificWorldJournal 9:1321-1344.

Raju DV, Shah DJ, Wright TM, Hall RA, Smith Y. 2006. Differential synaptology of vGluT2-containing thalamostriatal afferents between the patch and matrix compartments in rats. The Journal of comparative neurology 499(2):231-243.

Ravyn V, Bostwick JR. 2006. Functional coupling of the Galpha(olf) variant XLGalpha(olf) with the human adenosine A2A receptor. J Recept Signal Transduct Res 26(4):241-258.

Raz A, Vaadia E, Bergman H. 2000. Firing patterns and correlations of spontaneous discharge of pallidal neurons in the normal and the tremulous 1-methyl-4-phenyl-1,2,3,6-tetrahydropyridine vervet model of parkinsonism. J Neurosci. 20(22):8559-71.

Robelet S, Melon C, Guillet B, Salin P, Kerkerian-Le Goff L. 2004. Chronic L-DOPA treatment increases extracellular glutamate levels and GLT1 expression in the basal ganglia in a rat model of Parkinson's disease. The European journal of neuroscience 20(5):1255-1266.

Rochet JC, Hay BA, Guo M. 2012. Molecular insights into Parkinson's disease. Prog Mol Biol Transl Sci. 107:125-88.

Rodrigues RJ, Alfaro TM, Rebola N, Oliveira CR, Cunha RA. 2005. Co-localization and functional interaction between adenosine A(2A) and metabotropic group 5 receptors in glutamatergic nerve terminals of the rat striatum. Journal of neurochemistry 92(3):433-441.

Rosin DL, Robeva A, Woodard RL, Guyenet PG, Linden J. 1998. Immunohistochemical localization of adenosine A2A receptors in the rat central nervous system. The Journal of comparative neurology 401(2):163-186.

Rylander D, Iderberg H, Li Q, Dekundy A, Zhang J, Li H, Baishen R, Danysz W, Bezard E, Cenci MA. 2010. A mGluR5 antagonist under clinical development improves L-DOPA-induced dyskinesia in parkinsonian rats and monkeys. Neurobiol Dis 39(3):352-361.

Rylander D, Recchia A, Mela F, Dekundy A, Danysz W, Cenci MA. 2009. Pharmacological modulation of glutamate transmission in a rat model of L-DOPA-induced dyskinesia: effects on motor behavior and striatal nuclear signaling. The Journal of pharmacology and experimental therapeutics 330(1):227-235.

Samadi P, Gregoire L, Morissette M, Calon F, Hadj Tahar A, Dridi M, Belanger N, Meltzer LT, Bedard PJ, Di Paolo T. 2008. mGluR5 metabotropic glutamate receptors and dyskinesias in MPTP monkeys. Neurobiol Aging 29(7):1040-1051.

Sanberg PR. 1980. Haloperidol-induced catalepsy is mediated by postsynaptic dopamine receptors. Nature 284: 472–473.

Sardo P, Ravel S, Legallet E, Apicella P. 2000. Influence of the predicted time of stimuli eliciting movements on responses of tonically active neurons in the monkey striatum. Eur J Neurosci. 12(5):1801-16.

Sato F, Lavallee P, Levesque M, Parent A. 2000a. Single-axon tracing study of neurons of the external segment of the globus pallidus in primate. The Journal of comparative neurology 417(1):17-31.

Sato F, Parent M, Levesque M, Parent A. 2000b. Axonal branching pattern of neurons of the subthalamic nucleus in primates. The Journal of comparative neurology 424(1):142-152.

Scatton B, Javoy-Agid F, Rouquier L, Dubois B, Agid Y. 1983. Reduction of cortical dopamine, noradrenaline, serotonin and their metabolites in Parkinson's disease. Brain Res 275(2):321-328.

Schiffmann SN, Fisone G, Moresco R, Cunha RA, Ferre S. 2007. Adenosine A2A receptors and basal ganglia physiology. Progress in neurobiology 83(5):277-292.

Schiffmann SN, Jacobs O, Vanderhaeghen JJ. 1991a. Striatal restricted adenosine A2 receptor (RDC8) is expressed by enkephalin but not by substance P neurons: an in situ hybridization histochemistry study. Journal of neurochemistry 57(3):1062-1067.

Schiffmann SN, Libert F, Vassart G, Vanderhaeghen JJ. 1991b. Distribution of adenosine A2 receptor mRNA in the human brain. Neuroscience letters 130(2):177-181.

Schiffmann SN, Vanderhaeghen JJ. 1993. Adenosine A2 receptors regulate the gene expression of striatopallidal and striatonigral neurons. J Neurosci 13(3):1080-1087.

Sharott A, Doig NM, Mallet N, Magill PJ. 2012. Relationships between the firing of identified striatal interneurons and spontaneous and driven cortical activities in vivo. J Neurosci. 32(38):13221-36.

Shigemoto R, Nomura S, Ohishi H, Sugihara H, Nakanishi S, Mizuno N. 1993. Immunohistochemical localization of a metabotropic glutamate receptor, mGluR5, in the rat brain. Neuroscience letters 163(1):53-57.

Shindou T, Mori A, Kase H, Ichimura M. 2001. Adenosine A(2A) receptor enhances GABA(A)-mediated IPSCs in the rat globus pallidus. The Journal of physiology 532(Pt 2):423-434.

Shink E, Smith Y. 1995. Differential synaptic innervation of neurons in the internal and external segments of the globus pallidus by the GABA- and glutamate-containing terminals in the squirrel monkey. The Journal of comparative neurology 358(1):119-141.

Smith Y, Bolam JP. 1991. Convergence of synaptic inputs from the striatum and the globus pallidus onto identified nigrocollicular cells in the rat: a double anterograde labelling study. Neuroscience. 44(1):45-73.

Smith Y, Bevan MD, Shink E, Bolam JP. 1998. Microcircuitry of the direct and indirect pathways of the basal ganglia. Neuroscience 86(2):353-387.

Smith Y, Raju D, Nanda B, Pare JF, Galvan A, Wichmann T. 2009. The thalamostriatal systems: anatomical and functional organization in normal and parkinsonian states. Brain research bulletin 78(2-3):60-68.

Smith Y, Raju DV, Pare JF, Sidibe M. 2004. The thalamostriatal system: a highly specific network of the basal ganglia circuitry. Trends in neurosciences 27(9):520-527.

Smith Y, Wichmann T, Factor SA, DeLong MR. 2012. Parkinson's disease therapeutics: new developments and challenges since the introduction of levodopa. Neuropsychopharmacology 37(1):213-246.

Soares J, Kliem MA, Betarbet R, Greenamyre JT, Yamamoto B, Wichmann T. 2004. Role of external pallidal segment in primate parkinsonism: comparison of the

effects of 1-methyl-4-phenyl-1,2,3,6-tetrahydropyridine-induced parkinsonism and lesions of the external pallidal segment. J Neurosci 24(29):6417-6426.

Spooren WP, Gasparini F, Bergmann R, Kuhn R. 2000. Effects of the prototypical mGlu(5) receptor antagonist 2-methyl-6-(phenylethynyl)-pyridine on rotarod, locomotor activity and rotational responses in unilateral 6-OHDA-lesioned rats. European journal of pharmacology 406(3):403-410.

Stacy M, Silver D, Mendis T, Sutton J, Mori A, Chaikin P, Sussman NM. 2008. A 12-week, placebo-controlled study (6002-US-006) of istradefylline in Parkinson disease. Neurology 70(23):2233-2240.

Stowe RL, Ives NJ, Clarke C, van Hilten J, Ferreira J, Hawker RJ, Shah L, Wheatley K, Gray R. 2008. Dopamine agonist therapy in early Parkinson's disease. Cochrane Database Syst Rev(2):CD006564.

Stromberg I, Popoli P, Muller CE, Ferre S, Fuxe K. 2000. Electrophysiological and behavioural evidence for an antagonistic modulatory role of adenosine A2A receptors in dopamine D2 receptor regulation in the rat dopamine-denervated striatum. The European journal of neuroscience 12(11):4033-4037.

Svenningsson P, Hall H, Sedvall G, Fredholm BB. 1997. Distribution of adenosine receptors in the postmortem human brain: an extended autoradiographic study. Synapse (New York, NY 27(4):322-335.

Svenningsson P, Le Moine C, Aubert I, Burbaud P, Fredholm BB, Bloch B. 1998. Cellular distribution of adenosine A2A receptor mRNA in the primate striatum. The Journal of comparative neurology 399(2):229-240.

Tanganelli S, Sandager Nielsen K, Ferraro L, Antonelli T, Kehr J, Franco R, Ferre S, Agnati LF, Fuxe K, Scheel-Kruger J. 2004. Striatal plasticity at the network level. Focus on adenosine A2A and D2 interactions in models of Parkinson's Disease. Parkinsonism & related disorders 10(5):273-280.

Taverna S, Ilijic E, Surmeier DJ. 2008. Recurrent collateral connections of striatal medium spiny neurons are disrupted in models of Parkinson's disease. J Neurosci 28(21):5504-5512.

Tebano MT, Martire A, Rebola N, Pepponi R, Domenici MR, Gro MC, Schwarzschild MA, Chen JF, Cunha RA, Popoli P. 2005. Adenosine A2A receptors and metabotropic glutamate 5 receptors are co-localized and functionally interact in the hippocampus: a possible key mechanism in the modulation of N-methyl-D-aspartate effects. Journal of neurochemistry 95(4):1188-1200.

Testa CM, Standaert DG, Young AB, Penney JB, Jr. 1994. Metabotropic glutamate receptor mRNA expression in the basal ganglia of the rat. J Neurosci 14(5 Pt 2):3005-3018.

Thorsell A, Johnson J, Heilig M. 2007. Effect of the adenosine A2a receptor antagonist 3,7-dimethyl-propargylxanthine on anxiety-like and depression-like behavior and alcohol consumption in Wistar Rats. Alcohol Clin Exp Res 31(8):1302-1307.

Tozzi A, de Iure A, Di Filippo M, Tantucci M, Costa C, Borsini F, Ghiglieri V, Giampa C, Fusco FR, Picconi B, Calabresi P. 2011. The distinct role of medium spiny neurons and cholinergic interneurons in the D/AA receptor interaction in the striatum: implications for Parkinson's disease. J Neurosci 31(5):1850-1862.

Turle-Lorenzo N, Breysse N, Baunez C, Amalric M. 2005. Functional interaction between mGlu 5 and NMDA receptors in a rat model of Parkinson's disease. Psychopharmacology 179(1):117-127.

Valenti O, Marino MJ, Wittmann M, Lis E, DiLella AG, Kinney GG, Conn PJ. 2003. Group III metabotropic glutamate receptor-mediated modulation of the striatopallidal synapse. J Neurosci 23(18):7218-7226.

Verhagen Metman L, Del Dotto P, Blanchet PJ, van den Munckhof P, Chase TN. 1998. Blockade of glutamatergic transmission as treatment for dyskinesias and motor fluctuations in Parkinson's disease. Amino acids 14(1-3):75-82.

Vernon AC, Zbarsky V, Datla KP, Croucher MJ, Dexter DT. 2007. Subtype selective antagonism of substantia nigra pars compacta Group I metabotropic glutamate receptors protects the nigrostriatal system against 6-hydroxydopamine toxicity in vivo. Journal of neurochemistry 103(3):1075-1091.

Villalba RM, Lee H, Smith Y. 2009. Dopaminergic denervation and spine loss in the striatum of MPTP-treated monkeys. Experimental neurology 215(2):220-227.

Wachtel H, Kunow M, Loschmann PA. 1992. NBQX (6-nitro-sulfamoyl-benzo-quinoxaline-dione) and CPP (3-carboxy-piperazin-propyl phosphonic acid) potentiate dopamine agonist induced rotations in substantia nigra lesioned rats. Neuroscience letters 142(2):179-182.

Warnick JE, Maleque MA, Bakry N, Eldefrawi AT, Albuquerque EX. 1982. Structure-activity relationships of amantadine. I. Interaction of the N-alkyl analogues with the ionic channels of the nicotinic acetylcholine receptor and electrically excitable membrane. Mol Pharmacol. 22(1):82-93.

Weaver CD, Sheffler DJ, Lewis LM, Bridges TM, Williams R, Nalywajko NT, Kennedy JP, Mulder MM, Jadhav S, Aldrich LA, Jones CK, Marlo JE, Niswender CM, Mock MM, Zheng F, Conn PJ, Lindsley CW. 2009. Discovery and development of a potent and highly selective small molecule muscarinic acetylcholine receptor subtype I (mAChR 1 or M1) antagonist in vitro and in vivo probe. Current topics in medicinal chemistry 9(13):1217-1226.

Wenzel A, Fritschy JM, Mohler H, Benke D. 1997. NMDA receptor heterogeneity during postnatal development of the rat brain: differential expression of the NR2A, NR2B, and NR2C subunit proteins. J Neurochem. 68(2):469-78.

Westin J, Nyholm D, Palhagen S, Willows T, Groth T, Dougherty M, Karlsson MO. 2011. A pharmacokinetic-pharmacodynamic model for duodenal levodopa infusion. Clinical neuropharmacology 34(2):61-65.

Wichmann T, Bergman H, Starr PA, Subramanian T, Watts RL, DeLong MR. Comparison of MPTP-induced changes in spontaneous neuronal discharge in the internal pallidal segment and in the substantia nigra pars reticulata in primates. Exp Brain Res 1999;125:397–409.

Wichmann T, DeLong MR. 2003. Pathophysiology of Parkinson's disease: the MPTP primate model of the human disorder. Annals of the New York Academy of Sciences 991:199-213.

Wichmann T, Kliem MA, DeLong MR. 2001. Antiparkinsonian and behavioral effects of inactivation of the substantia nigra pars reticulata in hemiparkinsonian primates. Experimental neurology 167(2):410-424.

Wichmann T, Soares J. 2006. Neuronal firing before and after burst discharges in the monkey basal ganglia is predictably patterned in the normal state and altered in parkinsonism. Journal of neurophysiology 95(4):2120-2133.

Wingeier B, Tcheng T, Koop MM, Hill BC, Heit G, Bronte-Stewart HM. 2006. Intra-operative STN DBS attenuates the prominent beta rhythm in the STN in Parkinson's disease. Exp Neurol. 197(1):244-51.

Wirkner K, Assmann H, Koles L, Gerevich Z, Franke H, Norenberg W, Boehm R, Illes P. 2000. Inhibition by adenosine A(2A) receptors of NMDA but not AMPA currents in rat neostriatal neurons. British journal of pharmacology 130(2):259-269.

Wirkner K, Gerevich Z, Krause T, Gunther A, Koles L, Schneider D, Norenberg W, Illes P. 2004. Adenosine A2A receptor-induced inhibition of NMDA and GABAA receptor-mediated synaptic currents in a subpopulation of rat striatal neurons. Neuropharmacology 46(7):994-1007.

Wright CE, Sisson TL, Ichhpurani AK, Peters GR. 1997. Steady-state pharmacokinetic properties of pramipexole in healthy volunteers. J Clin Pharmacol 37(6):520-525.

Wu Y, Richard S, Parent A. 2000. The organization of the striatal output system: a single-cell juxtacellular labeling study in the rat. Neurosci Res 38(1):49-62.

Yamamoto N, Soghomonian JJ. 2009. Metabotropic glutamate mGluR5 receptor blockade opposes abnormal involuntary movements and the increases in glutamic acid decarboxylase mRNA levels induced by l-DOPA in striatal neurons of 6-hydroxydopamine-lesioned rats. Neuroscience 163(4):1171-1180.

Yung KK, Bolam JP, Smith AD, Hersch SM, Ciliax BJ, Levey AI. 1995. Immunocytochemical localization of D1 and D2 dopamine receptors in the basal ganglia of the rat: light and electron microscopy. Neuroscience 65(3):709-730.

**Non-printed sources**

National Parkinson Foundation. 2011. Parkinson's Disease (PD) Overview. Available at: http://www.parkinson.org/parkinson-s-disease.aspx. Accessed Nov 4, 2012.